Scuola Internazionale Superiore Studi Avanzati (S.I.S.S.A.)
Trieste, Italy

Neuroscience area

Program of Functional and Structural Genomics

SISSA 40!

MOLECULAR MECHANISM OF NEURITOGENESIS DRIVEN BY PRION PROTEIN

Thesis submitted for the degree of
Doctor of Philosophy

Supervisors
Prof. Giuseppe Legname

Dr. Dan Cojoc

Student
Nguyen Thi Anh Xuan

October 26th, 2018

ACKNOWLEDGEMENTS

First of all, I would like to express my deep gratefulness to Prof. Giuseppe Legname who gave me valuable opportunity to pursue my dream of studying neuroscience. He has encouraged and supervised me at important steps to accomplish this PhD study. Despite being busy with many responsibilities, he managed to have time for our discussion when necessary. He also supported me with many chances to learn scientific studies and other important skills.

I also highly appreciate Dr. Dan Cojoc for his kindness, friendliness and helpful supervision. Dan gave me important chance to learn advanced techniques in neurobiology from the first summer school I attended in Trieste. He also offered full support for the usage of his optical tweezer setup and tutored me in practicing Matlab.

I'm very thankful to Dr. Ladan Amin whom I had critical time working with during the first project. Following her, I could learn a lot about the technique and about her time management. I was lucky to participate in this exciting project started by her. I would like to thank also Dr. Hoa T. Tran for his kind collaboration and useful advices. I have learnt the technique of recombinant protein production and also other tips working in the lab from him. Besides, having him as a Vietnamese senior in the lab made me feel much supported. I send thanks to other lab seniors Dr. Silvia Vanni, Dr. Giulia Salzano and other members for useful discussions and their support in the lab.

I want to thank the staff at Sissa especially Beatrice who taught me dissection of mouse brain and primary cultures; Micaela who tutored me in using the confocal microscopes; students' secretariat Riccardo and Federica who kindly helped me with bureaucracy issues; and Tullio for his support in one of my part-time job at Sissa and for his jokes.

Next, I wish to show my appreciation to my dear friends Ulisse and Diletta who helped me a lot in transporting the cells to work in Elettra; deeply thanks to Nora and Kevin who always gave me strong encouragement to believe in myself, motivation to pursue academic life and full support as best friends. I want to thank also Katarina as a good friend who usually raised interesting topics to talk during lunch time and for the time we spent together.

I show my deepest gratitude to my parents who always provide me priceless love, care and support.

Last but not least, I appreciate the scientific committee who read and correct my thesis. For those who I did not mention specifically, I'm grateful for all whom I spent time with or met in life that helped fulfill my PhD life.

…And thanks for beautiful time I had in Trieste!

Abstract

The cellular form of prion protein (PrP^C) is a ubiquitous component of both the central and peripheral nervous systems from early stages of development to adulthood. Its misfolded isoform PrP^{Sc} is the pathological agent of prion diseases, a group of fatal neurodegenerative diseases. PrP^C has been suggested to play different roles in neuroprotection, synaptic activities, neuritogenesis and metal homeostasis. Particularly, we were interested in its neurotrophic function and molecular mechanism involved the prion protein (PrP) with the process. By combining genomic approaches, cellular assays and focal stimulation technique, we explored PrP could act as a guidance cue, attracting the growth cone (GC) protrusion forward and eventually neurite outgrowth.

In the study, we made different forms of the recombinant prion proteins (recPrP) from mouse without GPI anchoring residues mimicking secreted forms of PrP^C. Our data suggest that full-length and wild-type recPrP(23-231) protein, not its truncated forms at N or C-terminal (23-90, 23-120, 89-231), could attract GC turning toward the protein source and enhance neurite growth in a dose-dependent manner. recPrP may act through homophilic interaction with the GPI-anchor PrP^C and form trans-signaling complex with neural cell adhesion molecule (NCAM) on the target cells to induce multiple intracellular signaling cascades known for cell growth including the Src-family kinase Fyn, extracellular regulated kinases MEK-ERK and phosphatidylinositol 3-kinase (PI3K).

In addition, we discovered the functional sites for PrP function as a signaling molecule in neuritogenesis lying directly on N-terminal copper binding sites by mutating these residues to partially or completely prevent copper binding. In detail, minimal change in the copper binding site could lead to changes in the protein structure preventing PrP from functioning correctly and disrupting all the copper-binding sites at the N-terminus could turn the protein to be toxic to neurons. Especially, copper coordination at non-octarepeat (non-OR) region was shown to be essential for PrP to activate the proper growth signaling. GSS-linked mutation P102L (P101L in mouse numbering) that impacts indirectly to non-OR copper coordination could also abolish the function of PrP on neuritogenesis. Altogether, our findings indicate the crucial role of copper binding sites in maintaining functional structure for PrP interaction in neuritogenesis and suggest a potential link between loss-of-function of the protein and prion disease initiation.

Key words: prion protein, neuritogenesis, growth cone, copper binding site

Table of Contents

Pages

List of Abbreviations

AD – Azheimer's disease

ADAM – A Disintegrin and Metalloproteinase

ALS – Amyotrophic lateral sclerosis

AMPA - α-amino-3-hydroxy-5-methyl-4-isoxazolepropionic acid

Arg (R) – Arginine

Asn (N) – Asparagine

Aβ – Amyloid beta

Bax – Bcl-2-associated protein x

BBB – Blood brain barrier

BCA - Bicinchoninic acid assay

BDNF – Brain-derived neurotrophic factor

BSA – Bovine serum albumin

BSE – Bovine spongiform encephalopathy

cAMP – Adenosine 3′,5′-cyclic monophosphate

CD – Circular Dichroic

CJD – Creutzfeldt – Jakob disease

CNS – Central nervous system

CREB - cAMP response element-binding protein

CSF – Cerebrospinal fluid

CTR1 – Copper-transporter 1

CWD – Chronic wasting disease

DAPI – 4',6-diamidino-2-phenylindole

DCC – Deleted in Colorectal Carcinomas

DG – Dentate gyrus

D-PEN - D-Penicillamine

ECM – Extracellular matrix

EDTA - Ethylenediaminetetraacetic acid

ER – Endoplasmic reticulum

ERK – Extracellular regulated kinase

fCJD – familial CJD

FFI – Fatal familial insomnia

FNIII – Fibronectin III

GABA - Gamma-aminobutyric acid

GC - Growth cone

GdnHCl – Guadinine chloride

GFP – Green fluorescent protein

Gly (G) – Glycine

GPI – Glycosyl – phosphatidylinositol

GSS – Gerstmann – Strussler – Scheinker

HD – hydrophobic domain

His (H) – Histidine

HRP - Horseradish peroxidase

HuPrP – Human prion protein

IFN – Interferon

IL – Interleukin

IPTG - Isopropyl β-D-1-thiogalactopyranoside

IR – Infrared laser

KO – Knockout

LDCV – Large, dense-core vesicle

Leu (L) – Leucine

LN – Laminin

LR – Laminin receptor

LRP – Laminin receptor precursor

LTP – Long-tern potentiation

MAPK - Mitogen-activated protein kinase

MEK – downstream member of MAPK

MoPrP – Mouse prion protein

MVs – Microvesicles

MWCO – Molecular weight cut-off

NCAM - Neural cell adhesion molecule

NGF – Nerve-growth factor

NGS – Normal goat serum

NMDAR – N-Methyl-D-aspartate receptor

NMR – Nuclear magnetic resonance

NO – Nitric oxide

NRMSD - Normalized root mean square displacement

NSC – Neural stem cell

OR – Octarepeat

ORF – Open reading frame

PBS – Phosphate buffer saline

PC – Purkinje cell

PCR - Polymerase Chain Reaction

PFA – Paraformaldehyde

Phe (F) – Phenylalanine

PI3K – Phosphatidylinositol 3 kinase

PI-PLC – Phosphatidylinositol – specific phospholipase

PK – Proteinase K

PKA – Protein kinase A

Pro (P) – Proline

PrP - Prion protein

PrP^{C} - Cellular prion protein

PrP^{res} – Protease-resistant PrP

PrP^{Sc} – Scrapie prions (infectious form of prion protein)

PSD – Post-synaptic density

PVDF – Polyvinylidene difluoride

recMoPrP – Recombinant mouse prion protein

recPrP - Recombinant prion protein

RF – Restriction-free

ROS – Reactive oxygen species

SDS-PAGE – Sodium Dodecyl Sulfate Polyacrylamide Gel Electrophoresis

SPR – Surface plasmon resonance

STED - Stimulated emission depletion

STI1 – Stress-induced protein 1

SVZ – Subentricular zone

TBS-T - Tris buffer saline with Tween 20

TSEs – Transmissible spongiform encephalopathies

Tyr (Y) – Tyrosine

UV – Ultraviolet

Val (V) – Valine

vCJD – variant CJD

VGCC – Voltage-gated Ca^{2+} channel

Vn – Vibronectin

Wt – Wild-type

List of Figures

Pages

List of tables

CHAPTER 1 – INTRODUCTION

1.1. Research statement

Transmissible spongiform encephalopathies (TSEs) or prion diseases is a group of fatal neurodegenerative diseases found in both animals and humans which is featured by gliosis, neuronal loss [1, 2] and synaptic degeneration [3]. The prion protein has been believed as the only proteinaceous agent causing the disease by converting from its cellular form (PrP^{C}) to PrP^{Sc}. In the past 20 years, more than 280,000 cattle suffering from bovine spongiform encephalopathy (BSE) – a common type of prion disease [4]. In addition, transmission of BSE to humans have been considered as the reason of more than 200 cases of variant of Creutzfeldt-Jakob disease (vCJD) [5]. Although the epidemics of prion disease in animal have been in control and cases found in human are also rare, occurrences of the diseases are still found from time to time, for example a rise of chronic wasting diseases in elk and deer in the US [6] or cases of vCJD caused by blood transfusion [5]. Moreover, prion protein is getting more attention since it may mediate the neurotoxicity effect of amyloid beta (Aβ) oligomers that are associated with Alzheimer's disease [7, 8]; and prion-like mechanism has been proven in other neurodegenerative diseases [9] and even metabolic disorder [10].

Thereafter cellular prion protein (PrP^{C}) has been noticed widely in neurobiology research not only for its central role in prion disease and related disorders but also for its emerging function in the central nervous system (CNS) such as neuritogenesis [11], cell adhesion [12, 13], memory and cognition [14], neuroprotection [15, 16] and metal homeostasis [17]. For the reason, it is proposed that prion pathogenesis may involve alterations in the physiological function of PrP^{C}. Although loss of PrP^{C} function cannot, by itself, account for prion-induced neurodegeneration since PrP knockout (KO) mice do not develop prion disease [18]. However, it is possible that a loss of function mechanism exacerbates pathology caused by a toxic gain of function or other mechanisms [19].

PrP^{C} can be secreted from the cell membrane and released to the extracellular space through distinct mechanisms [11]. Therefore, PrP^{C} can interact with neighboring cells either in a soluble form or in exosomes, which are released by cells upon fusion of multivesicular bodies [20]. It has been suggested that the secreted form of PrP may contribute to neurotrophic activity and

promote neuritogenesis [11]. This phenomenon may help explain about loss in neuronal connection in prion diseases probably due to malfunction of PrP in neuritogenesis.

Therefore, attempts to study mechanism of neuritogenesis driven by soluble form of PrP will broaden important knowledge of emerging PrP functions in CNS which eventually can be helpful for understanding prion pathology and suggestions for therapeutic interventions.

1.2. Objective

Considering the potential importance of PrP role in neuritogenesis, we would like to investigate molecular mechanism on which extracellular PrP^C complex forms and induces intracellular signaling to guide neurons in that process. Taking advantage of a recently developed local delivery technique of molecules encapsulated in phospholipid vesicles [21-23], we combine with genomics manipulations to provide deeper mechanism of PrP function in specific neuronal compartment such as growth cone (GC) in addition to previous evidence from traditional cellular assays [24-26] . We also aim to explore which are the relevant components of the molecule for its function.

CHAPTER 2 – LITERATURE REVIEW

2.1. Prion diseases

Although prion disease is a group of rare neurodegenerative diseases, there are various types caused by different prion strains in both animals and humans. Despite variety of phenotypes and incidences, this group of disease is commonly believed to be caused by a unique proteinaceous agent, so called prion [27], that is resulted of pathogenic conversion of a highly conserved cellular prion protein PrP^C from α-helical structure to β-pleated sheet one [28, 29]. Common neuropathologic changes in prion diseases includes vacuolation, astrogliosis, and PrP deposition [30]. The diseases can occur by three mechanisms: spontaneous (sporadic), genetic (familial), and acquired (infectious/ transmitted) [31].

In humans, these diseases are Creutzfeldt-Jakob disease (CJD), Gerstmann-Strussler-Scheinker (GSS) syndrome, Fatal Familial Insomnia (FFI), and kuru. CJD accounts for approximately 85% of human prion diseases which are mostly sporadic and heritable [30]. Different types of CJD includes sporadic, familial, iatrogenic and variant CJD. Sporadic CJD is an acute disease and

predominantly at late middle-age around 60s with unknown cause [32]. The 129M/V polymorphism on *PRNP* gene and two types of protease-resistant prion proteins are the major determinants of neuropathological phenotypes in sCJD [33]. Iatrogenic and variant CJD (vCJD) are acquired prion diseases from neurosurgical instruments in transplantation or treatment and from food consumption respectively [34]. vCJD has earlier age of onset and more prolonged duration of illness than in sCJD (~13months) and featured by psychiatric symptoms and memory impairment [34, 35]. Higher prevalence in UK for vCJD is found with risk factors including young age and methionine homozygosity at codon 129 (129MM genotype) [34]. Remarkably, over 40 different mutations of *PRNP* gene have been shown to divide with the genetic human prion diseases [30] (Figure 1). Familial CJD (fCJD) as well as GSS occur inheritably as autosomal dominant trait with high penetrance and can transmit a scrapie-like disease to animal model with brain extract inoculation [36]. Insertions of two to nine additional octarepeats as well as point mutation E200K have been found in individuals within fCJD pedigrees [30]. Mutation D178N coupled with polymorphic V129 also causes fCJD with clinical signs including dementia and widespread deposition of PrP^{Sc} [30, 37]. Notely, point mutation at codon 102 (P102L) was found in unrelated families with GSS syndrome from several countries [30, 38, 39]. Other GSS-linked mutations include P105L, A117V, G131V, Y145Stop, Q160Stop, P198S, D202N, Q212P, and Q217R [40]. GSS typically begins at 40s to 60s age and progress slowly with cerebellar dysfunction, unsteady gait and/or mild dysarthria [40]. FFI similarly presents in midlife (40–50 years) with the onset of insomnia, a progressive sleep disorder that is ultimately fatal [30, 40]. The pathogenic mutation D178N if coupled with M129 results FFI instead of fCJD [37]. Concernedly, human-to-human transmission of prion disease is as well documented and occurred either through oral or mucocutaneous route of infection, for example from ritual cannibalism as in kuru [33, 34].

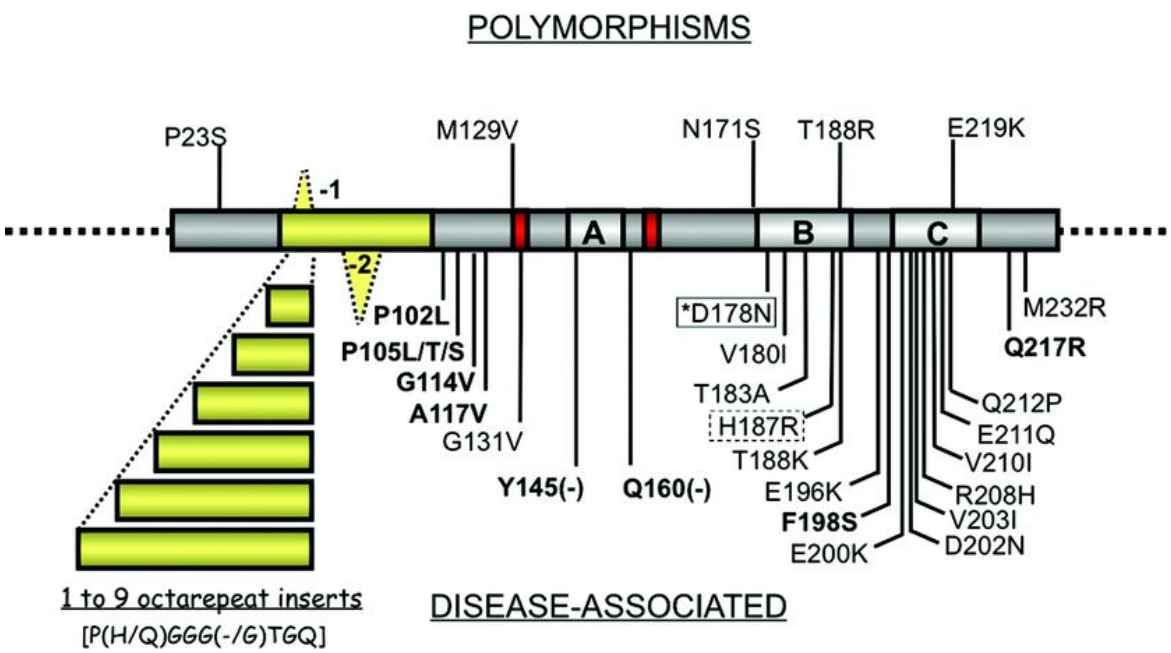

Figure 1 - PRNP gene polymorphisms and mutations. All mutations are associated with a CJD phenotype except those in bold (GSS), solid box (FFI or CJD, depending on codon 129 genotype), and dotted box (CJD phenotype but variable pathology). Adapted from [40]

In mammals, some well-known prion diseases include scrapie in sheep and goat, bovine spongiform encephalopathy (BSE), chronic wasting disease (CWD) in mule deer and elk [30]. Scrapie was probably the first prion disease documented since 1732 from which the infectious prion protein was named (PrP^{Sc}). Thanks to species barrier, humans are resistant to scrapie whereas laboratory animal models such as hamster and mouse are susceptible [30]. BSE was emerged in United Kingdom in early 90s probably due to prions-contaminated food supplement [36]. It has been suggested that a single prion strain responsible for BSE has infected humans, causing variant CJD (vCJD) [33, 41]. In classical BSE (BSE-C), the non-glycosylated PrP^{Sc} band migrates at ~17 kDa while in atypical BSEs, the band runs 0.5 kDa lower in low-type BSE (BSE-L) or 1–2 kDa higher in high-type BSE (BSE-H) [42]. The mean incubation time for BSE is approximately 5 years [30] while atypical BSE can be much shorter (less than two years) [43]. Atypical BSE is characterized by the presence of PrP-amyloid plagues, opposite to typical BSE, and to be similar with sporadic CJD (sCJD) [33]. The three natural host species for CWD are mule deer (Odocoileus hemionus), white-tailed deer (O. virginianus), and Rocky Mountain elk (Cervus elaphus nelsoni) and native to North America [44].The incidence of CWD in wild cervids was estimated to be as high as 15% [30]. CWD is infectious, transmitting horizontally

from infected to susceptible cervids potentially caused by shedding of prions in the feces or saliva [44].

2.2. Prion protein

2.2.1. Structure

Cellular prion protein (PrP^C) is a glycoprotein that is ubiquitous in mammals. It is mostly expressed from early to adult stage in central and peripheral nervous systems. Mature PrP^C molecules are normally localized on the cell surface attaching to the lipid bilayer via a C-terminal, glycosyl-phosphatidylinositol (GPI) anchor Ser-231 [45].

The premature PrP peptide is composed of around 250-254 amino acids that is encoded by a single chromosomal gene *Prnp*. After biosynthesis, it is processed at endoplasmic reticulum (ER) to remove a signal peptide with N-terminal 22 amino acids and 23 C-terminal residues upon the addition of the GPI anchor [46, 47]. The protein is also N-linked-glycosylated at Asn-180 and Asn-196 (mouse numbering) prior to being secreted to the cell membrane.

Mouse and hamster prion proteins contain a C-terminal globular domain that extends approximately from 121-231 [48] and 125–231 [46] respectively and an N-terminal flexibly disordered structure. The globular domain contains a two stranded anti-parallel β-sheet and three α-helices [49]. α2 and α3 helices are connected to each other through a disulfide link between residues 178 and 213 (mouse numbering). The flexible N-terminal tail is characterized mainly by five tandem repeats of eight amino acids forming an octarepeat region (OR) with the motif PHGGGWGQ and a hydrophobic linker region, also called hydrophobic domain (HD) [50]. (Figure 2)

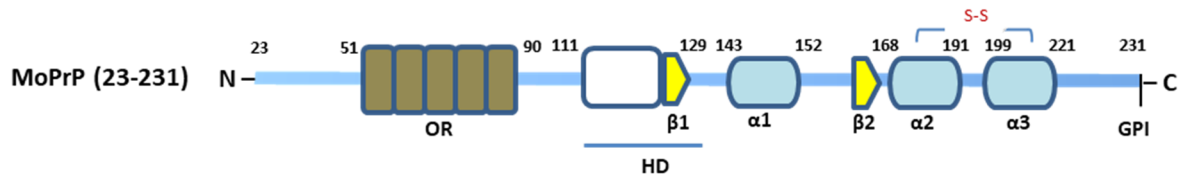

Figure 2 – Schematic representation of full-length, non-glycosylated form of major mouse prion protein MoPrP(23-231). The protein structure consists of five octarepeat regions (OR) and hydrophobic domain (HD) at the unstructured N-terminal; two short β-sheets (β1 and β2) and three α-helices (α1, α2, α3) with disulfide bond between α2 and α3; and GPI-attached at Ser231 at C-terminal.

The region from 50 to 111 residues at N-terminal sequence are claimed to bind metal ions such as Cu(II), Zn(II) or Mn(II) by the histidine residues at the OR and the adjacent site denoted as non-OR region (His95 and H111 - human numbering) [51, 52]. Although the metal-free PrP^C (apo-PrP^C) is natively unstructured at the N-terminal (Figure 3) but different stoichiometries of metal binding can impart different structures of this region (called 'component 1', 'component 2' and 'component 3' [50, 53] (Figure 4).

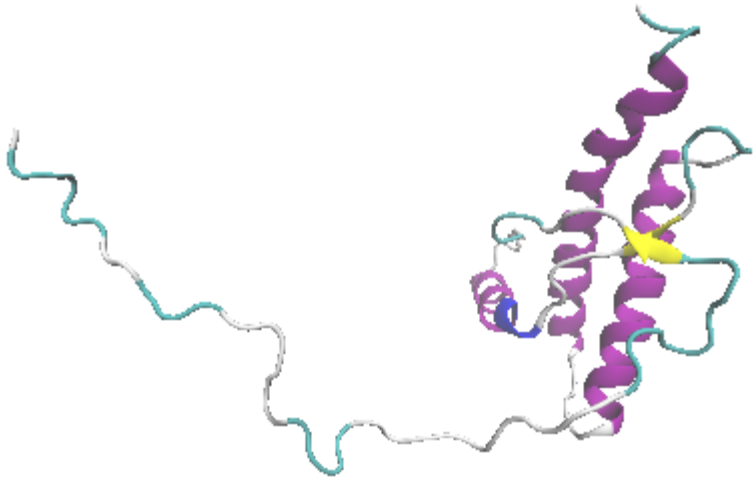

Figure 3 – apo-PrP^C structure with unstructured N-terminal tail. β-stranded antiparallel sheets are marked in yellow and α-helices are in pink. Modified from pdb: 2LSB

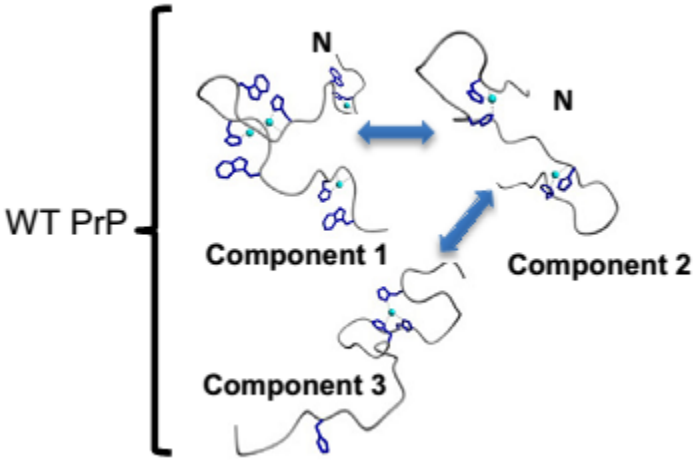

Figure 4 – **Different conformation of N-terminal PrP domain**. Different stoichiometries of metal binding at the N-terminal of PrP leading to potential different structure with interchangeable component 1, 2 and 3 geometries [50]

2.2.2. Proteolytic processing

After removal of the N-terminal signal sequence (aa 1-22) by signal peptidases in the ER and the C-terminal signal sequence for the attachment of the GPI-anchor (aa 231-254), mature PrP^{C} can be subjected to diverse proteolytic processing including α-cleavage within the neurotoxic domain (aa 105–125 in mice), β-cleavage around the residue 90, and shedding near the plasma membrane to release almost full-length PrP^{C} into the extracellular environment [54]. (Figure 5)

The α-cleavage is carried out by members of the ADAM (A Disintegrin And Metalloproteinase) enzyme family, including ADAM8, 10 and 17. ADAM8 cleaves PrPC at residue 109 (primary site) or 116 (minor site), while ADAM10 and 17 cleave at 119 [55]. Cleaving by ADAM8 at residue 109 (mouse numbering) yields two fragments, soluble N1 fragment of 11 kDa and a membrane-bound C1 fragment of 18 kDa [56, 57] although it was controversial ADAM10 was primarily responsible for this cleavage as well [57] and role of ADAM8 was proven mainly in muscle tissue [58]. Of note, this cleavage destroys the neurotoxic and amyloidogenic domain comprising aa 106-126. C1 can be glycosylated and is present in the normal human brain in substantial amount [56]. It has been shown that C1 could play a modulatory role as dominant-negative inhibitor of PrP^{Sc} formation probably because C1 competes with wild-type PrP for binding to PrP^{Sc} seeds [59]. However, *in vitro* study suggested that C1 potentiates staurosporine-induced caspase-3 activation through a p53-dependent mechanism displaying a pro-apoptotic function [60]. Conversely, compelling data suggesting N1 fragment is antiapoptotic, possibly acting through the inhibition of caspase-3 [55, 61].

The β-processing which was believed to be done by ADAM8 [55] is to make N2 (9 kDa) and C2 (20 kDa) fragments [57]. This cleavage appears to be driven by reactive oxygen species (ROS) [62, 63] that was proposed from these *in vitro* studies to be as a protective mechanism by the cell in response to oxidative stress. A longer C2 fragment that harbors the neurotoxic domain was thought to be conducive to prion replication since it is the main proteolytic product found in CJD brains [56]. In fact, C2 shares common features with the protease-resistant core of PrP^{Sc} denoted as PrP27-30 (i.e. detergent insolubility and the electrophoretic mobility) [57, 64]. The protective role of β-cleavage was suggestively modulated mainly by N2 fragment. N2(23-89) attenuated the production of intracellular ROS in response to serum deprivation and its activity depended on copper occupancy [65].

Recently a study by Lewis *et. al.* identified a potential γ-cleavage site on PrP producing C3 fragment of less than 10kDa. C3 is preferentially produced from unglycosylated form of PrP by a matrix metalloprotease. Even though the investigation was performed mainly with an engineered murine PrP (Myc-PrP), C3 was detectable readily in human sporadic CJD brains. [66]

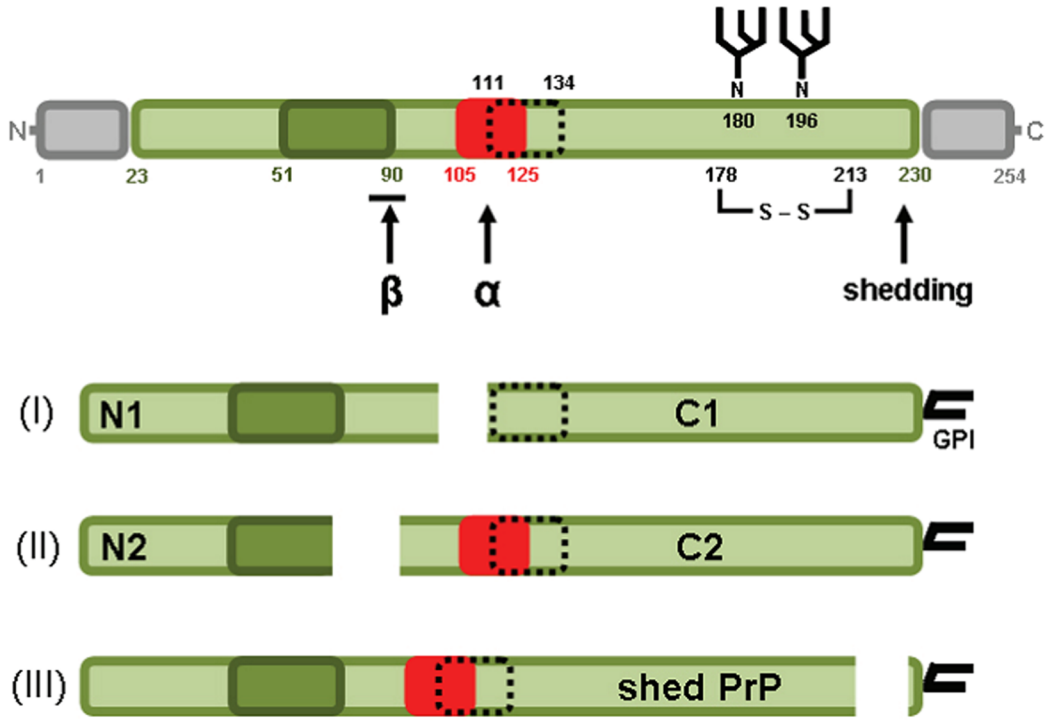

Figure 5 – Sites for proteolytic processing of PrP^C resulting in (I) N1, C1 fragments by α-cleavage gives or (II) N2, C2 by β-cleavage at the end of the OR region or (III) nearly full-length PrP by ectodomain shedding from the membrane close to the GPI-anchor. N-terminal signal sequence (aa 1-22) for directing the premature peptide to the ER and the C-terminal signal sequence for the attachment of the GPI-anchor (aa 231-254) are indicated as grey box; OR region (aa 51-90; dark green); a neurotoxic domain (aa 105-125; red box); a hydrophobic core (aa 111-134; dotted box); a disulfide bridge between aa 178 and 213 and two variably N-glycosylated sites aa 180 and 196 are also illustrated. [57]

2.2.3. Secretion

A secretory form of PrP^C was first evidenced since 1987 in the study with *Xenopus* oocytes and cell-free system [67]. Those experiments demonstrated that PrP was secreted as a soluble monomeric protein, not oligomer. Later, the relevance of this form was confirmed to be present in human cerebrospinal fluid [68]. A substantial amount of soluble PrP^C is also found in the

culture medium of splenocytes, cerebellar granule cells and in murine and human serum [69]. This secretion was suggested to be different from membrane budding [67] and happened after several possible mechanism. For example, ADAM10 could act as a sheddase to proteolyze the C-terminal component of PrP at position 227 (murine numbering) to release it from the GPI component [27]. Full-length PrP could be shed from the cell surface via phospholipase C cleavage of the GPI anchor [70] which mechanism is usually mimicked *in vitro* by usage of bacterial phosphatidylinositol-specific phospholipase C (PI-PLC). PrP^{C} could also be released to the extracellular space after loss of its GPI-anchor by post-translational modifications [71].

PrP secretion and its physiological relevance therefore has been implicated for its role in neuronal processes and spreading of prions. For example, soluble PrP was suggested to act as a neurotrophic factor promoting neurite outgrowth and neuronal survival [24, 72] thanks to different studies mimicking the function by using recombinant PrP [11]. Additionally, soluble PrP Fc fusion was shown to delay PrP^{Sc} accumulation and replication proposing its neuroprotective effect in prion disease [73]. On the other hand, infectious transgenic mice expressing anchorless PrP developed different amyloid pathogenesis with “new strain” of protease-resistant PrP (PrPres) and co-expression of wild-type PrP and GPI-negative PrP accelerates scrapie disease [74].

Secreted forms of PrP^{C} and PrP^{Sc} were both identified in exosomes and microvesicles (MVs) released from different cell cultures as well [20] which may contribute to intercellular spreading of prions. PrP^{C} was found in association with the lipid raft components in MVs from plasma of healthy human donors and culture supernatant of murine neuronal cells. In the same study, scrapie infected cells released PrP^{Sc}-containing MVs that could propagate prions *in vitro* and *in vivo* [75]. Interestingly, exosomal PrP^{C} was proposed to have neuroprotective role by accelerating fibrilization of toxic oligomeric Aβ42 into non-toxic Aβ aggregation [76].

Overall, secretion of PrP molecules may contribute significantly to both physiological and pathological conditions.

2.3. Physiology of prion protein (PrP) in central nervous system (CNS)

2.3.1. PrP and memory

A role of PrP^C in memory retention was early assumed from studies with comparison between wild-type animals to the knockout model. One of the first attempt was published since 1997. The authors found $PrP^{-/-}$ mice showed a significant disturbance in long-term memory retention and could not performed properly in the water-finding test indicating a disturbance in latent learning at nearly 6-month old [77]. The involvement of PrP^C was suggested to be age-dependent. While 3-month-old mice showed no difference between groups, 9-month-old $Prnp^{0/0}$ mice showed a clear impairment of short- and long-term memory retention [78]. In the same study, similar pattern could be observed in rats by infusion with anti-PrP^C antibody indicating the impairments were not a consequence by genetic ablation side effect yet by the loss of PrP^C function. Additional evidence came from the study by Criado R.J. *et. al.* in which PrP knockout mice from both homogenous or mixed background had deficits in hippocampal-dependent spatial learning and reduction in long-term potentiation in the dentate gyrus. Intriguingly, it was possible to rescue those phenotypes by re-expressing neuronal PrP^C [79].

Molecular mechanisms for PrP^C involvement in memory were investigated through interaction between PrP^C and its partner such as laminin (LN) and stress-induced protein 1 (STI1). Interfering interaction of PrP^C and LN by using LN-binding-site PrP^C173-192 peptide or either anti-PrP or anti-LN antibodies could impair memory consolidation probably by inhibiting the activation of hippocampal adenosine 3′,5′-cyclic monophosphate (cAMP) - dependent protein kinase A (PKA) and extracellular regulated kinase (ERK1/2) signaling [80]. In turn, blockage of PrP^C-STI1 interaction with intrahippocampal infusion of PrP^C or STI1 antibodies or PrP^C peptide 106–126 that spans the binding site for STI1 to PrP^C (aa 113-128) [81] inhibited both short and long-term memories for which performance could be enhanced by STI1 peptide 230–245 covering the PrP^C binding site [82].

Important roles of PrP^C in memory and cognition was found in human subjects as well. Polymorphic Val129 codon was associated with worsened cognitive performance in the elderly whereas healthy young adults expressing Met129 exhibit better [14, 83, 84]. Surprisingly, recent study pointed this function of PrP appears to be conserved among animals since zebrafish knocked out of PrP gene (*prp2*) showed an age-dependent memory decline [85]. Overall, compelling evidence support PrP^C as a significant component for memory formation and retention, especially during aging.

2.3.2. PrP and synaptic development

One of the first evidence for the presence of PrP^C at synaptic structure was shown from colocalization of PrP^C with the presynaptic vesicle protein synaptophysin using immunogold electron microscopy technique [86]. Later, Herms J *et. al.* used synaptosomal fractionation methods and immunohistochemical techniques which were claimed as a less destructive way to detect PrP^C expression in different brain tissue and confirmed that location of PrP^C is predominantly on the presynaptic plasma membrane rather than on the synaptic vesicle membrane [87]. In the same study, the authors could not detect PrP^C in the post-synaptic density (PSD) probably since postsynaptic PrP^C could be expressed only in particular type of neurons and at specific type of synapse. Indeed, the immune-reactivity for the protein was found more pronouncedly in Purkinje cell (PC) post-synaptic dendrites than in other type of cerebellar neurons like granular cells [88]. The expression of PrP^C in either pre- or post-synapses supports its potential function in synaptic regulation depending on specific type of synapses and inter-neuronal sites (Table 1).

Table 1 – Distribution of PrP^C-immuno-reactivity in the cerebellar synapses of the mouse and the hamster * [88]

Asymmetric synapses	PRE/POST		Symmetric synapses	PRE/POST	
PF/PC	+	-	PR/PC	+	-
	-	+		-	+
PF/IN	+	-	SC/PC	-	+
	-	-/+			
CF/PC	+	-	BC/PC	-	-/+
	-	+			
CF/GD	+	-	GO/GD	-	-
MF/GD	+	-			

* Presynaptic (PRE) or postsynaptic (POST) immuno-reactivity (+) is observed in the asymmetric and the symmetric synapses in the cerebellar cortex. (-/+) indicates occasional labeling. BC: basket cells, CF: climbing fiber, GD: granule cell dendrite, GO: Golgi neuron, IN: interneuron of the molecular layer, MF: mossy fiber, PC: Purkinje cell, PF: parallel fiber, PR: recurrent axon of Purkinje cell, SC: stellate cells.

PrP^C was found to localize on the surface of elongating axons and its retrograde transport is increased during axon regeneration [89-91]. Developmental expression of the protein in elongated axon in olfactory and hippocampal neurons is increased significantly after birth and maintained at high level in adult [89]. This evidence strongly suggest for PrP role in axonal growth, synaptogenesis and synaptic plasticity. It has been shown, furthermore, PrP^C regulates synaptic plasticity or long-term potentiation (LTP) through postsynaptic cAMP-dependent PKA signaling in developing hippocampus [92].

PrP^C expression at synapse was also linked with copper concentration since the latter was found being reduced by half in synaptosomes collected from *Prnp*$^{0/0}$ mice and could be rescued in *Prnp*-reconstituted *Prnp*$^{0/0}$ mice (tg20) [87]. This suggested for PrP function in synaptic copper homeostasis thanks to its copper-binding ability which will be discussed later in this thesis.

2.3.3. PrP and neuroprotection

The function of cellular prion protein in neuroprotection was early proposed from the observations in PrP null mice that showed to be more vulnerable to oxidative stress and apoptosis than the wild-type [93-95]. Deletion of PrP^C *in vivo* caused impairment in anti-apoptotic PI3K/Akt signaling and elevation of apoptotic caspase-3 activation in ischemic brain injury [94]. Markers for protein oxidation and lipid peroxidation were also found higher in brain lysate of Prnp$^{-/-}$ mice [96]. Furthermore, these mice in model of experimental autoimmune disease exhibited stronger proinflammatory cytokine gene expression such as IFN-γ and IL-17 accompanied with loss of spinal cord myelin basic protein and axons suggesting protective role of PrP in neuroinflammation [95].

Different studies had linked PrP^C and modulation of N-Methyl-D-aspartate receptors (NMDAR) as a neuroprotective mechanism. Taking advantage again of PrP-null mice, Khosravani *et. al.* explored that hippocampal slices prepared from these mice exhibited more neuronal excitability associated NMDAR activity which eventually mediated neuronal cell death; and overexpression of *Prnp* gene could rescue this phenotype. The study also pointed out PrP^C negatively modulates NMDAR by direct inhibition of its NR2D subunit [97]. Thereafter, this interaction of cellular prion protein and NMDAR was proven to be copper-dependent which copper binding to PrP^C reduced affinity of co-agonist glycine to the receptor [98, 99]. A detailed mechanism of the signaling complex between PrP^C, copper and NMDAR was already elucidated in the study by

Gasperini L *et.al.* The explanation is as following and summarized in Figure 6 adapted from the paper. PrP^C may bind copper usually released at the synapses. Then PrP^C-bound Cu^{2+} can oxidize NO to NO^+ and be reduced to Cu^+. NO^+ can react with extracellular cysteines thiols of NMDAR subunits resulting in the S-nitrosylation of the receptor which is inhibitory and helps protect neuron from excitotoxicity [16].

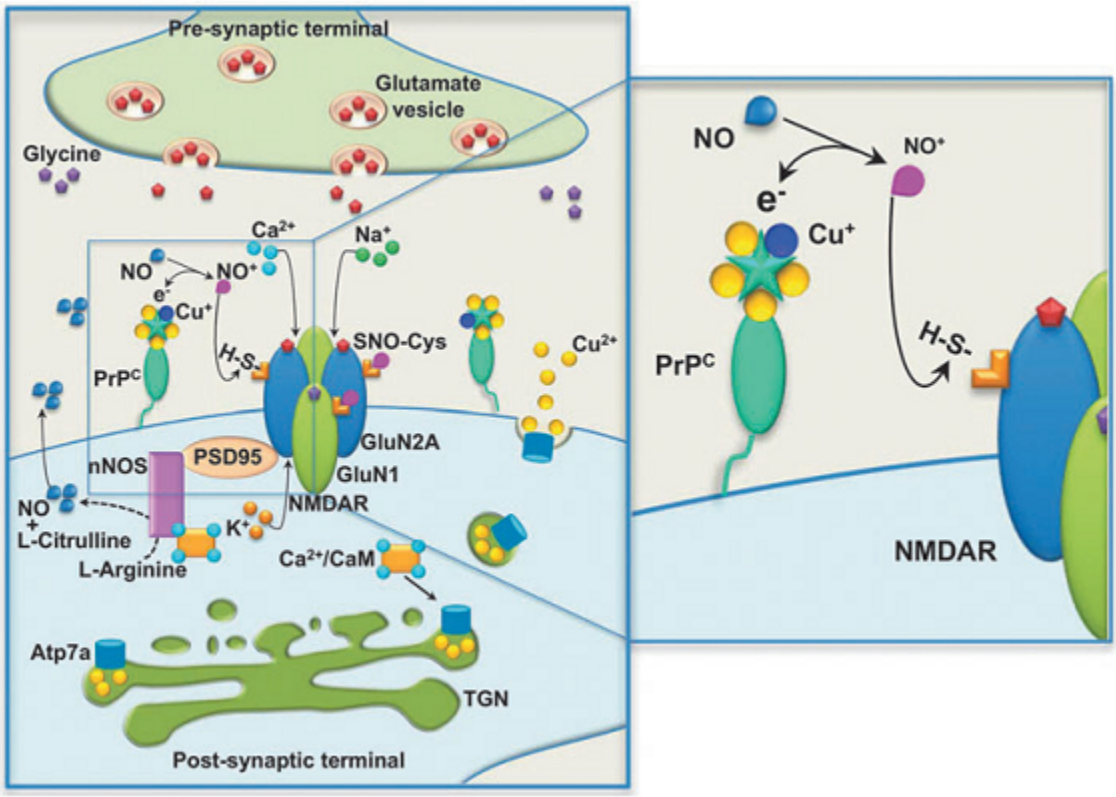

Figure 6 - Mechanism of PrP^C-mediated S-nitrosylation of NMDAR. According to this model, binding of copper ion to PrP^C facilitates the reaction of NO with thiols group on GluN1 and GluN2A subunits leading to the S-nitrosylation, thus inhibiting NMDAR channel. Copper and NO ions could be released from the post-synaptic terminal after NMDAR activation by glutamate released from the pre-synaptic cell. [16]

Intriguingly, soluble alpha-cleaved N1 fragment of PrP displayed neuroprotective function both *in vitro* and *in vivo* as well. It protects HEK293 cells, mouse cortical neurons and rat retinal ganglion cells from staurosporine-induced apoptotic caspase-3 activation and oxidative glucose deprivation respectively; reduces pressure-induced ischemia cell death in the rat retina by down-regulating p53 activity [61]. N1 can also bind early oligomeric intermediates during Aβ

fibrillization and strongly suppress Aβ oligomer toxicity in cultured hippocampal neurons and in a mouse model of Aβ-induced memory dysfunction [100].

2.3.4. PrP and neurogenesis

In 2006, Steele AD *et. al.* published strong *in vitro* and *in vivo* proofs for involvement of PrP^C in neurogenesis. Firstly, they found PrP^C expression was strongly high in the neurogenic region adjacent to proliferative subventricular zone (SVZ) and increased during neuronal development and differentiation. Secondly, PrP^C level positively correlates with neuronal differentiation from multipotent neural precursors *in vitro* and increases cell proliferation *in vivo* in SVZ and dentate gyrus (DG) where neurogenesis actively happens during development and adult stage. Although the study could not detect a direct increase in overall neurogenesis in these regions by PrP^C level, its important role in this process of mammalian CNS is unneglectable. [101]

It was then shown that the ablation of PrP^C reduced the number of neurospheres inferring the protein role in neurosphere formation, in other words, self-renewal capacity of neural progenitor/stem cells. Moreover, the augmentation in proliferation of these cells by PrP^C was proven to be dependent on its interaction with STI1 [102]. PrP^C – STI1 interaction was also discussed in memory formation in previous section. The involvement of PrP^C in both processes may represent additional evidence to support the relationship between adult neurogenesis and new memory formation [103].

Overexpression of PrP could enhance neurogenesis in the ischemic mouse model after 28 days post-stroke [104]. Although the authors also observed higher neurogenesis in the knockout brain slices comparing to the wt ones, this consequence exacerbated the brain injury whereas more neurons developed in $PrP^{+/+}$ mice accompanied with reduced proteasome activity leading to neurological recovery.

Intriguingly, prions – pathologic state of the PrP^C was found to accumulate and able to replicate in the neural stem cells (NSC) in ME7 prion-infected mice that eventually impaired the neuronal differentiation and might speed up the disease progression [105]. Adult neurogenesis can be helpful for regeneration of the central nervous system neurodegenerative disorders. Hence, the impairment of this process by prions could partly explain the pathology of the disease and

strongly imply the role of PrP^C in regulation of neural differentiation from endogenous neural progenitors.

2.3.5. PrP and neuritogenesis

The normal prion protein has been considered as a neurotrophic factor that promotes neuritogenesis through its *cis* or *trans* cell-cell interaction by either native GPI-anchor form or soluble secreted form [11]. Many interacting partners of PrP^C have been found involving this process for which interactions are important in memory consolidation and neuroprotection as well (Figure 7).

One of the first PrP^C cis interactor discovered was human 37-kDa laminin receptor precursor (LRP), also accepted as 37-kDa/ 67-kDa laminin receptor (LRP-LR) [106]. LRP-LR via its laminin binding domain aa 161-179 directly interact with C-terminal domain of PrP (aa 144-179) and indirectly interact with PrP octarepeat region mediated by heparan sulfate binding [107]. The binding of recombinant PrP to this receptor could lead to internalization of PrP as well [108]. Captivatingly, PrP^C showed high-affinity to the extracellular matrix (ECM) protein laminin (LN) and this interaction happening at γ-1 chain on laminin and probably 170-183 residues on PrP^C was involved in the neuritogenesis induced by nerve-growth factor (NGF) and LN in PC-12 cells [109]. PrP^C was also found co-localized and interacted with vibronectin (Vn), another ECM protein, via PrP^C domain 105-119 and Vn domain 307-320 to mediate axonal growth in embryonic dorsal root ganglia [110]. Altogether, PrP^C may form signaling complex with laminin receptor and ECM proteins at lipid raft and promote neurotrophic effects.

The interaction of PrP^C and the soluble ligand STI1 in *trans* resulted in memory formation and maintenance (discussed above) might propose for potential function in neuritogenesis at the cellular level. Binding of STI1 to PrP^C induced entocytosis of the prion protein via clathrin-coated vesicles triggering ERK1/2 activation that is essential pathway for neuritogenesis [111, 112]. These two proteins were found secreted by astrocytes resulting in stimulated neuronal survival and differentiation that support for importance of astrocyte-neuron cross talk in neuronal networking [72].

Lastly, an alternative pathway for PrP to promote neuritogenesis is via transmembrane receptor NCAM (neural cell adhesion molecule). It was found long ago from the *in situ* crosslinking study

about the direct interaction between the two proteins either in *cis* or in *trans* and the binding interfaces were between fibronectin III (FNIII) domain of NCAM and N-terminus plus helix A or helix 1 (residues 144-154) and the adjacent loop region of PrP [113]. Interaction of FNIII1,2 and human PrP (HuPrP) was then confirmed in the study with surface plasmon resonance (SPR) and nuclear magnetic resonance (NMR) technique that the affinity of binding was strong (K_d of 337 nM) and appeared to be stronger in case of HuPrP peptide with P102L mutation [114]. The study also revealed residues Tyr669, Val673, His686, Phe687, and Val688 of the FNIII2 domain constitute critical binding site to the PrP N-terminal peptide (23-144) [114]. However, the functional residues on PrP could not be detailed probably due to disordered N-terminal tail limiting the complete NMR structure of PrP. In hippocampal neurons, both cellular and soluble prion protein could recruit to and stabilize NCAM in lipid draft and activate Fyn kinase signaling to enhance neurite outgrowth [26]. In addition, PrP could act through different receptor to activate cAMP-PKA signal transduction for increasing significantly neurite growth [24].

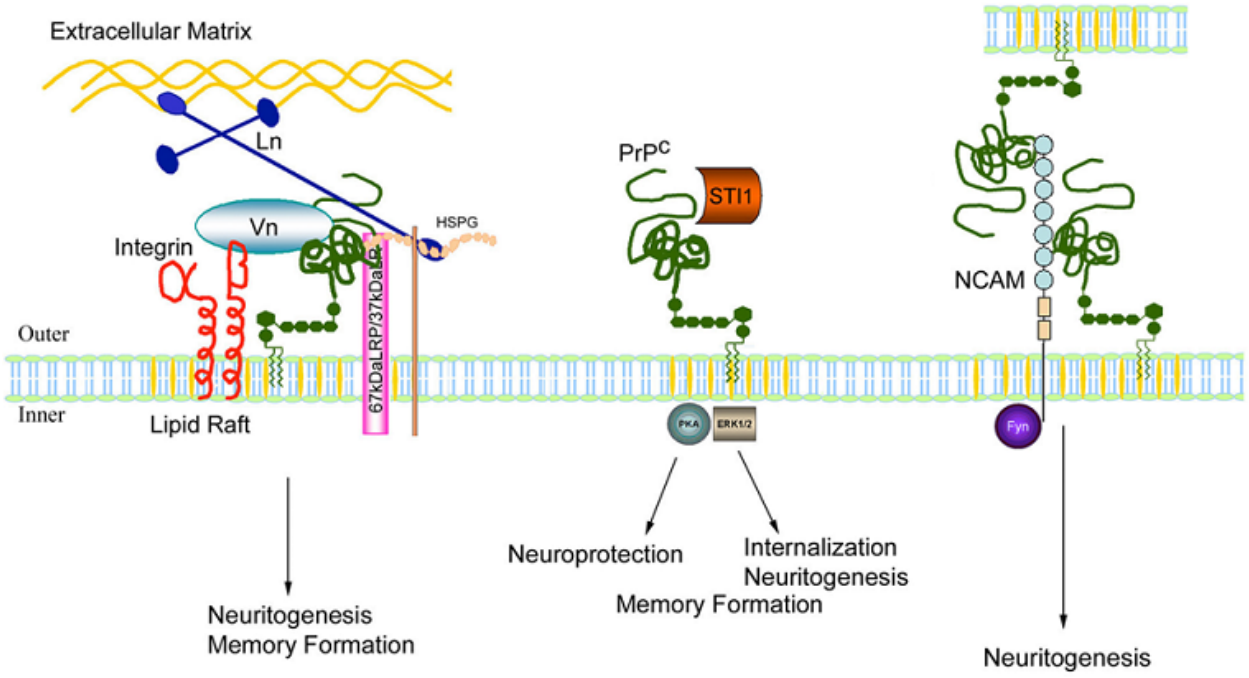

Figure 7 – Interacting partners of PrP^C (green) involving neuritogenesis and other processes. The first signaling complex would consist of PrP^C and ECM proteins such as Laminin (Ln) and Vitronectin (Vn), laminin receptor (37LRP/67LR) and integrins (red) as ECM receptors. The second possible pathway could be mediated by PrP^C-STI1 interaction. Lastly,

PrP^C might interact with neural cell adhesion molecule (NCAM) either in cis or in trans, and promotes neuritogenesis through the activation of Fyn kinase. Adapted from [11]

2.4. Role of copper in CNS

Copper ions play essential roles in many biological processes and are found highly rich in mammalian brain [115]. In human, copper content together with zinc was found higher in inner molecular and granular layers of the dentate gyrus of hippocampus than in insular and central region [116]. Intracellular level of Cu is usually higher than in extracellular concentrations which vary from 0.5-2.5 μM in cerebrospinal fluid (CSF) to 10-25 μM in blood serum and up to 30 μM at the synaptic cleft [117]. The entries of Cu ions into the brain are effectuated via CTR1 (copper-transporter 1) and ATP7A [118]. Cellular uptake of copper requires reduction of Cu^{2+} to Cu^{+} that is transported by Ctr1 and this protein remains intracellularly till the need of more Cu [117]. ATP7A facilitates copper transport from the blood brain barrier (BBB) to the brain parenchyma [119]. In fact, P-Type ATPases including ATP7A and ATP7B are main copper transporter in and out the cells and mutations on these proteins caused Menkes and Wilson diseases [117, 119].

Due to its redox ability of changing between oxidized state (Cu^{2+}) and reduced state (Cu^{+}), copper is able to bind a wide range of proteins as a catalytic or structural cofactor [120]. It is widely known that copper serves as a catalytic cofactor for cuproenzymes such as cytochrome c oxidase, superoxide dismutase, dopamine β-hydroxylase and peptidylglycine α-amidating monooxygenase required for processes critical to neuronal function including mitochondrial respiration, antioxidant activity, catecholamine production and hormonal processing respectively [121]. Other non-enzymatic proteins bind copper involving in neuronal signaling, especially at synapses [118] (Figure 8) which could explain why copper is abundant at synaptic vesicles [122]. Cu^{2+} inhibited AMPA and NMDA receptors with IC_{50} of 4.3 and 15 μM respectively in primary rat cortical neurons [118, 123]. While blockade of AMPA receptor by copper is based on an oxidative mechanism [123], inhibitory effect of NMDAR is due to S-nitrosylation mediated by the binding of copper to PrP^C [16]. Competing with zinc ion, Cu(II) also inhibit $GABA_A$ receptor on channel gating by binding distinctly from GABA binding site [118]. Residues V134, R135, and H141 in a VRAECPMH motif of α1 subtype of the receptor compose the main binding pocket for Cu(II) and the H141 residue was the major determinant [124].

Interestingly, the extracellular domain of APP which cleaves Aβ peptides implicated in Alzheimer's disease binds Cu^{2+} with attomolar affinity at the binding site on amyloid beta 1-42 [125]. Cu^{2+}-glycine (1 µM) promotes Aβ production and potentiates Aβ-mediated neuronal toxicity [126]. Lastly, Cu ions bind cellular PrP which is expressed pre- and post-synaptically with high nM to low µM affinity [52]. Notely, Aβ may compete with PrP in Cu binding that prevents it from inactivation of NMDAR and leads to neurotoxicity – a potential mechanism for synaptic loss and neuronal death in AD [127]. Role of Cu-PrP^C interaction in neuronal processes and prion pathology will be discussed further in the next part.

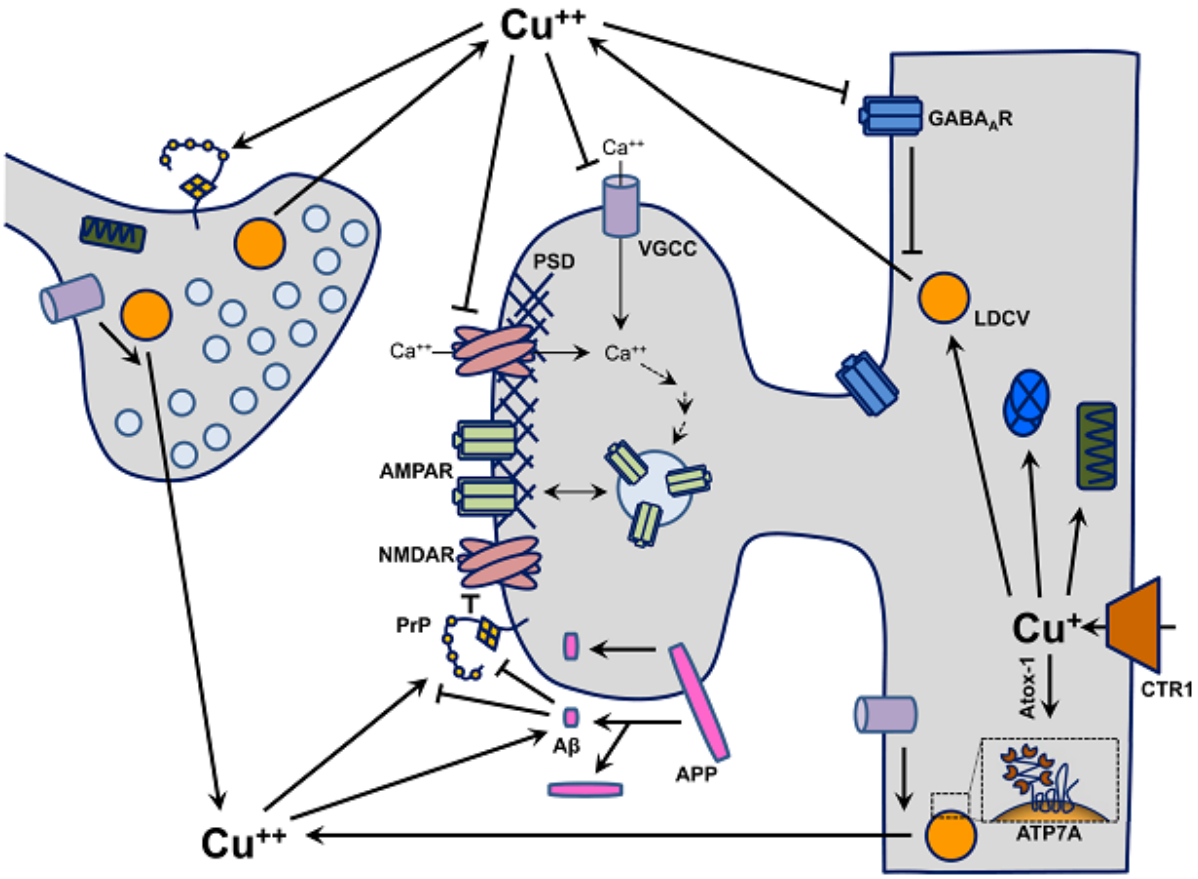

Figure 8 – Role of Cu in synaptic function. Cu enters cells through CTR1 and is delivered to ATP7A by Atox-1 chaperone. Cu^{2+} could be delivered to secretory pathway via ATP7A and is stored in LDCVs (large, dense-core vesicles) prior to secretion or to mitochondria (green rectangular) and cuproenzymes (blue round) for ATP production and antioxidative activity respectively. Influx of Ca^{2+} through NMDARs and VGCCs (voltage-gated Ca^{2+} channel) results in LDCV release and Cu secretion. Extracellularly, Cu has inhibitory effects on NMDARs, VGCCs and $GABA_A$Rs. Cu binds PrP and APP, which are located at synapses. Binding of Cu to

APP facilitates extracellular Aβ yield which also binds Cu with high affinity. Adapted from [118]

Under physiological condition, copper concentration needs to be strictly regulated. While copper deficiency or genetic mutation of copper-transporting proteins could lead to developmental defects [115, 120, 121], excess copper load would increase toxic-free radicals and cause oxidative damage within the cell [121, 128]. Hence, there are several neurodegenerative diseases involved perturbation of copper homeostasis such as Menkes disease, Wilson disease, amyotrophic lateral sclerosis (ALS), Alzheimer's disease and prion disease [129].

2.5. Role of copper in PrP physiology

2.5.1. Copper binding sites on PrP

Metal-binding sites on human prion protein (HuPrP) were characterized since 2001. There are two high-affinity binding sites for divalent transition metals lying on N-terminal octarepeat region (aa 60-91) (OR) and the adjacent non-OR region around His96 and His111 [52] (Figure 8). Affinity of PrP^C for copper is higher than zinc and other metals (Ni^{2+}, Mn^{2+}) [52, 130]. N-terminus of PrP can coordinate up to six Cu ions while there may be other potential site with histidine residues at the C-terminus (Figure 9) [51].

OR domain composes of four or five tandem repeats of conserved eight-residue sequence PHGGGWGQ that at full occupancy, each OR His can coordinate to single Cu ion [53]. This region has the K_d for Cu(II) of 10^{-14} M at pH 7.4 [52]. An electron pramagnetic resonance (EPR) spectroscopic study revealed three distinct binding modes of Cu into OR segments of PrP at pH 7.4 which are component 1 at high Cu^{2+} concentration, component 2 at intermediate Cu^{2+} occupancy and component 3 at low Cu^{2+} load [53] (Figure 4). In component 1 at pH above 7, coordination pocket consists of octarepeat subsegment HGGGW and involves the nitrogen Nδ1 of the His imidazole and deprotonated amide nitrogens from the following two Gly residues [53, 131]. Each octapeptide tandem binds Cu^{2+} through a 1:1 ratio and so the coordination stoichiometry composes of four Cu ions and four bridging imidazolate ions [132]. In component 2, two His residues in sequential repeat segments are required to stabilize the structure or in other words, one copper is coordinated by both the His imidazole and its exocyclic nitrogen [53]. Multi-OR binding mode or component 3 appears in an environment of low copper load meaning

that three or four neutral imidazoles involve [53]. Similar multiple imidazole binding mode was also observed at mild acidic pH 5.5 [133].

Non-OR copper binding site, also known as "fifth site" starts after residue 90 and extend prior to the hydrophobic domain. Copper coordination was involved His96 and/or His111 (H95 & H110 in mouse) with affinity of almost four folds to that in OR; this strong binding was observed in oxidized α-helical PrP and almost similar in reduced β-sheet conformation [52]. This non-OR domain of PrP has the most relevance to disease since it corresponds to the protease resistance core and contains pathogenic mutations such as P102L and P105L in Gerstmann–Sträussler–Scheinker (GSS) prion disease [51]. Moreover, alteration in copper coordination in this region particularly at acidic pH 5.5 was suggested as a key switch of prion conversion [134]. Interestingly, in a competitive environment with both Zn^{2+} and Cu^{2+}, preference binding of Zn ions to the OR regions can shift copper to non-octarepeat binding sites [130]. Non-OR region with the sequence GGGTH coordinates Cu in a distinct fashion from the octarepeat HGGGW motif in which Cu^{2+} is directed toward the C-terminal side of histidine whereas the ion interacts with backbone amides on the N-terminal side of His96 in case of non-OR site [135]. Notely, the presence of H96 seemed to increase the Cu-binding affinity at the entire OR segment since the peptide containing this residue had higher affinity to copper than the OR peptide alone [136, 137] indicating that the possible preference as primary binding site for copper at histidine residues of non-OR facilitates the sequential coordination at the OR [137].

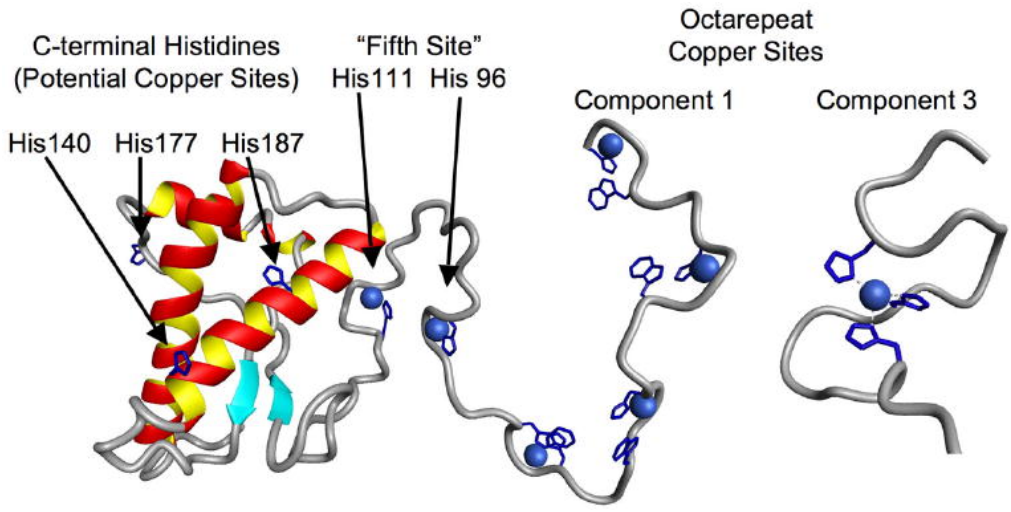

Figure 9 – Copper-binding sites on the prion protein (human numbering). Two copper (blue round) coordinated components at octarepeat region are presented (component 1 at high copper

load and component 3 at low copper concentration). The PrP protein may coordinate up to six coppers with involvement of the fifth site consisting of His96 and His111. Other potential histidine residues for copper binding are suggested at the C-terminus as well. Adapted from [51].

2.5.2. Effects of copper binding to PrP functions

Binding of metal ions, especially copper can affect biochemical and biological characteristics of the prion protein.

Principally, one of the first PrP function suggested is metal homeostasis. PrP may help buffer copper concentration, especially at synapses [138] and cerebrospinal fluid [139]. Free Cu^{2+} is highly cytotoxic, since redox reactions of Cu^{2+} generate reactive oxygen species (ROS) [140]. At synapses, the copper concentration may exceed 10 μM due to significant copper efflux during neuronal activity [139]. Hence, the copper-buffering activity of PrP^{C} at synaptic cleft can provide part of neuroprotective mechanism together with inhibiting NMDAR excitotoxicity as mentioned. Of note, deletion of the octapeptide repeats found to abolish the ability of PrP to protect cortical neurons from Bax (Bcl-2-associated protein x)-mediated apoptosis strongly implies for the role of copper in neuroprotection by PrP [141].

Whilst unbound N-terminus of PrP is unstructured, copper binding to the OR and adjacent region at different pH and copper concentration leads to various conformations of the tail (as discussed above) which may have certain functionality. This could suggest PrP as a copper-sensor. Copper concentration of more than 100 μM stimulate PrP endocytosis which could be triggered by the transition between component 3 and 1 with component 2 as intermediate [139]. Indeed, both copper and zinc could stimulate the translocation and endocytosis of surface PrP^{C} into transferrin-containing early endosomes and Golgi compartments [142, 143]. PrP endocytosis, thus, may transport Cu from the extracellular space to the cell interior. In turn, lowered pH in the endosomal compartment may facilitate the release of PrP-bound coppers and recycle of the ions [144]. Therefore it is suggested that PrP^{C} may function as recycling receptor for the cellular uptake and efflux of ions [142]. At high copper load, PrP with component 1 conformation may exhibit its antioxidant activity by sequestering free copper ions [139]. Then the presence of PrP in the endosome can reduce Cu(II) to Cu(I) and facilitate the copper trafficking by other copper chaperones [145].

Additionally, binding of copper to OR region was shown to suppress beta-cleavage in the absence of a reducing agent. Of note, copper coordination at His110 suppresses α_1-cleavage by ADAM8 [146]. Since β-cleavage provided N2, C2 fragments found extensively in prion-infected samples whereas α-cleavage has mostly neuroprotective role [57], binding of Cu at different position on PrP facilitates production of variously functional fragments that may explain for controversial role of copper in prion disease.

In prion pathology, interaction of copper with PrP^{Sc} may not be beneficial since it can restore the PK resistance and infectivity of scrapie after inactivation by GdnHCl (guadinine chloride) [147]. Conformations of PrP^{Sc} also depend on metal-ion occupancy (copper and zinc) indicating the role in prion strain determination [148]. Intriguingly, high concentration of copper (~200μM) *in vitro* could turn PrP^{C} into detergent insoluble and protease resistant form but not PrP^{Sc} and the effect requires the presence of a single octapeptide repeat [149]. *In vivo* study with copper chelator D-PEN suggested a delay in the onset of prion disease in mice for 11 days; yet copper levels might be only one of many factors influencing the progression rate of prion disease [150]. Conversely, Cu ions inhibited conversion of full-length recombinant PrP (recPrP 23-230) into amyloid fibrils at pH 7.2 although they have opposite effect to enhance aggregation of preformed amyloid fibril [151]. This may indicate copper has different effects on the soluble form of PrP and membranous PrP^{C}.

Copper binding into OR or non-OR region may have distinct importance to the development of prion disease. It was shown that in PrP-KO mice overexpression of truncated PrP retaining only one of the five ORs, still restored the susceptibility of these mice to scrapie and development of disease [152]. Further study confirms for the unimportance of OR copper-binding site in prion propagation since PrP devoid of this whole region could sustain scrapie infection in the knockout mice even though they appeared to have longer incubation times and 30 fold lower prion titers than the wild-type [153]. These mice showed no typical histo-pathological changes but neuronal loss and astrogliosis in the cervical spinal cord. In contrast, expansions of OR tandems correlates with earlier Creutzfeld-Jakob disease (CJD) onset [154]. Particularly, eight total repeats exhibit a conformation with two equivalents of component 3 coordinations and have approximate 10-fold Cu^{2+} binding affinity [155]. Very interestingly, copper binding in the non-octarepeat sequence GGGTH can protect against PrP^{C}-to-PrP^{Sc} conversion [156]. Recent study has directly proposed

the key role of non-OR region in prion conversion which is in agreement with the implications from previous findings related to OR deletion [134]. Altogether, it is very likely that there is a strong relationship between copper binding properties and prion pathology. Although role of the OR domain in prion disease is enigmatic, significance of non-OR copper binding site has been increasingly recognized.

2.6. Loss-of-function hypothesis in prion pathology

It is widely discussed that the converted prion species (PrP^{Sc}) may have toxic gain-of-function in prion disease since amyloid fibrils or oligomeric aggregates have been proven to be very harmful for neurons [157, 158]. PrP^{C}, however, involves in various neuronal processes suggesting that it is very likely the loss-of-function of the protein may be one of initiation factor of the disease and/or the consequences obtained after being converted. In addition, mice lacked the protein showed different abnormalities and were prone to neurodegeneration, especially in stress conditions [159, 160]. Hence, prion toxicity may be caused by perverting the normal function of PrP and in return the loss-of-function of the protein can exacerbate the pathology caused by toxic gain of function of the converted one [12].

Notely, the PrP knock-out mice are widely known to resist to develop prion disease making them debatable model for loss-of-function hypothesis in prion disease. Mice expressing structurally artificial or pathogenic mutations, instead, may give good insights for the possibility of incorporation between structural change and functional loss in the pathology [161]. In fact, some of these mutant PrP showed alterations in thermodynamic stability and biochemical properties favoring misfolding and formation of PrP^{Sc}-like structure [134, 162]. Mutated PrPs, for example, octapeptide insertional mutation or GSS-linked mutations, also exhibited impairments in PrP functions such as cytoprotective activity [12] and neurite outgrowth [163] that would largely potentiate neurodegeneration in the disease context.

Furthermore, loss-of-function mechanism was as well suggested in other neurodegenerative disorders such as Parkinson's and Huntington's diseases in which huntingtin (Htt) and α-synuclein, like PrP, possess neuroprotective roles [164].

Chapter 3 – MATERIALS AND METHODS

3.1. Plasmid constructions

The sequence encoding for the mature mouse prion protein (MoPrP) from residue 23 to 231 was amplified by PCR from pcDNA3.1::MoPrP(1-254) and cloned into pET-11a by restriction-free (RF) method [165]. Then the plasmids containing truncated mouse PrP(23-120) were cloned from the full-length protein sequence. Plasmid with truncated mouse PrP(89-231) sequence was available in the lab. The peptide corresponding to the truncated mouse PrP(23-90), N-terminal acetylated and C-terminal amidated, was chemically synthesized (Chematek Inc, Milano, Italy). Sho protein was a gift from Prof. David Westaway (University of Alberta; Edmonton, AB, Canada).

For neuronal transfection, the open reading frame (ORF) encoding for the pre-pro MoPrP(1-254) was amplified by PCR from genomic murine DNA and cloned in pcDNA3.1(-) vector (Invitrogen). To generate the construct of GFP-PrP targeted to the membrane, the sequence coding for GFP from the plasmid pEGFP-N1 (Clontech) was amplified and inserted downstream of N-terminal PrP signal peptide sequence (1-23) by RF cloning method. The plasmid pcDNA-GFP-PrP was verified by DNA sequencing, isolated and purified by Maxiprep kits (Qiagen) prior to transfection.

The single point mutations (H60Y, H68Y, H76Y, H84Y, H95Y, H110Y and P101L) were introduced step-by-step into pET-11a::MoPrP(23-231) using the Quick Change site-directed mutagenesis kit (Stratagene). These plasmids were then used to produce recombinant mutant prion proteins at the N-terminal copper-binding sites denoted as recMoPrP(H1234Y) with octarepeat H-to-Y mutations, recMoPrP(H56Y) with non-OR mutations and recMoPrP(H123456Y) with all 6 histidine residues mutated or recMoPrP(P101L).

The primers used for constructing the necessary plasmids are summarized in table 2.

Table 2 – List of primers used for constructing plasmids containing different mouse prion protein sequences

Primer - forward	Primer - Reverse	Usage	Template

ctttaagaaggagatatacatatgaaaaaacgcccgaaaccggg	ggctttgttagcagccggatcctattagctggatcttctcccgtcgtaat	To amplify MoPrP23-231 DNA sequence	* pcDNA-MoPrP(1-254) → pET-MoPrP(23-231) * pcDNA-MoPrP(1-254, H1234Y) → pET-MoPrP(23-231, H1234Y) * pcDNA-MoPrP(1-254, H56Y) → pET-MoPrP(23-231, H56Y) * pcDNA-MoPrP(1-254, H123456Y) → pET-MoPrP(23-231, H123456Y)
agctggggcagtagtgtaataggatccggctg	cagccggatcctattacactactgcccagct	To remove 121-231 region	pET-MoPrP(23-231) → pET-MoPrP(23-120)
ggactgatgtcggcctctgcaaaaagcggatggtgagcaagggcgaggagctgttcacc	gttccaccctccaggctttggccgctttttcttgtacagctcgtccatgccgag	To amplify GFP ORF from pEGFP	* pEGFP → megaprimer * megaprimer + pcDNA-MoPrP(1-254) → pcDNA-GFP-PrP
ggttggtttttggtttgctgagcttgttccactgattatg	cataatcagtggaacaagctcagcaaaccaaaaaccaacc	To substitute P by L at aa101	pET-MoPrP(23-231)
cagccctacggtggtggctgggacaa	ttgtccccagccaccaccgtagggctg	To substitute H by Y at aa60	
ggggacaaccctatggggg cagctgg	ccagctgccccccatagggttgtcccc	To substitute H by Y at aa68	
agctggggacaaccttatggtggtagttggg	cccaactaccaccataaggttgtcccagct	To substitute H by Y at aa76	

tggggtcagccctatggcgg tggatgg	ccatccaccgccatagggctgac ccca	To substitute H by Y at aa84	
caaggaggggtacctataa tcagtggaacaagc	gcttgttccactgattataggtaccc cctccttg	To substitute H by Y at aa95	
aaaaaccaacctcaagtatgt ggcaggggctgc	gcagcccctgccacatacttgagg ttggttttt	To substitute H by Y at aa110	

3.2. Recombinant protein production

Generally the protocol for protein expression and purification was referred to [166] with some modifications. The pET-11a plasmids containing sequences for recombinant proteins were expressed in Rosetta-GAMI *E.Coli* cells by 0.8mM IPTG overnight (~16 hours) induction. Inclusion bodies containing the proteins were isolated after cell homogenization by Homogenizer Panda Plus 2000 (Gea Niro Soavi) at around 1500 bar and following centrifugation at 13'000 g for 30 min, 4ºC. They were washed in 25 mM Tris-HCl pH 8.8, 5 mM EDTA pH 8, 0.8% Triton X100 and two times in bi-distilled water. Then they were solubilized in 6M GdnHCl and 25 mM Tris base pH 8, shake overnight and the supernatant was collected for further purification. In case of MoPrP(23-120), the protein is soluble and found in cell extract instead of inclusion bodies. Thereafter the protein is purified from the supernatant phase after cell homogenization. The samples with wild-type MoPrP(23-231), truncated MoPrP(23-120), MoPrP(H56Y) and MoPrP(P101L) proteins were purified using 5mL HisTrap column chromatography (GE Healthcare) whereas MorecPrP(89-231), MoPrP(H1234Y) and MoPrP(H123456Y) were purified using size-exclusion chromatography (column HiLoad 26/60 Superdex 200pg, GE Healthcare) because of lacking the histidine residues. All the purified protein samples were *in vitro* refolded by dialysis against refolding buffer (20 mM sodium acetate, 0.005% NaN3, pH 5.5) using a Spectrapor-membrane (MWCO 3500) and exchanged to PBS pH7.4 buffer prior to treatments in cell cultures.

3.3. Circular Dichroic (CD) measurement

Purified and refolded proteins were dialyzed in phosphate buffer pH7.2 and diluted at concentration ~ 0.1mg/mL for CD measurement by spectrophotometer JASCO J- 810. Measurements were carried out at room temperature using 0.1cm optical path length quartz cell. Spectra were obtained in the 190 to 260 nm far-UV region and accumulated at least 3 times. Samples subjected for CD measurement were unexposed, UV or UV+IR exposed full-length recPrP and mutant PrP proteins at copper-binding sites. CD data were reconstructed by CDSSTR program with reference data set 7 (Sreerama and Woody 2000), NRMSD < 0.05 on DichroWeb server (http://dichroweb.cryst.bbk.ac.uk/).

3.4. Neuronal culture and transfection

P1-P2 FVB wild-type (wt) and PrP-deficient (*Prnp*$^{0/0}$) mice were sacrificed by decapitation in accordance with the guidelines of the Italian Animal Welfare Act. After decapitation, hippocampi were dissected, cut into slices and washed twice with the dissection medium. The enzymatic dissociation was performed treating the slices with 5 mg/ml trypsin (Sigma-Aldrich, St. Louis, MO) and 0.75 mg/ml DNase I (Sigma-Aldrich, St. Louis, MO) in digestion medium (5 min, 37ºC). Then, trypsin was neutralized by 1 mg/ml trypsin inhibitor (Sigma-Aldrich, St. Louis, MO) in the dissection medium for 10 minutes at 4ºC. After the wash in the dissection medium, mechanical dissociation was performed in the dissection medium with 0.6 mg/ml DNase I by approximately 50 passages through a Gilson P1000 tip. The cell suspension was then centrifuged at 800 rpm for 5 min, and the pellet re-suspended in the culture medium. Finally, hippocampal neurons were plated on 50 µg/ml poly-L-ornithine (Sigma- Aldrich, St. Louis, MO) coated coverslips. The hippocampal neuronal culture was incubated (5% CO2, 37°C) in the minimum essential medium with Earle's salts and Glutamax I with 10% FBS, 2.5 µg/ml gentamycin (all from Invitrogen, Life Technologies, Gaithersburg, MD, USA), 6 mg/ml D-glucose, 3.6 mg/ml Hepes, 0.1 mg/ml apo-transferrin, 30 µg/ml insulin, 0.1 µg/ml biotin, 1.5 µg/ml vitamin B12 (all from SigmaAldrich, St. Louis, MO). To find isolated neuronal growth cone (GC) we performed local delivery experiments 24- 48 h after plating the neurons. PrP KO neuronal culture could be transfected with pcDNA-EGFP-PrP using Lipofectamine 3000 for primary cells (Life Technologies, Grand Island, NY) according to the manufacturer's instructions.

In experiments with treatments of PrP mutants, dissociated neurons were cultured in B27 supplemented neurobasal medium (Thermo Fisher Scientific) with around 2 x 10^4 cells per coverslip after filtration through 40µm cell strainer (Corning). About 22 hours post-plating, the cells were treated in bulk with 2µM of the recombinant proteins or PBS control for further neurite outgrowth assay by immunofluorescence.

3.5. Liposome preparation and local stimulation

The following composition of lipid mixture was used for liposomal vesicle preparation: Cholesterol: 9 µmol, L-α-Phosphatidylcholine: 63 µmol, Stearylamine: 18 µmol (Sigma-Aldrich). The lipid solution was prepared at the concentration of 10 mg/mL in chloroform: methanol (2:1v/v). The solution obtained was then saturated with nitrogen and stored at -20 °C. Vesicles with a diameter of 1 –5 µm were obtained by using the lipid film rehydration method [21, 167]. In this method the lipid solution was dried in vacuum condition for 24 h and then the lipid film was rehydrated with solution containing the desired concentration of recPrP. Sucrose 100 mM was also included in the hydration solution to allow better vesicle washing and to improve vesicle trapping. After overnight incubation, vesicles were gently centrifuged (5,000 rpm for 3 min) and rinsed 3 times with PBS to wash the external solution. Final vesicles solution was then administered to the cell cultures. Single vesicles were subsequently identified, trapped and positioned at the location of interest. The behavior of the stimulated growth cone was recorded and analyzed by Matlab software.

The optical manipulation setup was developed starting from an inverted microscope (Nikon Eclipse TE-2000-E, Japan) equipped with phase contrast imaging and epi-fluorescence. The microscope was completed by installing custom IR optical tweezers and an UV laser-dissection system (MMI-cellCut Plus, Switzerland). Briefly, the IR laser beam (1064 nm, CW) was collimated and coupled to the optical path of the UV laser beam (355 nm, ns pulsed laser). Both beams were directed into the microscope lens (Nikon 60X, NA 1.25) by a dichroic mounted above the fluorescence cube [168]. The sample chamber containing the differentiating neurons and the vesicles was placed on the motorized microscope stage. The temperature of the dish was kept at 37°C by a digital temperature controller (PeCon GmbH, Er-back, Germany). During the experiments the cells were monitored by time-lapse phase contrast imaging using a digital camera (Orca Flash 4.0, Hamamatsu, Japan) at a frame rate of 5 Hz.

Estimation of the spatial and temporal distribution of the concentration at the GC. To perform this simulation, we used the point source approximation for the vesicle [23] and the following equation that describes three-dimensional free diffusion from a point source:

$$C(r,t) = 2 * \frac{C}{(4\pi Dt)^{3/2}} e^{-\frac{r^2}{Dt}}$$

where C is the initial concentration in the vesicle, D the diffusion coefficient and C(r,t) the concentration in a point at distance r from the vesicle, at time t. The concentration vs time curves for three points positioned at distances r, 1.25r and 1.5r are represented in the top inset of the Figure 10A, indicating a steep temporal gradient. The concentration at a distance r from the vesicle reaches a maximum after few seconds and then decreases fast to a value which is maintained almost constant in time after t=10s. From the concentration curves represented for different distances we notice also the spatial gradient and the fact that the spatial gradient tends to vanish after about 10 s from vesicle photolysis. However, when an obstacle as the cell membrane is reached, the molecules might stop their free diffusion, bind and accumulate on the membrane. Assuming that all the molecules reaching the membrane bind to it, we calculate the spatial and temporal distribution of the cumulative concentration CC(r, t) by summing C(r, t) values:

$$CC(r,t) = \sum_t \sum_r C(r,t)$$

As a numerical example, we consider a vesicle of 4 μm diameter, initial concentration inside the vesicle C_0= 4μM, the diffusion coefficient of the encapsulated molecules D= 40 μm2/s, the distance r ranging from 10 to 50 μm measured from the vesicle and t from 0 to 5 min. The spatio-temporal distribution of the concentration is shown in Figure 10B, showing that for a given distance the concentration increases fast immediately after the photolysis and tends to a constant value after about 2 min, while a significant spatial gradient is maintained constant in time after about 3 min. The concentration isolines are represented in Figure 10C. Notice that after 3 min the concentration decreases from 90 nM to 20 nM for a distance range of about 40 μm. The vesicle is typically positioned at 10-20 μm from the leading edge of the neurite, creating a spatial gradient of molecules concentration of about 2 nM/μm at the GC, which promotes the outgrowth and guidance mechanisms.

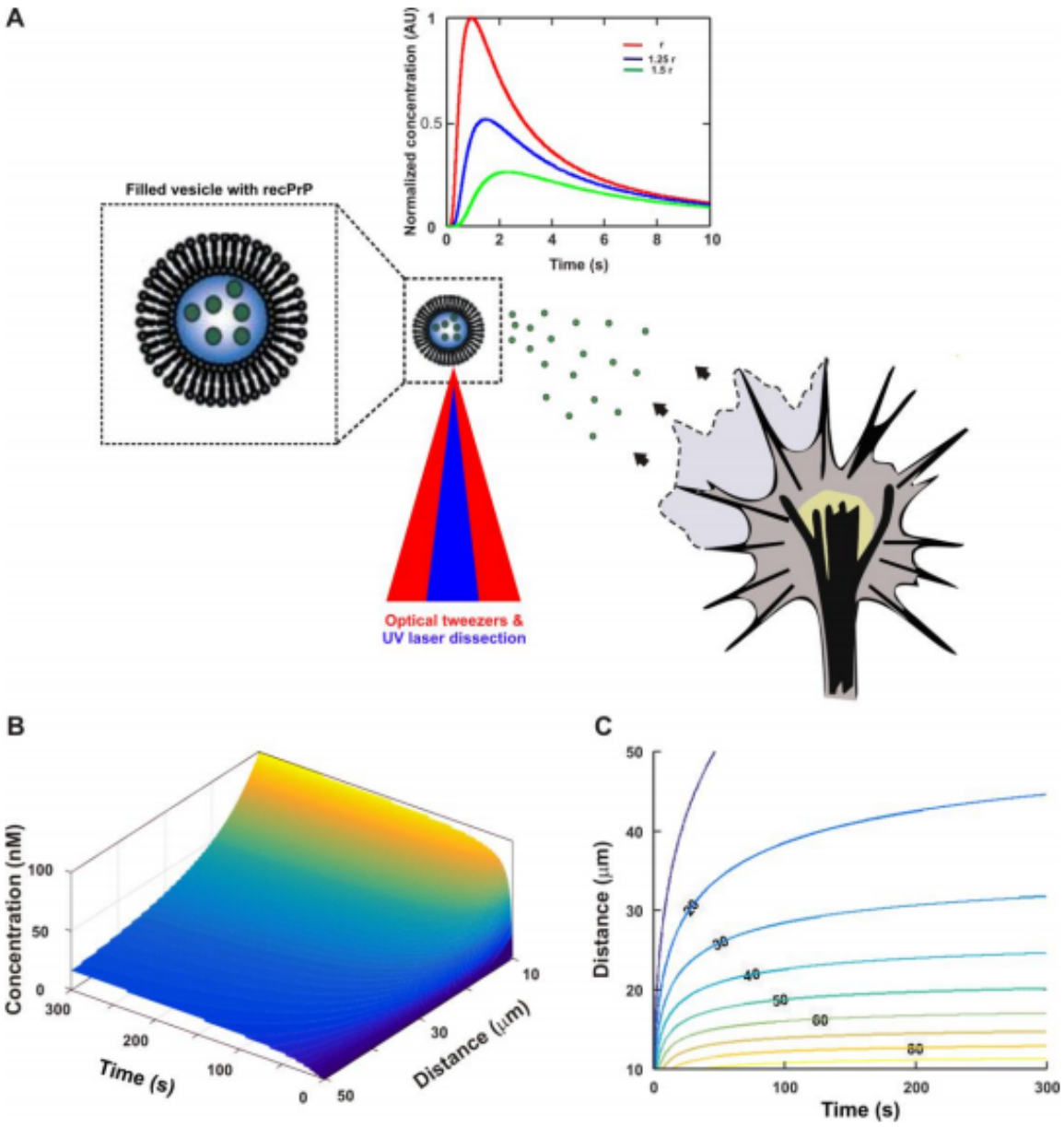

Figure 10 - Schematic representation of the focal stimulation assay. (A) The vesicle, trapped by the IR laser tweezers (red) is positioned near the GC and the molecules are released by photolysis of the membrane vesicle with an UV laser pulse (blue). The normalized concentration vs time curves for three points positioned at distances r, 1.25r and 1.5r are represented in the top inset, indicating a steep temporal gradient. The maximum concentrations are reached in 1 -2 seconds and the values decrease from 1 (for r) to 0.5 (1.25 r) and 0.25 (1.5r), indicating also a steep concentration spatial gradient. To generate these curves we have used r = 15 μm and D= 40

μm2/s. (**B**) The spatiotemporal distribution of the concentration at the GC, under the assumption that all the molecules reaching the membrane by free diffusion, bind to it. (**C**) The concentration isolines (numbers on the isolines indicate concentration in nM).

3.6. Immunofluorescence

After around 20hrs of treatments with wt or mutant recombinant mouse PrP (recMoPrP) proteins, the hippocampal neurons were fixed by 4% paraformaldehyde (PFA) in 20 min, washed 3 times in PBS and quenched with glycine 0.1M. The fixed cells were blocked in 5% normal goat serum (NGS, Sigma) for 30 min, permeabilized in 0.3% Triton and blocked again in 5% NGS solution. To appreciate the total neurite morphology, the cells were incubated with monoclonal antibody to β3-Tubulin (Thermo Fisher Scientific) in blocking solution for 2 hours at room temperature, washed three times with PBS, and incubated for additional 1 h at room temperature with the goat anti-mouse fluorochrome-conjugated secondary antibody in blocking solution. After three washes with PBS, nuclear staining was performed by incubated with 4',6-diamidino-2-phenylindole (dapi) for 5 min. The coverslips were eventually mounted on slides with Vectashield mounting medium (Vector Laboratories). Fluorescent images were acquired at 40X, oil immersion objective by a Leica or Nikon laser scanning confocal microscope with a Krypton-Argon and UV lasers. Five to six projections of six optical sections were randomly taken per coverslip at the region with cells evenly distributed and similar density between treatments, usually away from the edge and from center of the coverslip. Data were collected from at least three independent experiments per treatment and analyzed with ImageJ software (http://rsb.info.nih.gov/ij/).

Immunostainings for PrP^{C} localization and STED experiment were performed with some slight differences. Cells were fixed in 4% paraformaldehyde containing 0.15% picric acid in phosphate-buffered saline (PBS), saturated with 0.1 M glycine, permeabilized with 0.1% Triton X-100, saturated with 0.5% BSA (all from Sigma-Aldrich, St. Louis, MO) in PBS and then incubated for 1 h with primary antibodies followed by the 30 min incubation with secondary antibodies. Secondary antibodies used for STED measurements were conjugated with STAR580 or STAR635P (Abberior, Göttingen, Germany).

STED microscopy. 2-color STED microscopywas performed at the NanoBiophotonics Department (Max Plank Institute for Biophysical Chemistry, Göttingen, Germany) on a setup

previously described in [169] or on a two-color Abberior STED 775 QUAD Scanning microscope (Abberior Instruments GmbH, Göttingen, Germany) equipped with 561 nm and 640 nm pulsed excitation lasers, a pulsed 775 nm STED laser, and a 100x oil immersion objective lens (NA 1.4)

3.7. Western blotting

For standard immunoblotting procedure to detect PrP^C, primary hippocampal neurons were lysated in lysis buffer (50 mM-Tris HCl, pH 7.5, 150 mM NaCl, 0.5% CHAPS, 1 mM EDTA, 10% glycerol) supplemented with protease inhibitor mixture (Roche), and processed for Western blot detection. Samples were loaded onto SDS-PAGE gel and transferred to nitrocellulose membranes (GE Healthcare). After blocking in 5% non-fat dried milk in TBS-T for 1 hour at RT, membranes were incubated overnight at 4°C with primary antibody diluted in blocking solution. Incubation for 1 hour at RT with secondary antibody followed.

For detecting phosphorylated proteins in the treated cultures, hippocampal neurons were plated at 4 x 10^5 cells/mL in a 6-well plate. At day 1 *in vitro*, each well was treated with mock control or 2µM recMoPrP(wt) or recMoPrP(H56Y) for 25 min. Cells were then washed with ice cold PBS 1X (pH7.4) twice and lysed by lysis buffer (50mM Tris HCl pH 7.5, 150mM NaCl, 0.5% NP-40 and 0.5% sodium deoxycholate) supplemented with protease and phosphatase inhibitor cocktails (both from Roche). Cells extracts were collected after centrifugation at 14,000xg, 4°C, 15 minutes. Total protein amount was measured using BCA kit (Euroclone). Same amount of protein in each sample were loaded on SDS-PAGE gel 10%. Proteins were transferred onto polyvinylidene difluoride (PVDF) membrane (Immobilon-P, Milipore) at 300mA, 4°C, 150 minutes and then blocked in 5% BSA (for detecting phosphorylated protein) or skim milk in TBST (TBS with 0.5% Tween-20) for 45min-1h. Membranes were probed with primary antibody diluted in blocking solution overnight at 4°C, washed 2 times (5 min each) with TBST and then probed with HRP conjugated secondary antibody for 1 h. Immunoreactivity was detected by chemiluminescence HRP substrate (Milipore) and imaged with UVITEC Cambridge Imaging system. Densitometric analysis of band intensities was performed using Alliance v16.14 software.

The antibodies used were as follows: mouse monoclonal anti-PrP (W226, 1:1000), mouse monoclonal anti-PrP (EB8, 1:1000), mouse monoclonal anti-β-Actin HRP conjugated (A3854,

SIGMA, 1:10000), β3-tubulin rabbit polyclonal antibody (pAb) from Sigma was diluted at 1:5000. Phospho-p44/42 MAPK (Erk1/2) (Thr202/Tyr204) rabbit mAb (197G2, Cell Signaling Technology) was prepared at 1:4000; p44/42 MAPK (Erk1/2) mouse mAb (3A7, Cell Signaling Technology) was diluted 1:3000. Horseradish peroxidase (HRP) or fluorochrome-conjugated secondary antibody conjugated goat anti mouse or rabbit secondary antibodies (1:1000) was from DAKO.

3.8. Viability/cytotoxicity test

After incubation with recMoPrP proteins for about 22 hours, neuronal cultures were subjected to cytotoxicity test by using the LIVE/DEAD Viability/Cytotoxicity Kit (Thermo Fisher Scientific). The staining protocol was applied from the manufacturer manual. Briefly, the dye mix was prepared in PBS 1X with 2 μM calcein AM for live cell staining and 4 μM EthD-1 for dead cell staining at final concentration. After being washed twice in warm PBS, the cells were incubated with the dye mix for 20min at 37^{o}C. Then the coverslips containing the cells were proceeded for observation under 20X objective of the Nikon confocal microscope at laser 488 for the signal of calcein AM and laser 561 for the signal of EthD-1. Numbers of live and dead cells from each image in each treatment were analyzed by the plugin Analyze Particles of ImageJ 1.49 software.

3.9. Statistical analysis

Statistical data are presented as mean (SD) or ± SE depending on data type. Circular statistics is used to compute mean and SE for angle analysis (MATLAB Circular Statistics Toolbox [170]). Statistical significance of the differences between the mean values was evaluated using the *t*-test for outgrowth and colocalization data. For some cases in which we had multiple comparisons we used Holm-Bonferroni correction to adjust the p-values. For angle data we used Watson-Williams test as one-way ANOVA and Harrison-Kanji test as two-way ANOVA [170].

Statistics for multiple comparisons were also analyzed using one-way ANOVA with Games-Howell or Dunnett's T3 post-hoc test by IBM SPSS statistics 23. Minimum significance was set at $p < 0.05$.

CHAPTER 4 – RESULTS

The project contains two parts. The first part involves the characterization of neurite outgrowth by the prion protein in a focal stimulation manner which was already published on Journal of Cell Science by Amin L. *et. al.*, 2016 [171]. The second part investigates on the role of copper binding in regulating the prion function in the neuritogenesis process.

4.1. Recombinant PrP (recPrP) induces neurite outgrowth and rapid GC turning

Although prion protein has been indicated to contribute in neurite outgrowth [25, 172], its role in neurite navigation has not yet been investigated. To test whether recPrP molecules can directly influence neuronal growth cone (GC) steering, we used an *in vitro* assay for axon guidance based on local stimulation technique [21]. This technique employs an infrared (IR) laser tweezers to trap and position a lipid vesicle carrying guidance molecules in the proximity of the cell. The molecules are then released by vesicle photolysis, using a pulse from a second ultraviolet (UV) laser. Here, we employed recombinant PrP (recPrP) molecules. Despite the lack of posttranslational modifications (*e.g. N*-glycosylation at residues N180 and N196 and glycosylphosphatidylinositol- (GPI) anchor), full-length recPrP is structurally equivalent to brain-derived PrP^C [173] thus, it represents a valuable model for structural and functional studies. Considering that UV light might induce protein damage by direct photo-oxidation and radical reactions [174], we investigated the structural consequences of UV and IR radiations on recombinant murine PrP. Protein samples were exposed to 7 min UV (355 nm) followed by 2 h of IR irradiation (1064 nm) to mimic the irradiation conditions during the stimulation experiment, based on the lasers characteristics (energy and beam size). Circular Dichroism (CD) spectra of each sample were recorded before and immediately after laser irradiation (Supplementary Figure S1). We found that in both conditions (UV and UV+IR irradiated samples) the spectra of the protein remain unaffected, indicating that neither UV nor IR radiation alter recPrP structural features in our experimental assays.

After vesicle photolysis, molecules freely diffuse in all directions and only a fraction of them reaches the GC membrane. The number of molecules reaching the leading edge depends on the starting concentration of the molecules inside the vesicle, distance between the GC and vesicle,

and the diffusion coefficient of molecules [21]. Assuming the concentration inside the vesicle and the size of vesicle were known, we calculated the spatial and temporal distribution of the concentration of the molecules at the GC (see section 3.5). The numerical example in section 3.5, using the set of parameters consistent with the real experiments, shows that a spatial gradient of about 2 nM/μm can be delivered to the GC from the micro-vesicle.

In our experimental assay, 4 μM of recPrP were encapsulated in lipid vesicles with a diameter varying between 1 and 5 μm. Vesicles were introduced to the cell culture media and a single vesicle was trapped and positioned by an infrared (IR) laser tweezer near an exploring hippocampal GC (Figure 11A-B). Using a short ultraviolet (UV) laser pulse the membrane of the vesicle was then broken, and the protein content was released and allowed to reach the GC by free diffusion. With this assay, the outgrowth and turning of neurite can be measured in response to a defined stimulus of recPrP over a short time period (Figure 11A-D). Following the release of recPrP (4 μM), we observed a rapid neurite outgrowth and a significant turning towards the source of the stimuli (Figure 11E-F). Rapid GC motions started 1-2 min after vesicle breaking and within 600s the neurite outgrowth enhanced 2-3 folds, compared to control (Figure 11F, maximum neurite growth within entire duration of experiment reached to 6.73 ± 0.80 μm). Quantification of the turning angle revealed that neurites had a significant bias toward the source (Figure 11E blue rose distribution). Control vesicles, filled with phosphate-buffered saline (PBS), were positioned and photolysed in proximity of exploring GC (Figure 11A). Following vesicle photolysis, the GC continued the spontaneous navigation without significant changes in growth or direction (Figure 11E-F, maximum neurite elongation in this case reached to 2.88 ± 0.36 μm). Remarkably, the neurite outgrowth induced by recPrP was significantly correlated with the turning angle (Figure 11G; correlation coefficient $R = -0.64$, p-value <0.05), but no significant correlation was observed in the control. This confirms that local recPrP stimulation was concomitant with simultaneous fast neurite growth and GC turning toward the protein source. Indeed, these experiments strengthen the evidence that PrP^C is involved in neurite outgrowth and differentiation but also suggest a putative physiological function for soluble PrP as a guidance molecule for mouse hippocampal GC, which promote neurite outgrowth and influence the directional motion of neurites.

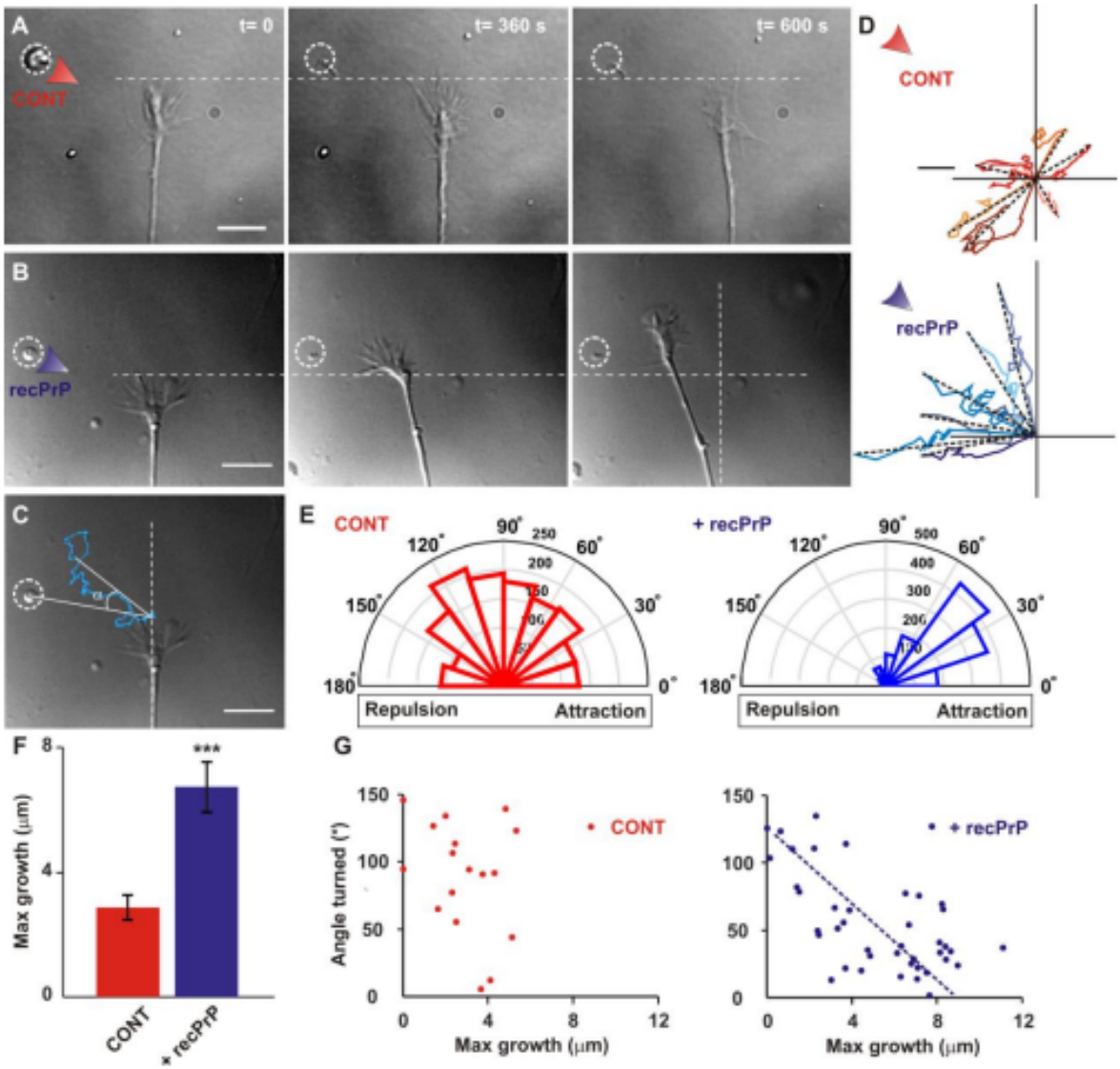

Figure 11 – Local delivery of PrP induces fast neurite outgrowth and turn toward the source. (**A-B**) DIC images of GC dynamics after vesicle photolysis at t=0 s. Red arrowheads indicate the position of vesicle encapsulating PBS (A) and 4 µM recPrP (B). Scale bar 8 µm. After recPrP release, GC clearly grew faster and turned towards the vesicle. **(C)** Definition of the growth and turning angle, α. The growth was derived from the position of the leading edge in successive frames, while the turning angle was defined as the angle between the direction of neurite extension and vesicle position for each frame. The blue line represents the detected leading-edge position at different time. (**D**) Superimposed trajectories of neurite extension after PBS (up) and recPrP (down) stimulations for 6 GC. Trajectories were normalized to the distance between initial position of GC and vesicle position. Scale bar 2 µm. Dotted lines indicate the principal direction of growth. **(E)** Distributions of turning angle (absolute value) for control and recPrP (N= 22 and 49 GC respectively) showing large angular distribution for control and a

much narrower distribution for stimulation with recPrP. **(F)** The value of maximum neurite outgrowth defined with respect to t= 0 s. recPrP stimulation enhanced neurite outgrowth up to 3-fold. Data represent mean ± SE and significance indicates *** $p < 0.001$ (Student's *t*-test). **(G)** Scatterplot of the maximum neurite outgrowth versus turning angle for control (left) and after recPrP release (right)

We next wondered whether changing the concentration of recPrP reaching the GC could influence its navigation. Therefore, GC were stimulated with different concentrations of recPrP. As expected, at low concentration (0.5 μM), the maximum growth was similar to control and no significant turning was observed. Increasing the concentration of recPrP from 1 to 4 μM, both neurite elongation and GC turning toward the source increased significantly (Figure 12). However, these effects were diminished by increasing the concentration to 6 μM and the opposite effects were observed at 15 μM (Figure 12B-D). Altogether, these data suggest that recPrP influences GC navigation in a dose-dependent manner: outgrowth and turning are stimulated progressively only when the concentration increases up to a certain value. For higher concentration the outgrowth is decreased or even reverted into retraction (at concentrations 3-4 folds higher the threshold). Low concentration of recPrP at the plasma membrane is sufficient to initiate signaling, while increased recPrP concentration may interfere with signaling cascades or activate different pathway leading to GC retraction and collapse.

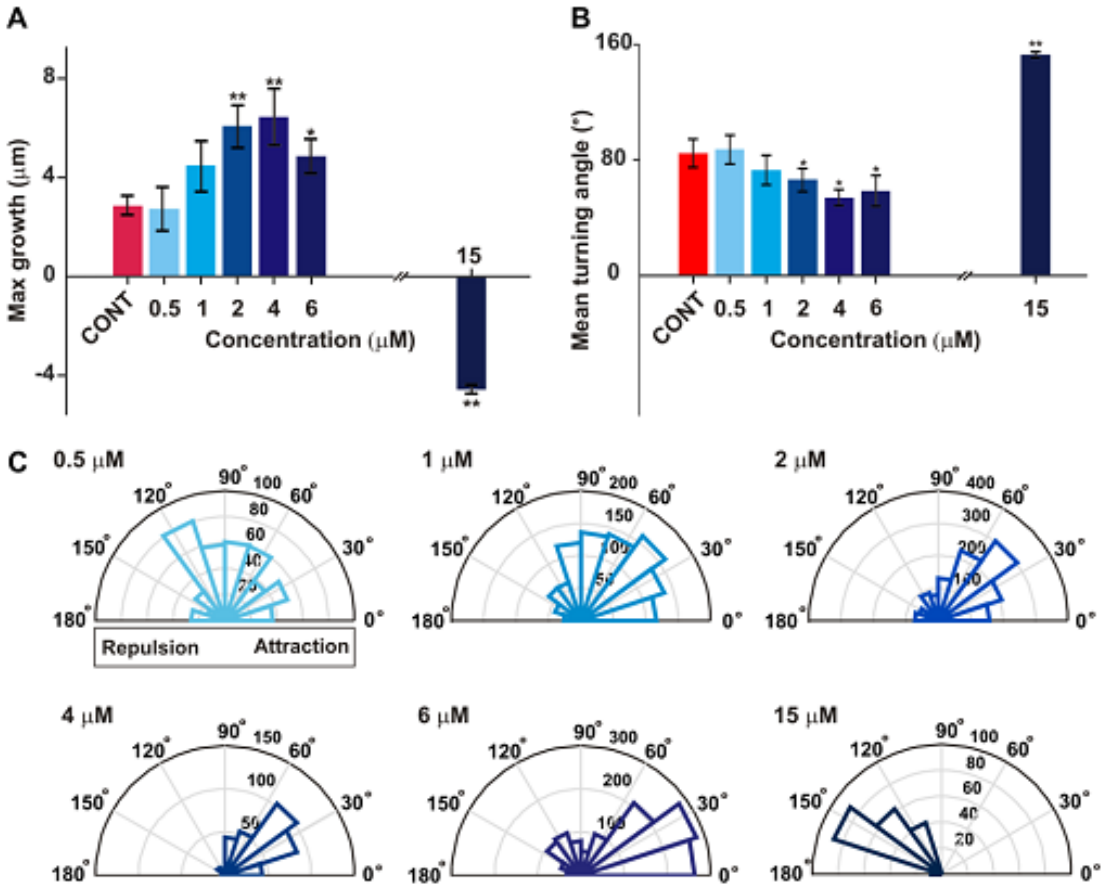

Figure 12 - GC response to recPrP stimulation depends on the recPrP concentration. (A) Color coded bars indicate maximum neurite outgrowth with respect to concentration of recPrP inside the vesicle. Data represent mean ± SE; p<0.05, one-way ANOVA; stars indicate p-values of t-test with Holm-Bonferroni correction for multiple comparison (* $p < 0.05$, ** $p < 0.01$). **(B)** Mean turning angle with respect to concentration of recPrP inside the vesicle. Data represent circular mean ± SE; p<0.001, one-way ANOVA for circular data. Stars indicate p-values of Watson-Williams test with Holm-Bonferroni correction for multiple comparison (* $p < 0.05$, ** $p < 0.01$). N > 10 GC**. (C)** Color coded rose distributions indicate the change of GC direction as a function of concentration. By increasing the concentration of recPrP inside the vesicles maximum neurite elongation increased significantly and GC turn toward the source in dose dependent manner. For very high concentration GC retracted completely (dark blue bar)

4.2. The function is specific to full-length wild-type PrP molecule

Next, we examined whether the stimulatory effect of recPrP was dependent on the full-length molecule or if a similar effect could be reproduced by truncated forms of PrP. To ensure that the recombinant proteins were not degraded or cleaved by proteases during incubation time in

neuronal medium before or during the experiments, we analyzed by Western blotting the integrity of each PrP fragment at different time points (0, 20, 40, 60 and 120 minutes) after addition to the medium. We found that all fragments of PrP used in this study remained stable for the entire duration of the experiments (Figure 13A-B).

Local delivery of N-terminal (23–90) domain of recPrP (up to 8 μM) slightly increased the average growth in comparison to control condition but did not result statistically significant (Figure 13D-F). Surprisingly, local delivery of C-terminal [89-231] domain (4 μM) caused an opposing effect on GC dynamics and in some cases, GC retracted completely (Figure 13C). Quantification of the turning angle indicated that none of the fragments was able to induce GC orientation toward the source (Figure 13D and F). Notably, the mixture of 4 μM of recPrP (23-90) and 4 μM recPrP (89-231) had a very similar effect to what was observed after local delivery of C-terminal domain [89-231], no significant growth or turn was detected (Figure 13E-F). We also performed experiments using 4 μM recPrP (23-120) and the mixture of recPrP (23-120) and recPrP (89-231). We found that although recPrP (23-120) can slightly enhanced the maximum growth with respect to control condition, the mixture of this fragment and recPrP (89-231) is functionally not active (Figure 13E-F). These results are consistent with associated pro- and anti-apoptotic functions of the C- and N-terminal domain of PrP^C [11], confirming that the growth-promoting function of recPrP is more pronounced in the presence of the full-length protein.

Previous studies identified the biochemical similarities between the flexible N-terminal domain of PrPC, and a newly discovered GPI-linked glycoprotein called Shadoo (Sho). This protein is also expressed in the adult brain. Furthermore, it has been suggested that Sho exhibits PrP-like protective properties [175]. Therefore, we examined the role of this protein on neurite outgrowth and GC navigation. Local delivery of 4 μM Sho, did not influence the GC navigation (Supplementary Figure S2).

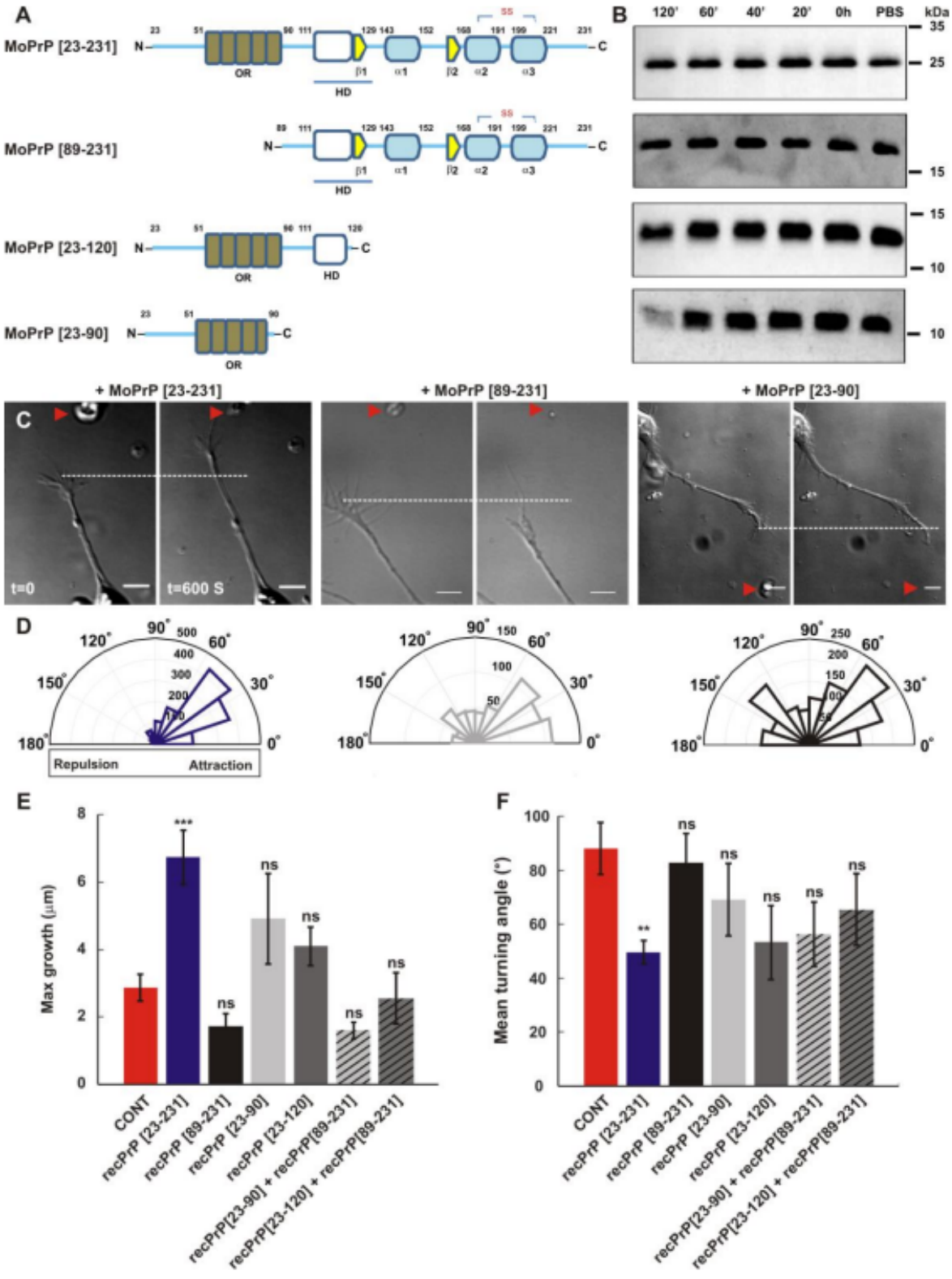
A
MoPrP [23-231]
MoPrP [89-231]
MoPrP [23-120]
MoPrP [23-90]
OR
HD
B
120'
60'
40'
20'
0h
PBS
kDa
35
25
15
15
10
10
+ MoPrP [23-231]
+ MoPrP [89-231]
+ MoPrP [23-90]
C
t=0
t=600 S
D
Repulsion
Attraction
E
Max growth (μm)
F
Mean turning angle (°)
CONT
recPrP [23-231]
recPrP [89-231]
recPrP [23-90]
recPrP [23-120]
recPrP[23-90] + recPrP[89-231]
recPrP[23-120] + recPrP[89-231]

Figure 13 - Full-length PrP had a more active role in GC navigation. (A) Mouse full-length PrP and its different domains proteins used in this study. **(B)** Western blot analysis indicates different PrP fragments in neuron medium (NM) supplemented with FBS and incubated for different time (0, 20, 40, 60 and 120 minutes). Protein in PBS was used as a positive control. W226 (binding epitope: 145-155) was used to detect full-length recPrP (23-231) and C-terminal fragment (89-231) but EB8 (binding epitope: 26-34) was used for N-terminal fragments detection (23-120 and 23-90). **(C)** DIC images of a GC before and after vesicle photolysis. Red arrowheads indicate the position of vesicle encapsulating 4 μM of full-length recPrP, N-terminal (23-90) and C-terminal of recPrP (89-231). Scale bar 8 μm. (**D**) Angle distributions when full-length, C-terminal and N-terminal of PrP were delivered to GC. (**E**) Maximum neurite outgrowth in control condition and in presence of different fragments and their mixture. Data represent mean ± SE. $p<0.001$, one-way ANOVA, stars indicate p-values of t-test with Holm-Bonferroni correction for multiple comparison (*** $p < 0.001$). (**F**) Mean turning angle. Data represent circular mean ± SE. $p<0.05$, one-way ANOVA for circular data. Stars indicate p-values of Watson-Williams test with Holm-Bonferroni correction for multiple comparison (** $p < 0.01$). N > 10 GC

4.3. Membrane-anchored PrP^C acts as a signaling receptor

We then investigated how neurons respond to extracellular recPrP stimuli and where the primary site of this interaction could be. Previous studies suggested that GPI-anchored PrP^C itself could be one of the candidates for mediating the effect of PrP [13]. To test this hypothesis PrP knockout mouse (*Prnp*$^{0/0}$) models were used. As a preliminary control of the neuronal cultures used in this study, endogenous PrP^C expression was evaluated in PrP wild-type (wt) and knock-out neurons, 24 and 48 h after plating the neurons. PrP^C is expressed in wt neurons with its normal glycosylation pattern (Figure 14A), presenting three isoforms (unglycosylated, monoglycosylated and di-glycosylated protein). After PNGase F (Peptide -N-Glycosidase F, an amidase that cleaves oligosaccharides from N-linked glycoproteins) digestion, PrP^C is mainly deglycosylated. PrP^C-ablated neurons do not show PrP expression as expected. Comparing GC dynamics in wt and *Prnp*$^{0/0}$ neurons we found that PrP-null GC were insensitive to recPrP release (Figure 14B-C), undergoing the repetitive cycles of protrusions and retractions, without any significant growth or change in direction (Figure 14D-E). Although PrP-null GC were growing at a slower rate in comparison to wt neurons (Figure 14C), they were able to respond to other guidance cues such as Netrin-1. When GC were exposed to Netrin-1 stimulation, within a few minutes GC clearly turned toward the vesicle position (Figure 14F-G). These results suggested that these two signaling events followed two different signaling pathways. In all species, the

attractive effects of Netrin are meditated by well documented receptors of the DCC (Deleted in Colorectal Carcinomas) family [176] while our experimental data on *Prnp*$^{0/0}$ mice model predicted that the potential function of recPrP as a signaling molecule requires membrane-anchored PrP^{C} to exert its functions. To further clarify this issue, *Prnp*$^{0/0}$ neurons were transfected with GFP-PrP constructs and examined for local stimulations with 4 μM recPrP (Figure 14H-I). GFP-tagged PrP is expected to have the same glycosylation pattern as the endogenous protein, previous studies showed that GFP-tagged PrP is correctly localized and functionally active in the brains of transgenic mice [177]. Moreover, it has been shown that GFP-PrP expressed in prion-infected cells have the same pattern as wt PrP after PK-digestion [178]. Notably, in our assay GFP-PrP expressing GC acquired the ability to respond to recPrP stimuli and neurite outgrowth enhancement was rescued compared to control (Figure 14J).

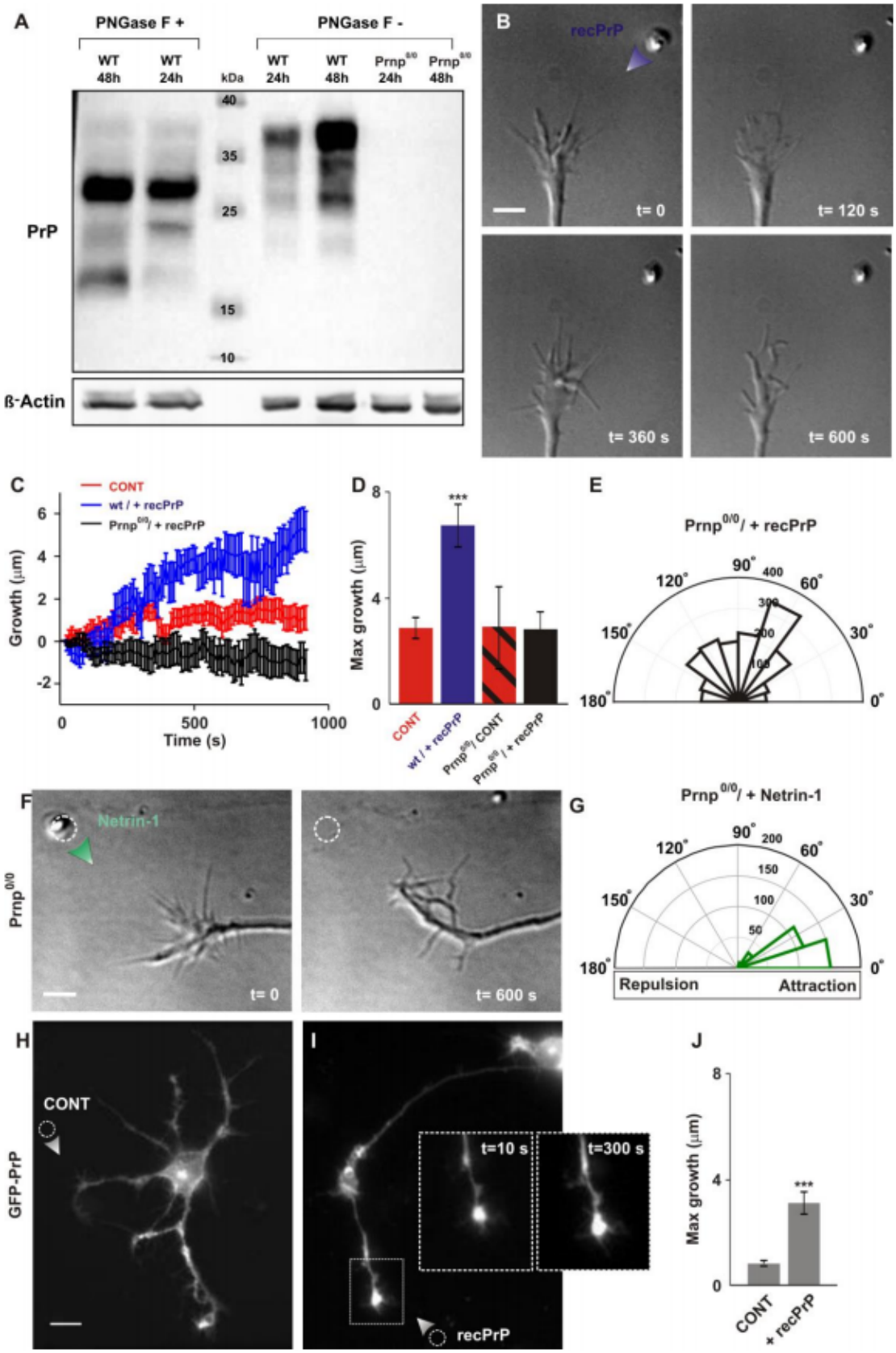
A
PNGase F +
PNGase F -
WT 48h
WT 24h
kDa
WT 24h
WT 48h
Prnp0/0 24h
Prnp0/0 48h
40
35
25
15
10
PrP
ß-Actin
B
recPrP
t= 0
t= 120 s
t= 360 s
t= 600 s
C
CONT
wt / + recPrP
Prnp0/0/ + recPrP
Growth (µm)
Time (s)
D
Max growth (µm)
***
CONT
wt / + recPrP
Prnp0/0/ CONT
Prnp0/0/ + recPrP
E
Prnp0/0/ + recPrP
F
Netrin-1
Prnp0/0
t= 0
t= 600 s
G
Prnp0/0/ + Netrin-1
Repulsion
Attraction
H
CONT
GFP-PrP
I
t=10 s
t=300 s
recPrP
J
Max growth (µm)
***
CONT
+ recPrP

Figure 14 - recPrP requires expression of PrP^C on the membrane to exert its functions. (A) PrP^C expression in primary hippocampal neurons 24 and 48 h after dissection. Western blot analysis using anti-PrP W226 antibody was performed. PrPC expression was evaluated in wt neurons before (right) and after (left) PNGase F treatment. *Prnp*$^{0/0}$ neurons were used as negative control. β-actin was used as loading control. **(B)** DIC images of a *Prnp*$^{0/0}$ GC after recPrP stimulation. Any significant growth was observed after vesicle photolysis. **(C)** Time evolution of neurite outgrowth after recPrP release in *Prnp*$^{0/0}$ GC superimpose with collected data from wt GC. **(D)** Bars indicate the value of maximum neurite outgrowth in control conditions and after 4 μM recPrP stimulation in wt and *Prnp*$^{0/0}$ GC. N > 10 GC. Data represent mean ± SE. Stars indicate p-values of t-test with Holm-Bonferroni correction for multiple comparison (*** $p < 0.001$). **(E)** Distribution of angle after local delivery of recPrP to *Prnp*$^{0/0}$ GC (N= 25 GC). **(F)** DIC images of a *Prnp*0/0 GC after local delivery of Netrin-1. After vesicle breaking GC clearly turned toward the source. Scale bar 4 μm. **(G)** As in **(E)** but vesicle encapsulating Netrin-1. **(H-I)** Fluorescence images of GFP-PrP expressing neurons immediately after local stimulation with PBS (H) and 4 μM recPrP (I). Arrowheads indicate the position of the vesicles. Scale bar 8 μm. Insets indicate the time-lapse images of GC marked in (I). **(J)** Bars indicate the value of maximum neurite outgrowth after local stimulation of GFP-PrP expressing GC (N= 9 and N=10 GC for control and recPrP stimulated conditions, respectively). Restoring PrP to the GC membrane rescued neurite outgrowth enhancement.

To check the accuracy and reliability of our experimental data we compared data from two different mouse strains, FVB and C57 black6 mice, either wt or *Prnp*$^{0/0}$ (Supplementary Figure S3). The recPrP effects were identical, indicating that recPrP stimulation enhanced neurite outgrowth in a similar manner in both mouse strains. Neither significant growth, nor GC turning was observed in experiments using *Prnp*$^{0/0}$ neurons originating from both FVB and Zurich I mice.

Considering the relevance of homophilic interaction between PrP^C molecules in our experimental assay, we then asked which region of PrP^C is mediating this interaction. To address this question, PrP^C was probed with three different monoclonal antibodies (mAb) to test their ability to bind distinct epitopes situated in the distal region of both the PrP^C N- and C- terminus. The localization of PrP^C was investigated by immunostaining with W226 [179] (binding epitope: 145- 155), SAF34 [180] (binding epitope: 59-89) and EB8 [181] (binding epitope: 26-34). All three mAbs recognized the PrP^C in wt mouse hippocampal neuronal culture, showing similar staining patterns (Figure 15A). After 30 minutes of incubation with mAbs [1 μg/ml], they were washed out and recPrP was delivered locally to GC. Interestingly, the growth promoting effect of recPrP was completely abolished after treatment with W226 and SAF34 (Figure 15B and C)

while EB8 was not able to block the effect of recPrP at the used concentration. These data suggest that the homophilic interaction of recPrP and PrP^C is necessary to provide distinct signaling events and that defined epitopes of PrP^C might regulate this homophilic interaction.

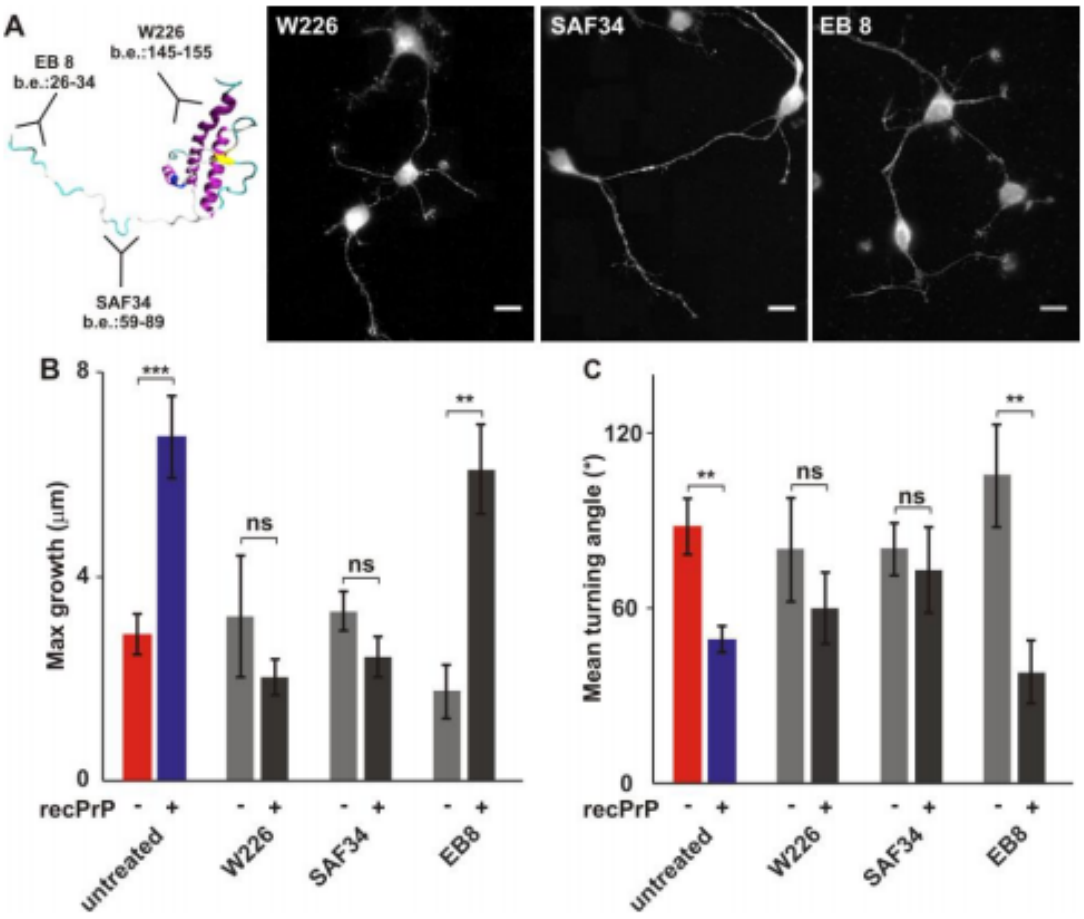

Figure 15 - mAbs against PrPC block growth promoting effect of recPrP. (A) Hippocampal neurons were fixed and were immunostained with the three mAbs. All the antibodies show a similar pattern. Scale bars, 10 µm. Cartoon indicates three-dimensional structure of mouse PrPC and binding epitopes of mAbs **(B-C)** Maximum neurite outgrowth **(**B**)** and mean turning angle **(**C**)** in control condition and in presence of 4 µM recPrP. Cells were pre-treated with different mAbs against PrPC (W226, EB8 and SAF34, [1 µg/ml]). In the presence of W226 and SAF34 any significant growth and turn was observed while EB8 did not block the growth promoting effect of recPrP. Data in (B) represent mean ± SE, p<0.001, two-way ANOVA, stars indicate p-values of t-test with Holm-Bonferroni correction for multiple comparison (** $p < 0.01$, *** $p < 0.001$). (**F**) Mean turning angle. Data represent circular mean ± SE. p < 0.001, two-way ANOVA for circular data. Stars indicate p-values of Watson-Williams test with Holm-Bonferroni correction for multiple comparison (** $p < 0.01$).

4.4. recPrP- PrP^C mediates multiple signaling pathways through transmembrane receptor NCAM

We showed that murine recPrP may interact with PrP^C as a putative receptor or part of receptor complex to exert its function. However, it remains largely unclear how recPrP stimuli are transduced in the cell interior. To gain preliminary insight into the intracellular signaling mechanisms involved in recPrP-mediated neurite outgrowth on mouse hippocampal culture, a panel of kinase inhibitors was tested for their ability to inhibit the effect of recPrP on neurite elongation (Figure 16). Src family kinases, including p59fyn (fyn), are known to have roles in mediating both prion neurotoxicity and PrP-mediated cell signaling. In addition to the src family kinases, extracellular regulated kinases (ERK) and phosphatidylinositol 3-kinase (PI3-kinase) can regulate a broad range of cellular process including cell differentiation, adhesion and migration, reviewed in [182]. In this set of experiments, neurons were incubated with different inhibitors for 30 min and then 4 μM recPrP (stripped blue bars in Figure 16) or PBS (stripped red bars in Figure 16) was delivered to the GC. As summarized in Figure 16, PP2 (1 μM), a selective inhibitor of the Src kinase, blocked the enhancing and guiding effects of recPrP by more than 70%, this is in agreement with previous studies which introduced Src kinase as important kinase involved in PrP^C-mediated intracellular signaling and its role in neurite outgrowth [24, 25, 182]. Furthermore, to investigate whether other kinase activation, including ERK and PI3-kinase, are necessary for recPrP-mediated neurite outgrowth we tested PD98059 (50 μM), inhibitor of MEK-ERK, and LY294002 (20 μM), inhibitor of PI3-kinase. Collected data indicated that inhibition of ERK and PI3 kinase abolishes the effect of recPrP on neurite elongation. Therefore, in our experimental assay neurite outgrowth and turning triggered by recPrP in cultured mouse hippocampal neurons require the activity of the Src kinase family, including p59fyn, ERK and PI3-kinase activation, thus these data indicated that multiple signaling pathways were involved in transduction of recPrP-mediated signals.

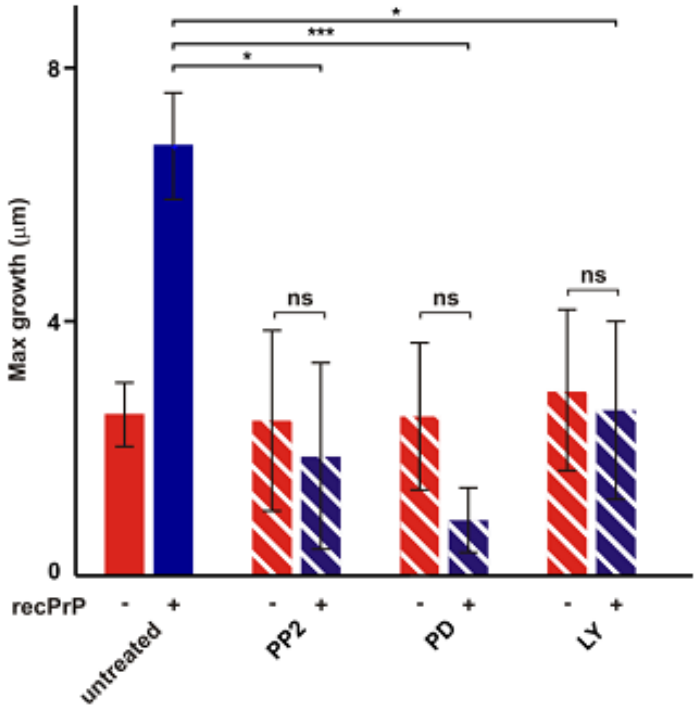

Figure 16 - Effect of kinase inhibitors on PrP-induced neurite outgrowth. Quantification of the maximum neurite outgrowth in control conditions (red bars) and after stimulation by 4 µM recPrP (blue bars). Solid bars indicate untreated experiments and stripped bars indicate 30 min incubation with different kinase inhibitors. Treatment with 1 µM PP2 (a selective inhibitor of the Src family kinase. N= 12 GC), 50 µM PD98059 (PD, inhibitor of ERK. N= 11 GC) and 20 µM LY294002 (LY, inhibitors of PI3-kinase. N= 10 GC) block the effect of recPrP indicating that multiple signaling pathways were involved in transduction of recPrP-mediated signals. Data represent mean ± SE. p <0.001, two-way ANOVA, Stars indicate p-values of t-test with Holm-Bonferroni correction for multiple comparison (* $p < 0.05$, *** $p < 0.001$).

PrP^C is anchored to the outer leaflet of the plasma membrane via a GPI-anchor, therefore it is unlikely to physically associate with cytosolic molecules. Nevertheless, several transmembrane and intracellular molecules are known to functionally cooperate with PrP^C to transduce signals into the cell interior [14]. Among them, neural cell adhesion molecules (NCAM) have attracted interest because both PrP^C and NCAM have been implicated in signaling cascades involving the Src kinase family and because Src is also involved in NCAM-driven neurite outgrowth [26, 113]. First, we investigated the role of NCAM in GC motility by using mAb against NCAM. Surprisingly, the growth promoting effect of recPrP was abolished after treatment with [1 µg/ml]

mAb against NCAM (Figure 17 F). These data suggest that NCAM may be involved in signal transduction.

To further investigate the role of NCAM in our assay, we analyzed the co-localization of PrP^C and NCAM in cultured mouse hippocampal neurons in control condition (Figure 17A) and in the presence of 2 μM recPrP (bulk treatment) (Figure 17B) using STimulated Emission Depletion (STED) nanoscopy [183]. Low co-localization was measured between PrP^C and NCAM in control cultured while after recPrP treatment co-localization increased significantly (Figure 17B). In control condition both molecules showed uniform distribution along neurites (Figure 17A). In contrast, in recPrP-treated cultures, clusters of NCAM overlapped with PrP^C (Figure 17B) suggesting that recPrP treatment can affect NCAM clustering in plasma membrane.

To exclude the contribution of recPrP from observed colocalization we pre-treated the cells with EB8 antibody against PrP. After 30 min of incubation, unbounded antibodies were washed out and cultures were treated in bulk with 2 μM of recPrP for 2h. We found a slightly lower colocalization (not significant difference, $p > 0.4$) than for the case when the cells were exposed directly to recPrP (Figure 17 C and E). Notably, this value was also significantly different from the control, suggesting that recPrP treatment recruits NCAM to lipid rafts, and would increase the association between NCAM and PrP^C. We then asked whether increased association between PrP^C and NCAM is specific to recPrP treatment or other growth-promoting factor can cause similar effect on distribution of NCAM and/or PrP^C. To address this issue, samples were treated in bulk with 1 μM NGF (Nerve Growth Factor) and examined with STED nanoscopy (Figure 17 D and F). Surprisingly, we also observed higher colocalization between PrP^C and NCAM in NGF treated samples, suggesting that recruitment of NCAM to lipid rafts is a generic property of neurite outgrowth stimulation.

Higher co-localization of NCAM and PrP^C in recPrP treated cultures suggested that these proteins might form a complex in lipid rafts, activate Src and downstream members of Src kinase, which in turn trigger the growth. This is in line with previous studies in cultured mouse hippocampal neurons [26] where PrP^C was found to directly interact with NCAM via *cis* or *trans* interaction, stabilizing NCAM within lipid rafts, and thereby stimulating neurite outgrowth.

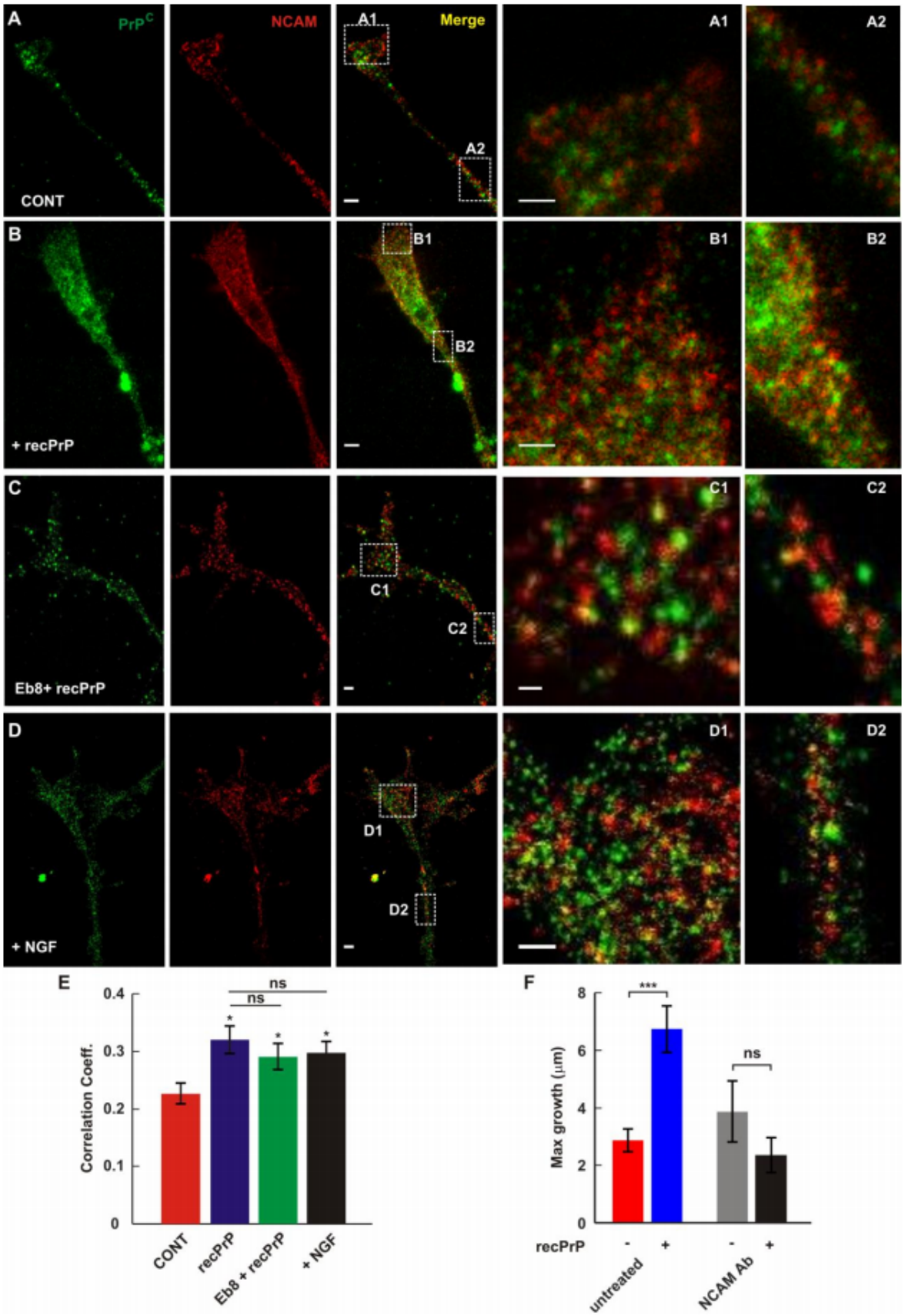
A
PrP^C
NCAM
A1
Merge
A2
CONT
B
B1
B2
+ recPrP
C
C1
C2
Eb8+ recPrP
D
D1
D2
+ NGF
E
Correlation Coeff.
0.4
0.3
0.2
0.1
0
ns
ns
*
CONT
recPrP
Eb8 + recPrP
+ NGF
F
Max growth (µm)
8
6
4
2
0
***
ns
recPrP
-
+
untreated
NCAM Ab

Figure 17 - recPrP treatment increase the colocalization between PrP and NCAM. (A) STED images of GC stained for PrP, NCAM and merge of the two staining in control condition. Scale bar 500 nm. (**A1-A2**) High-resolution images of areas indicated in (A). Scale bar 250 nm. **(B)** As in (A) but neurons were incubated in bulk with 2 μM recPrP (2 h). (**C**) As in (A) but in this case cells were pre-treated with mAb against PrP ([1 μg/mL] of EB8 for 0.5 h) and then incubated with 2 μM recPrP (2 h). **(D)** As in (A) but neurons were treated in bulk with 1 μM NGF for 2 h. (**E**) Mean correlation coefficients comparing the co-localization between PrP and NCAM in different conditions. $p < 0.05$, one-way ANOVA (**F**) Maximum neurite outgrowth in control condition and in presence of recPrP. Cells were pre-treated with mAbs against NCAM [1 μg/mL]. In the presence of mAb any significant growth was observed. Data represent mean ± SE. $p < 0.001$, two-way ANOVA. Stars indicate p-values of t-test with Holm-Bonferroni correction for multiple comparison (* $p < 0.05$, *** $p < 0.001$).

4.5. Structural integrity of N-terminal copper-binding sites of the prion protein is crucial for its function in neuritogenesis

To investigate whether copper-binding sites play an important role in the function of PrP^C in neuritogenesis, we mutate the histidine residues of the N-terminal of PrP involved in copper coordination [184]. In addition we produced the homologous GSS-linked mutation P101L (P102L in human) that was shown to alter copper coordination at the non-OR region [134] (Figure 18a). The purified and folded proteins were assessed using Circular Dichroism spectra. As result, substitution of histidine to tyrosine at the OR denoted as H1234Y changed critically the PrP secondary structure with very high α-helix rich content comparing to the wild-type (wt) protein. The same structure was observed in the construct were all 6 histidine residues were mutated to tyrosine (6-H toY mutant (H123456Y)). However, mutations at non-OR including H-to-Y substitutions or P101L had similar structural patterns with the wt protein although minimal changes favor more β-sheet contents were observed. (Figure 18b & 18c)

(a)

Denotation	Octarepeat 1	2	3	4	Non-octarepeat 5		6
	60	68	76	84	95	101	110
recMoPrP(wt)	…**H**GGGWGQP**H**GGSWGQP**H**GGSWGQP**H**GGGWGQGGGT**H**NQWNK**P**SKPKTNLK**H**…						
recMoPrP(H123456Y)	…**Y**GGGWGQP**Y**GGSWGQP**Y**GGSWGQP**Y**GGGWGQGGGT**Y**NQWNK**P**SKPKTNLK**Y**…						
recMoPrP(H1234Y)	…**Y**GGGWGQP**Y**GGSWGQP**Y**GGSWGQP**Y**GGGWGQGGGT**H**NQWNK**P**SKPKTNLK**H**…						
recMoPrP(H56Y)	…**H**GGGWGQP**H**GGSWGQP**H**GGSWGQP**H**GGGWGQGGGT**Y**NQWNK**P**SKPKTNLK**Y**…						
recMoPrP(P101L)	…**H**GGGWGQP**H**GGSWGQP**H**GGSWGQP**H**GGGWGQGGGT**H**NQWNK**L**SKPKTNLK**H**…						

(b)

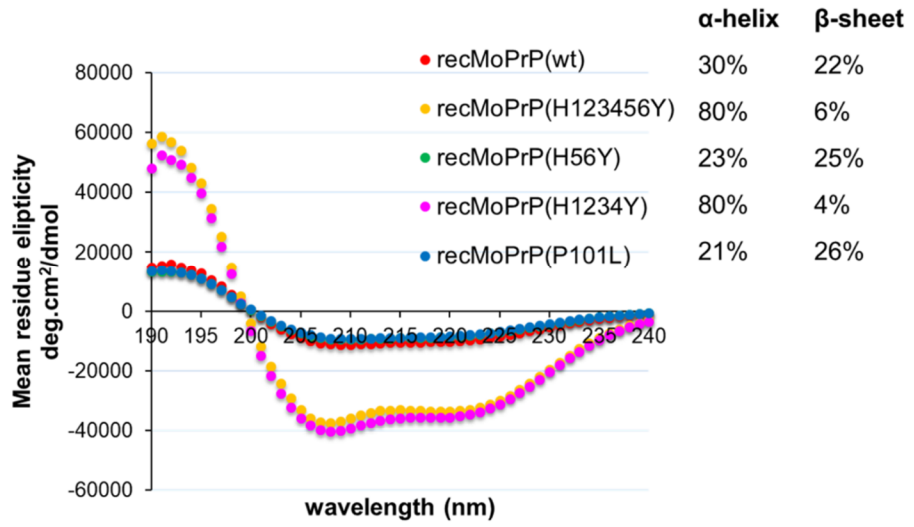

(c)

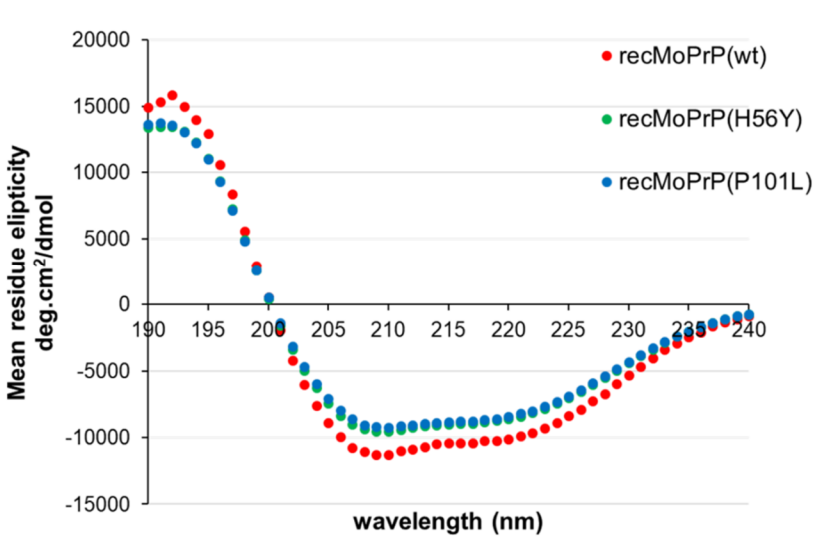

Figure 18 - Assessment of secondary structure for recombinant wild-type (wt) and mutant prion proteins by Circular Dichroism (CD). (a) Point mutation positions shown on part of sequences of the recombinant mutant MoPrP proteins compared to the wt recMoPrP; **(b)** Superimposed CD spectra representative of the purified and refolded recombinant MoPrP

proteins indicating that OR mutant (recMoPrP(H1234Y)) and recMoPrP(H123456Y) have completely different structure from the wt MoPrP whereas non-OR mutants including recMoPrP(H56Y) and recMoPrP(P101L) have minimal changes but mostly the beta-sheet content. **(c)** Detailed superimposed CD spectra indicating minimal changes in secondary structures between recMoPrP(wt) and non-OR mutants. CD data were reconstructed by CDSSTR program with reference data set 7 (Sreerama and Woody 2000), NRMSD < 0.05 on DichroWeb server (http://dichroweb.cryst.bbk.ac.uk/)

Recombinant PrP proteins were without GPI anchoring residues to mimic the soluble form of PrP which may act as a signaling molecule for neuronal processes. They were then delivered into the neuronal culture following overnight incubation. Different concentrations of wt recMoPrP at 0.5 μM, 1 μM or 2 μM were used to treat the P2 hippocampal neurons in bulk. After about 22 hrs of incubation in the presence or absence of recMoPrP, the cells were fixed for the immunostaining with β3- Tubulin as s specifically neuronal marker. Neurites in cultures treated with 2 μM of wt recMoPrP sample showed significant outgrowth and connection than the mock control treatment though the increase in neurite growth could already be observed at 1 μM treated condition (Figure 19).

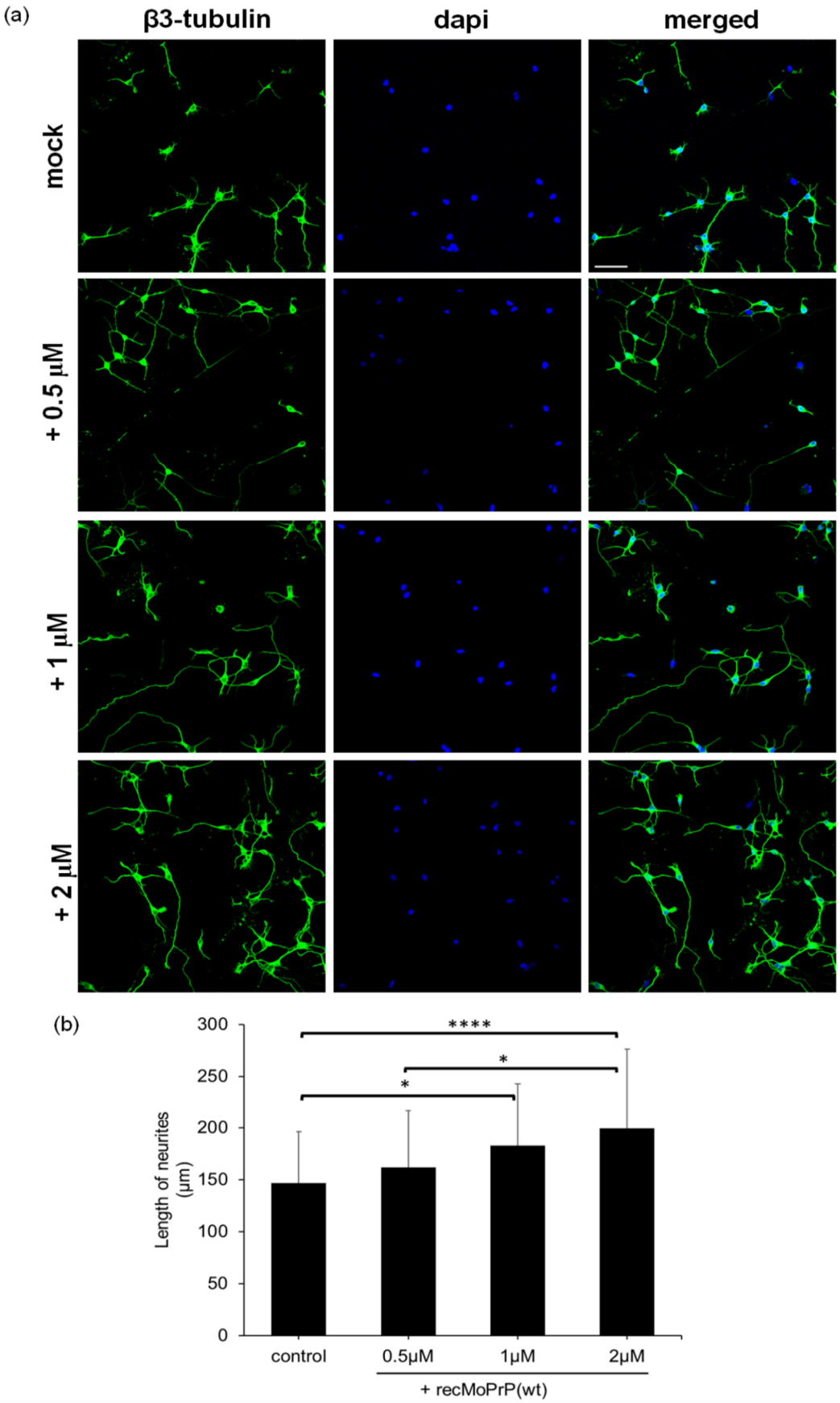
(a)
β3-tubulin
dapi
merged
mock
+ 0.5 μM
+ 1 μM
+ 2 μM
(b)
Length of neurites (μm)
300
250
200
150
100
50
0
****
*
*
control
0.5μM
1μM
2μM
+ recMoPrP(wt)

Figure 19 – Assessment on effects of different concentrations of recMoPrP(wt) on average neurite length of hippocampal cultures. Culture treated with 2μM recMoPrP(wt) showed significant neurite outgrowth and connections comparing to the mock control and 0.5μM concentration. **(a)** Representative immunofluorescent images of β3-tubulin for P2 hippocampal mouse neuronal cultures after about 22 hours of incubation with mock control or different concentration of recMoPrP(wt). Images were taken at 40X oil immersion objective by the Leica confocal microscope; scale bar 50μm, nuclear staining with dapi. **(b)** Quantitative analysis of average length of neurites in different treatments by ImageJ; data represent mean (SD) from at least three independent experiments with 28 to 88 images analyzed; statistical comparison by one-way ANOVA with Games-Howell post hoc test (****$p < 0.0001$; *$p < 0.05$)

We next investigate the effect of minimally structural change in non-OR copper-binding site on the neuritogenesis process using two mutants recMoPrP(H56Y) and recMoPrP(P101L). After the cells were plated for one day, the neuronal cultures were treated with either the mutant or wt recombinant proteins at 2 μM concentration. As a result, neither recMoPrP(H56Y) or recMoPrP(P101L) could enhance neurite outgrowth comparing to the effect of wt recMoPrP treatment versus control (Figure 20a). The cultures treated with the non-OR mutants appeared to have shorter neurites than in the mock control despite the differences were of non-statistical significance. Average length of neurites in wt recMoPrP treatment could reach almost 200μm after two days in culture whereas in recMoPrP(H56Y) and recMoPrP(P101L) mutant treatments neurites were about 80 and 70 μm shorter respectively. (Figure 20b)

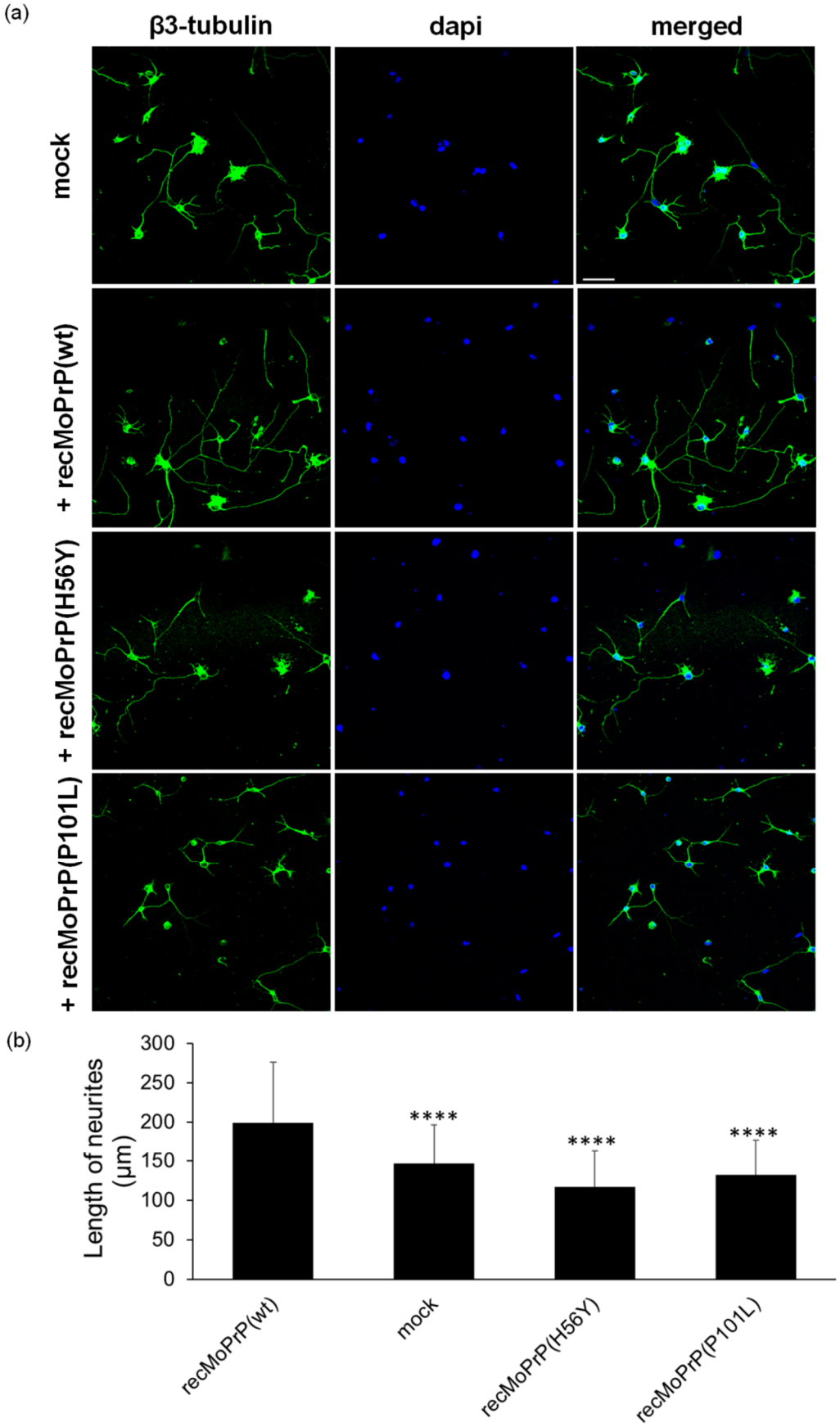
(a)
β3-tubulin
dapi
merged
mock
+ recMoPrP(wt)
+ recMoPrP(H56Y)
+ recMoPrP(P101L)
(b)
Length of neurites (μm)
300
250
200
150
100
50
0
****
****
****
recMoPrP(wt)
mock
recMoPrP(H56Y)
recMoPrP(P101L)

Figure 20 – Effects of non-OR mutants on neuronal growth. Neuronal culture treated with recMoPrP-wt showed significant neurite outgrowth and connections whereas non-OR mutant PrP(s) failed to promote the neuritogenesis in those treated cultures. **(a)** Representative immunofluorescent images of β3-tubulin for P2 hippocampal mouse neuronal cultures after about 22 hours of incubation with mock control or 2μM recMoPrP(wt) or non-OR mutants including recMoPrP(H56Y) and recMoPrP(P101L). Images were taken at 40X oil immersion objective by the Leica confocal microscope; scale bar 50μm, nuclear staining with dapi. **(b)** Quantitative analysis of average length of neurites in different treatment by ImageJ; data represent mean (SD) from at least three independent experiments with 23 to 88 images analyzed; statistical comparison by one-way ANOVA with Games-Howell post hoc test (****$p < 0.0001$)

With dramatic changes in the protein structure, it is expected that the OR and 6-H toY mutant proteins would show altered PrP function. Indeed, while recMoPrP(H1234Y) failed to increase the neurite growth comparing to the mock control, recMoPrP(H123456Y) could surprisingly cause high toxicity to neurons (Figure 21 and Figure S4). This data suggests that copper binding may contribute to stabilize the unstructured N-terminal of PrP maintaining its proper conformation for the signaling function. Particularly, the toxic effect was observed only with the additional substitution at the non-OR region together with the OR-region. Hence the total disruption of copper-binding at N-terminal of PrP, especially at the non-OR region leads the protein become more vulnerable to structural alteration and conversion to toxic species.

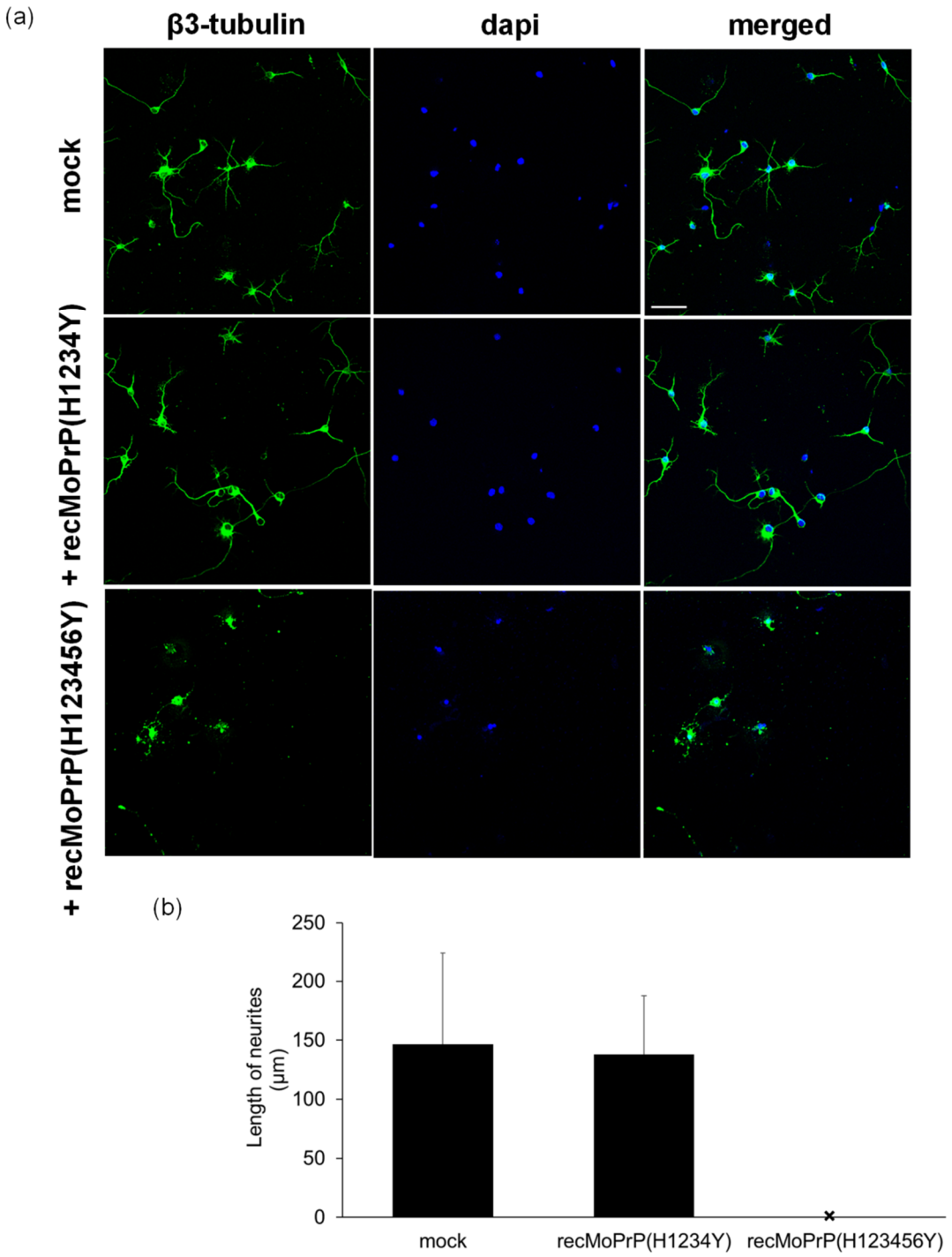

Figure 21 – Effects of OR mutant and 6-His mutant on the neuronal growth. Neuronal cultures treated with the OR mutant (H1234Y) and the all 6 His to Tyr (H123456Y) mutant recMoPrP that folded into completely different structures from the wild-type protein also failed to promote the neuritogenesis. Especially, the latter induced lethal toxicity to neurons. **(a)** Representative immunofluorescent images are shown as β3-tubulin (green) and nuclear staining dapi (blue) for P2 hippocampal mouse neuronal cultures after about 22 hours of incubation with

mock control or 2μM or mutant proteins. Images were taken at 40X oil immersion objective by the Leica confocal microscope; scale bar 50μm. **(b)** Quantitative analysis of average length of neurites in treatments with control and OR-mutant by ImageJ; data represent mean (SD) from at least three independent experiments with 30 to 88 images analyzed. Images from cultures treated with recMoPrP(H123456Y) could not be analyzed due to neuronal death

4.6. Mutant prion proteins at the N-terminal copper binding sites fail to induce neuronal growth cone polarity and protrusion

After assessing the overall effect of the above PrP mutants to general growth of the neuronal network in cultures, we moved to evaluate single neuronal focal stimulation to understand how the mutants could affect the cell dynamics leading to the reduction in neuritogenesis. For this, we applied the established neuronal guidance assay based on optical tweezer technique in the first part of the study (see section 3.5) [171] to monitor the growth cone polarity and protrusion-retraction movement after the stimuli delivery. Briefly, recombinant PrP proteins were encapsulated in liposomes at concentration of 4μM. With the help of optical tweezer composed of two focused IR laser beams, the liposome was trapped and placed near a dynamic growth cone at a distance around 10-20μm. The proteins were released after photolysis by the UV (ultraviolet) pulse laser and diffused toward the growth cone.

Upon stimulation with wt recMoPrP, the GC trace (red line) showed that it protruded forward and turned towards the protein source (Figure 22) which replicated our previous finding about the function of wt PrP in promoting fast GC navigation (section 4.1) [171]. As for the OR and the non-OR mutants as well as the PBS control, GC(s) have only spontaneous movements around the original positions showed clearly from the rose diagrams with angle distributions covering 0-180 degree (Figure 23). Stimulation with recMoPrP(P101L) showed only few GC moving toward the source, and the mutant protein failed to significantly promote GC polarity (Figure 22, Figure 23, supplementary video 1). As far as neurite growth was concerned, wt recMoPrP stimulated GC outgrowth immediately following vesicle photolysis and sprouted after 3 min whereas all other cases started decreasing at the same time or maintained minimal changes in length (Figure 24b). Wt PrP could increase the GC maximum growth up to 12 μm within few minutes, 3 folds more than the control and 4 folds than the H56Y mutant (Figure 24a). On average, GC stimulated with the non-OR mutant (H56Y) did not increase growth and in some cases even retracted indicating the protein may have inhibitory effect (Figure 24b, supplementary

video 2). Interestingly, the difference in behavior of GC upon stimulation with H56Y and P101L mutants infer that the direct blocking of copper binding has a strong impact on PrP function in neurite outgrowth than the putative conformational changes at the non-OR region.

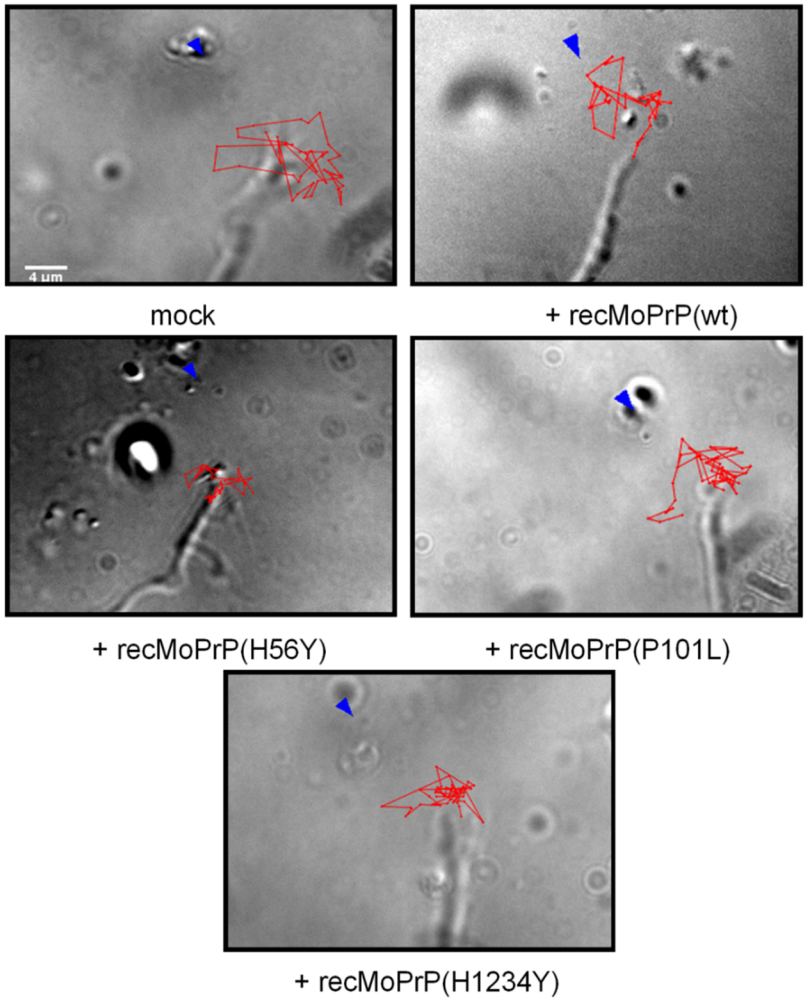

Figure 22 - Trajectories (red) of representative growth cones 'responses to wt or mutant prion proteins. The GC movements were monitored for about 15min after the deliveries of recMoPrP(wt), OR (H1234Y) or non-OR (H56Y & P101L) mutants by photolysis of the encapsulating liposomes. Only the growth cone stimulated with the recMoPrP(wt) protruded dynamically toward the protein source. Blue arrows indicate original positions of the chosen liposomes before photolysis. Red lines indicate traces of the growth cone movement every 25s analyzed by our custom code developed in Matlab

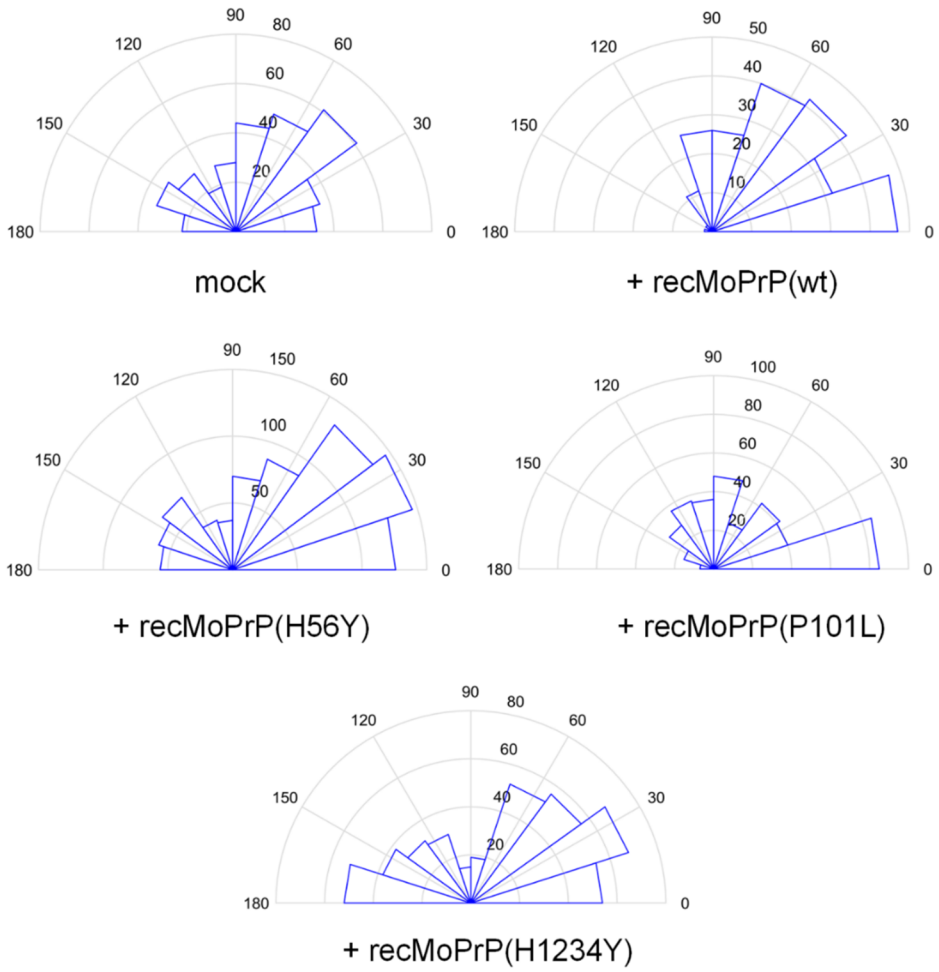

Figure 23 – Effects of OR and non-OR mutant PrP on GC polarity. Rose diagrams showing angle α distribution between the target GC(s) and the liposome positions (protein delivery points) during different stimulation conditions. $0 < \alpha < 90^0$ indicates the GCs are attracted toward the protein source; vice versa $90 < \alpha < 180^0$ indicates the GCs are repulsed from the protein source. The GC responses to recMoPrP(wt) show a clear polarity toward the signaling cue whereas in the other conditions, the GCs turn to the opposite direction many times. The angles are analyzed every 50 frames from all the experiments for each treatment by our custom code developed in Matlab

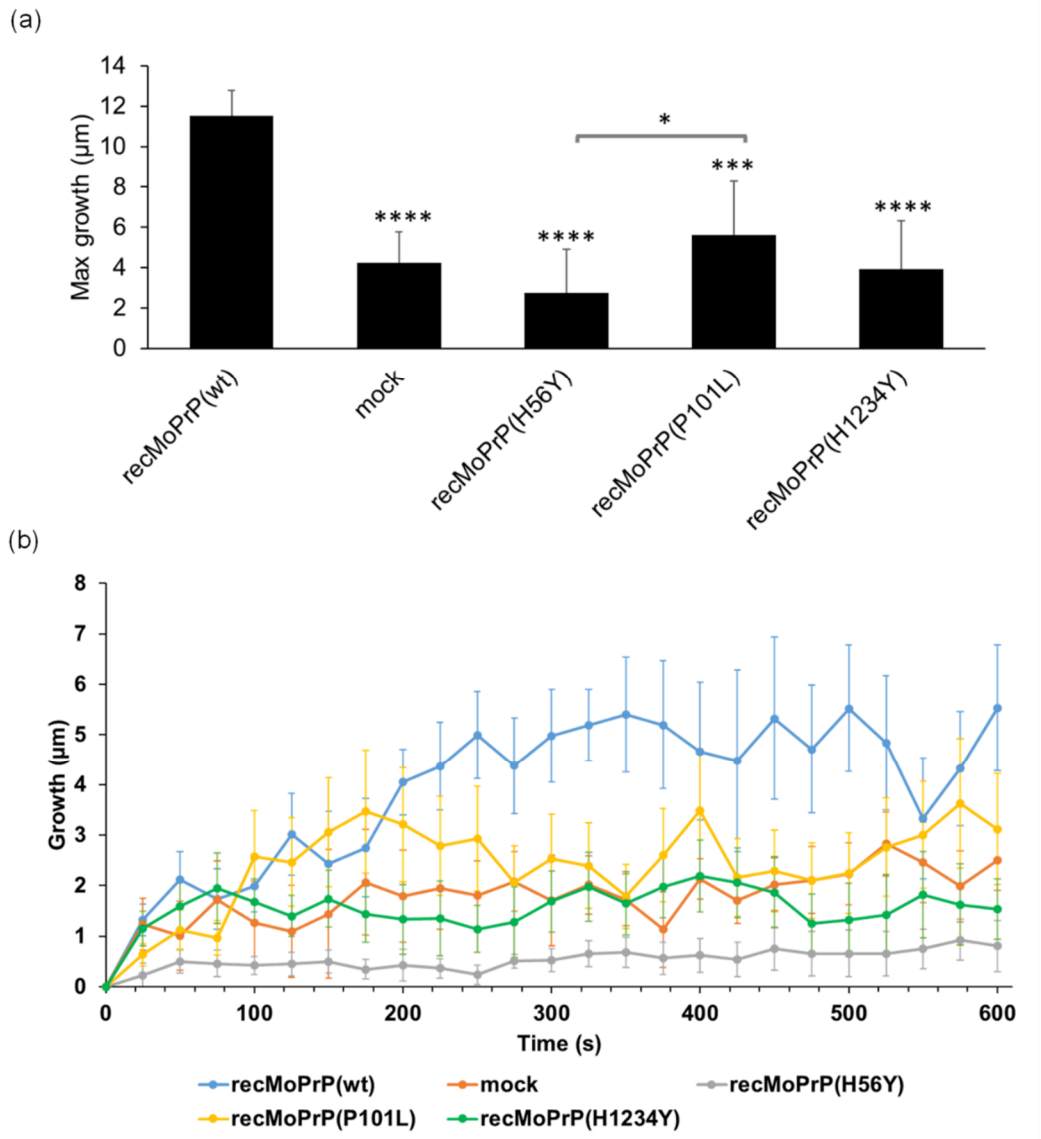

Figure 24 – Effect of OR and non-OR mutants on GC protrusion. The OR mutant recMoPrP(H1234Y) (n = 9) and non-OR mutants including recMoPrP(H56Y) (n = 18) and (P101L) (n = 8) failed to enhance growth-cone protrusion and neurite outgrowth as well as the mock control (n = 8) whereas the wild-type protein (n = 6) could increase remarkably the neurite growth. **(a)** Maximum growth of neurites measured from each stimulation conditions; growth-inhibiting effect of the non-OR mutant recMoPrP(H56Y) is most pronounced indicating the importance of copper binding in this region on growth-promoting function. Data represent mean (SD), one-way ANOVA with Gabriel post hoc test (*$p < 0.05$, *** $p < 0.001$ and **** $p < 0.0001$). **(b)** Superimposition of GC protrusion from all the experiments of different stimulation conditions during 10 min after liposome photolysis. Data represent mean ± SE every 25s

4.7. Non-octarepeat (non-OR) copper binding site is essential for PrP trans-signaling in neuritogenesis

Data from the previous neuritogenesis assays showed that non-OR mutant recMoPrP(H56Y) treated culture had shorter average neurite length (~117 ± 46.7 μM) comparing to control (~147 ± 49.6 μM) (Figure 20b) and GC protrusion dynamic was even significantly lower than the one stimulated by other non-OR mutant recMoPrP(P101L) (Figure 24a). This set of data confirms that copper coordination in both His95 and His110 (mouse numbering) is relevant for PrP function. Hence, recMoPrP(H56Y) is chosen for further experiment to understand how non-OR copper binding site affects PrP trans-signaling in neuritogenesis. It can be implied from our previous study of this project that wt recMoPrP could promote growth signaling through NCAM-Fyn-ERK pathway (section 4.4) [171]. In this part, we could show direct activation of this pathway by detecting phosphorylated form of ERK in the hippocampal cultures after treatment with the recMoPrP (Figure 25a). Mitogen-activated protein kinases (MAPK) are activated by phosphorylation cascade. p44/42 MAPK- ERK1 and 2 are phosphorylated by MEK 1 and 2 at Thr202/Tyr204 and Thr185/Tyr187 respectively which eventually activate downstream transcription factors [185] such as CREB for neuritogenesis [186].

To detect phosphorylation of ERK, the hippocampal neurons after one day of plating were treated with 2μM wt recMoPrP or recMoPrP(H56Y) for 25 min prior to cell lysis. As a result, wt recMoPrP could promote significantly phosphorylation of p44/42 ERK 1/2 up to almost 20% (1.2 fold) comparing to the mock control (Figure 25b). The mutation H56Y failed to induce this signaling event resulting in nearly 40% less phosphorylated ERK ratio comparing to the wt sample (Figure 25a & b). The total expression of ERK after being normalized to the loading control β-tubulin in the recMoPrP treated samples were higher than in the control although not statistically significant due to small sample size (Figure 25c). Interestingly, while the possible upregulation of ERK could lead to more activation of the kinase by MEK in case of wt recMoPrP treated culture, the phosphorylating cascade was much less efficient in the mutant treated culture. Mutant PrP however could act through other unknown mechanism to increase ERK expression. Spontaneous activity of the pathway was still present since phosphorylation of ERK was not diminished indicating other growth factors could compensate the normal growth in

the cells. As a conclusion, the non-OR copper binding site in PrP seems to play a major role in inducing outgrowth signaling in hippocampal neurites.

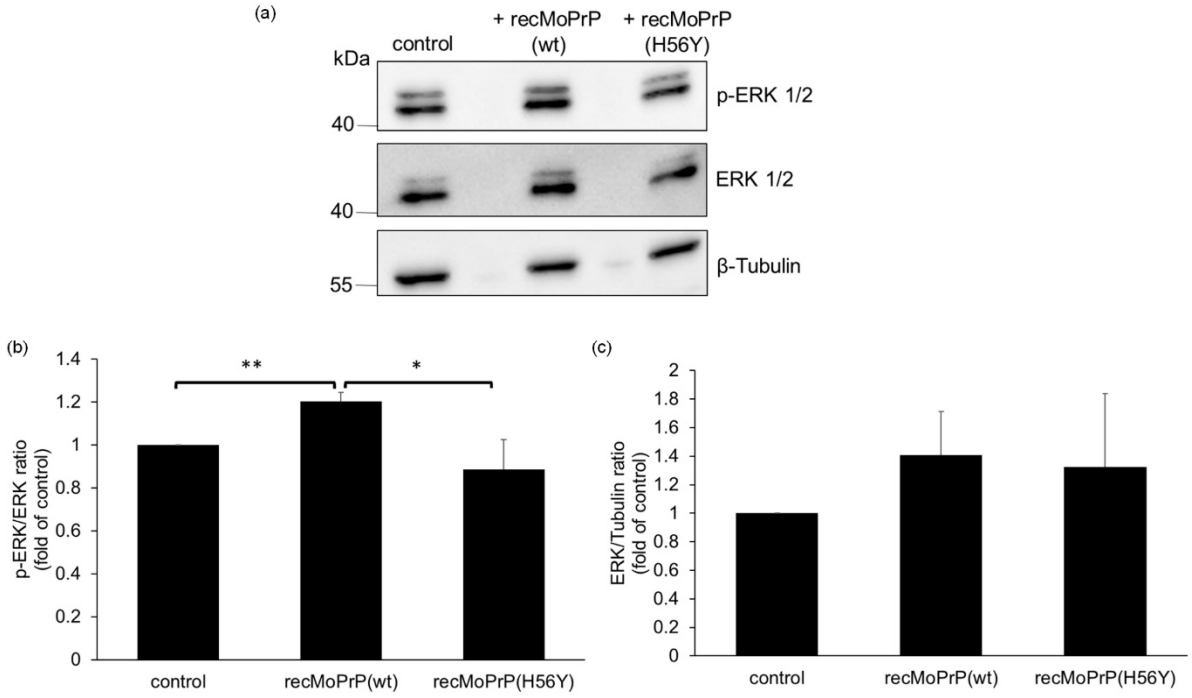

Figure 25 - Non-OR mutant recMoPrP(H56Y) did not increase activation of ERK pathway observed in treatment with the wt protein. **(a)** Representative western blot of phosphorylated ERK 1/2, total ERK 1/2 and β-Tubulin as loading control. Around 18µg of proteins were loaded in each well. **(b)** Ratio of phosphorylated ERK normalized to total ERK calculated from densitometric volume of each blotted signal; ratios of the control samples were set to 1 and data are presented as fold of control. Only recMoPrP(wt) treatment could significantly enhance phospho-p44/42 MAPK (Erk1/2) indicating elevated activation of the cascade whereas the recMoPrP(H56Y) treated culture had a reduction of the ERK phosphorylation level; * $p < 0.05$, **$p < 0.01$ one-way ANOVA with Dunnett's T3 multiple comparison. **(c)** Ratio of ERK densitometric signal normalized to β-Tubulin amount; PrP treated cultures appeared to have higher expression of ERK in spite of non-statistical significance. **(b) & (c)** data represents mean (SD), n=4

Chapter 5 – DISCUSSION

5.1. Soluble PrP may act as a non-canonical guidance cue by forming signaling complex with membranous PrP^C and NCAM

In the present study we assayed experimental conditions to mimic the interaction between a single GC and locally released recPrP molecules, unraveling long-awaited putative physiological function for soluble full-length PrP as a signaling molecule and GPI-anchored PrP^C as its receptor. Previous studies indicated that PrP^C can be secreted from the cell membrane and released to the extracellular space through distinct mechanisms [11]. The GPI-anchor can be removed by posttranslational modification [71, 187] or cleaved by phospholipase C [70]. Moreover, PrP^C can reach the extracellular space in exosomes, which are released by cells upon fusion of multivesicular bodies [20]. Therefore, PrP^C may interact with neighboring cell in a soluble form. Our methodology enabled experimental condition to examine and visualize the function of soluble PrP as a guidance molecule.

Comparing neurite navigation in wt and *Prnp*$^{0/0}$ GC, we found that *Prnp*$^{0/0}$ GC were insensitive to recPrP stimulation, but they are still able to respond to other biochemical cues such as Netrin-1. These results strongly suggest that physiologically active PrP^C on the membrane is required to mediate recPrP stimulation and activate downstream signaling events. There is evidence supporting the notion that PrP^C functions as a part of cell surface platform to interact selectively with various sets of ligands and transmembrane modules, providing distinct signaling events, which in turn convert into specific physiological processes or behavior [2, 14].

Moreover, we show that local accumulation of recPrP at wt GC leading edge requires the activation of multiple intracellular tyrosine kinases including the Src-family kinases and other kinases such as ERK and PI3-kinase to initiate any motile behavior. There is a general agreement that PrP-mediated signaling in neurons can trigger activation of Src-related kinases, such as fyn [24, 182]. More importantly, the non-receptor Src-related kinases are able to regulate a broad range of cellular process in physiology and disease. For instance, Src-related kinases are known to regulate cell adhesion *via* direct phosphorylation of $p120^{ctn}$ and β-catenins [188]. Thus, PrP^C signaling may modulate cell adhesion and consequently reorganize actin cytoskeleton dynamics through the activation of Src-related kinases. Furthermore, consistent with a previous

investigation [24], our experimental data support that the ERK kinase and PI3 kinase are involved in recPrP signal transduction. PI3 kinase, is involved in various cellular functions, including proliferation, cell migration, and axon guidance [189, 190]. It has been reported that PI3 kinase activity mediates GC attractive turning responses to guidance cues such as NGF, BDNF, and netrin-1 [191].

The observation that full-length recPrP is more active in inducing physiological responses poses intriguing issues about the role of N- and C-terminal domains for PrP^C function: while the C-terminus moiety possesses well-defined secondary and tertiary structures, the N-terminus is unstructured. These segments are often considered independent and non-interacting with each other [192]. However, recent studies are attributing a significant role to the N-terminus in driving tertiary structure contacts with the C-terminus, and this structural proximity appears to be mediated by metal ions (*i.e.* copper and zinc) binding the octarepeats domain located in the N-terminal moiety [193, 194]. Interestingly, we found that treatments of wt mouse hippocampal neurons with SAF34 and W226 mAbs -targeting the N- and C-terminus, respectively- completely abolished the growth promoting effect induced by recPrP. On the contrary, EB8 mAb –binding a region adjacent the octarepeats domain does not show any inhibitory effect. These results seem to support a model whereby PrP^C exerts its growth promoting function through a mechanism mediated by the interplay between the flexible octarepeat region and the structured domain. Cellular prion protein may undergo multiple processing by disintegrins. These cleavages occur within the putative toxic domain comprising the 106-126 residues. The processing is carried out by members of the ADAM (A Disintegrin And Metalloproteinase) enzyme family, including ADAM8, 10 and 17. ADAM8 cleaves PrP^C at residue 109 or 116, while ADAM10 and 17 cleave at 119. ADAM10 can also process the C-terminal domain of PrP at position 227. This complex posttranslational process harbors different fragments displaying various physiological functions. The first such processing carried out by ADAM8, which cleaves at residue 109, yields two moieties denoted N1 and C1, for the N-terminal and C-terminal domains, respectively. These two fragments have been shown to possess opposing biological activities [56, 146]. In our experiments, we have used either PrP(23-89) or PrP(23-120) to test whether the N-terminal domain may retain GC guidance properties. Although some limited effect was observed, the results were not statistically significant. Altogether, we propose a defined mechanism underlying the interaction of recPrP with GC. Local accumulation of recPrP at wt GC sites and its

homophilic interactions with membrane PrP^C activate Src-related kinase (including fyn), along with downstream signaling pathway to transduce the recPrP signal into the cell interior. Focal adhesion molecules and actin cytoskeleton are the major targets of these signaling cascades at GC periphery. Therefore, local stimulation with recPrP may activate new adhesion formation at the leading edge nearest to the guidance cue and may promote actin remodeling at GC periphery, which in turn facilitates neurite outgrowth and mediate attractive guidance response. Most likely, the association of PrP^C is not the sole player in transduction of recPrP-mediated signals and other cell-surface proteins such as NCAM are implicated in activation of signaling cascade by forming complexes on the membrane. This mechanism is consistent with a role of PrP^C in the modulation of cell adhesion *via* signaling [14] and supports the previous evidence in a zebrafish study, showing that PrP^C itself promotes Ca^{+2}-independent homophilic cell adhesion and suggested a functional link between PrP^C and E-cadherin to modulate Ca^{+2}-dependent cell adhesion [13]. Other studies reported that over expression of PrP^C modulates focal adhesion dynamics by regulating Src and Focal adhesion kinase phosphorylation both in mammals and *Drosophila* [195].

5.2. Role of copper in maintaining functions of PrP

In the last few years, many attempts to investigate the physiological role of PrP^C and its partners have been intensively carried out. In the CNS, different proposed functions of PrP have been proposed: synaptic regulation [25, 92], neuroprotection [16, 196] , neurogenesis [196, 197] and neuritogenesis [11, 26]. The latter may account for PrP^C role in memory and cognition [14]. PrP^C and Cu are found abundant at synaptic clefts [87, 88, 198] and some activity of PrP^C at synapses has been proposed to act as a copper-binding protein to regulate Ca^{2+} influx signaling [14]. In addition, PrP^C and copper cooperate in regulating NMDA receptor activity to protect neurons from glutamate excitotoxicity [16, 99]. Interestingly, PrP^C expression increases proliferation and differentiation at subventricular zone (SVZ) and dentate gyrus (DG) of hippocampus where neurogenesis constitutively occurs in both developing and adult CNS [197]. Copper is also found at high concentration in SVZ than in other brain regions and its increased concentration during aging could reduce neurogenesis [199]. On the other hand, moderate copper deficiency at early developmental stage can affect to dentate gyrus and hippocampal maturation [200]. Since either

high or low copper concentration can disturb neurogenesis, the involvement of PrP^C in neurogenesis should relate with its regulating activity in metal homeostasis.

PrP^C has been also considered a neurotrophic factor that facilitate neuritogenesis process either through cis or trans interactions between PrP^C and other soluble ligands (laminin, vibronectin, STI1) and transmembrane receptors (NCAM, integrin) [11, 24, 25, 171]. However most of these studies neglect to assess the role of copper binding in PrP^C activity, although it has been shown that extracellular copper can regulate PrP^C expression and release of its GPI anchorless form [201]. Following the observations about co-existence and co-function between Cu and PrP^C, we have attempted to study the role of copper binding in regulating PrP signaling. Altogether, in this study, we could provide evidence for the involvement of copper coordination in PrP signaling in neuritogenesis using specific point mutations to disrupt copper binding sites on the protein. Our data shows that copper binding stabilize the unstructured part on PrP. Whilst disrupting copper binding at OR region may change the protein structure, altered copper coordination at non-OR cause minimal but sufficient alteration in PrP structure that could prevent it from inducing neuritogenesis signaling. Cu^{2+} has high affinity to PrP with a K_d of 10^{-14} M for OR region and 4 x 10^{-14} M for non-OR region with His 96 and 111 (as human numbering) [52]. Therefore, higher affinity for copper at non-OR may explain its vulnerability in structural alteration due to different copper coordination.

Intriguingly, the GSS-linked mutation P102L (P101L as mouse numbering) seems to cause dysfunction of the protein. This result supports the loss-of-function hypothesis for prion pathology, particularly in case of GSS syndrome. It has been shown in previous studies that this mutant protein could alter copper coordination at non-OR region making the His96 unable to participate in the interaction with copper at both neutral and acidic pH [134]. This result suggests that copper-coordination at non-OR region may be critical to ensure correct conformation for this region, for correct interaction of PrP^C with its partners in signaling complexes. Indeed, the non-OR mutant tested in our study failed to activate the ERK signaling cascade - the central pathway for neurite outgrowth [171, 202, 203] comparing to the wt PrP protein. Moreover, this region has been suggested as a key site for prion conversion [134] . Thus, conformational changes in this region that would prevent copper binding could affect either PrP^C function or increase its susceptibility to pathologic prion conversion.

Chapter 6 – CONCLUSION

In this project we could define molecular function of PrP^C, which may provide new insights into understanding of its physiological roles during developmental stage and adult life. PrP^C in its soluble form might act as a signaling guidance cue. Its action needs homophilic interaction with the active PrP^C on adjacent cell membrane to form a signaling complex with NCAM and induce intracellular cascades for neurite outgrowth such as Fyn, PI3K and ERK. Further investigations may establish whether PrP^C has a potential role in affecting axon regeneration in the adult nervous system.

Our data also provide evidence about the critical role of copper binding in regulating PrP^C function in neuritogenesis. All copper binding sites are important to preserve the functional conformation of PrP^C. The ability of PrP^C in binding copper is key maintaining the protein function and preventing its conversion to the prion state. Indeed, minimal structural changes at non-OR copper binding site may be sufficient to alter PrP^C conformation and function, which may modulate its propensity to prion conversion. Overall, this study contributes to shed light between PrP^C physiology and prion pathology.

SUPPLEMENTARY DATA

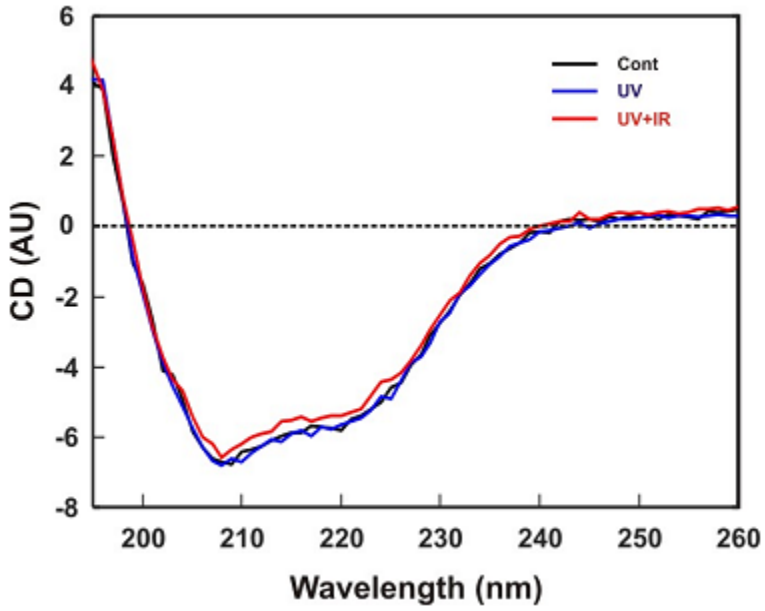

Figure S1 - CD spectroscopy monitoring possible changes in the structure of the PrP molecules by UV and IR radiation. The CD spectrum of a non-exposed sample of murine full-length PrP was first measured (black). CD spectra for the sample exposed to 7 min UV (355 nm) laser radiation (blue) and the sample exposed both to 7 min UV and 2 h IR (1064 nm) laser radiation (red) do not show significant changes with respect to the control spectrum (black) meaning that the laser radiation does not damage the protein

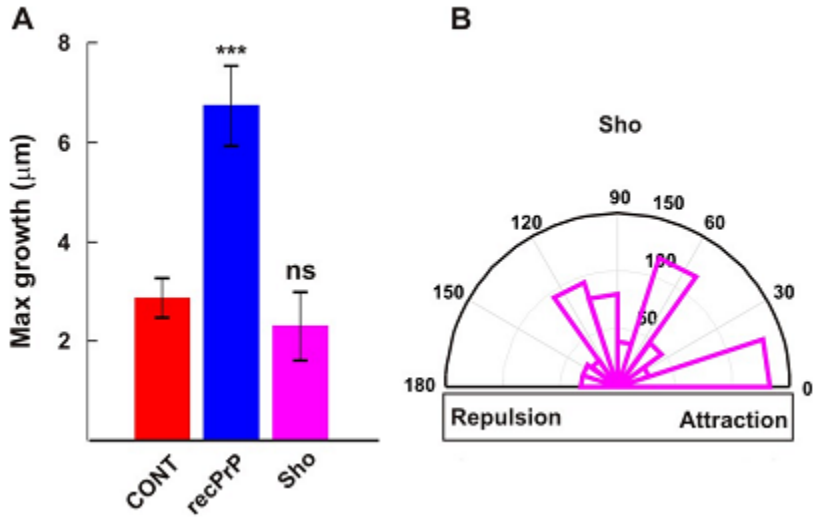

Figure S2 - The role of Shadoo (Sho) on GC motility. (A) Maximum neurite outgrowth in control condition and after local delivery of 4 µM Sho. Sho was not able to influence GC navigation at used concentration (N=9 GC). Data represent mean ± SE, Significance indicates *** $p < 0.001$ (Student's t-test)

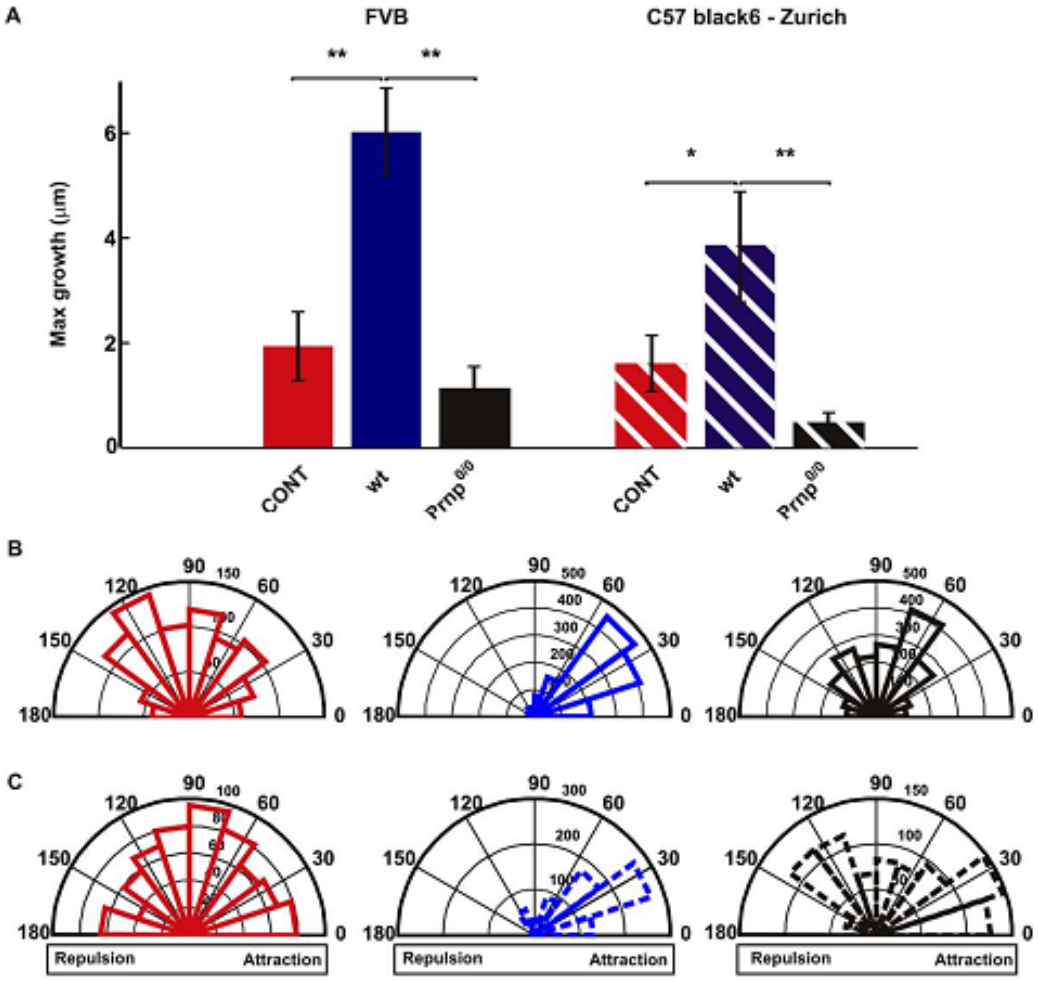

Figure S3 - The recPrP stimuli have a similar effect on two different mouse strains. (A) elongation measurement in two different mouse strains. RecPrP stimulation enhanced neurite outgrowth in similar manner in FVB (solid blue bar) and C57BL/6 (striped blue bar) cultured neurons. No significant growth was observed in two different types of *Prnp* neurons (solid black bar indicates the FVB $Prnp^{0/0}$ and striped black bar indicates Zurich I $Prnp^{0/0}$ mice. **(B-C)** After recPrP release GC turned towards the vesicle position in both FVB (B, blue rose distribution) and C57 Black (C, blue rose distribution) but FVB $Prnp^{0/0}$ (B, black rose distribution) and Zurich I $Prnp^{0/0}$ (C, black rose distribution) were insensitive to recPrP stimulation

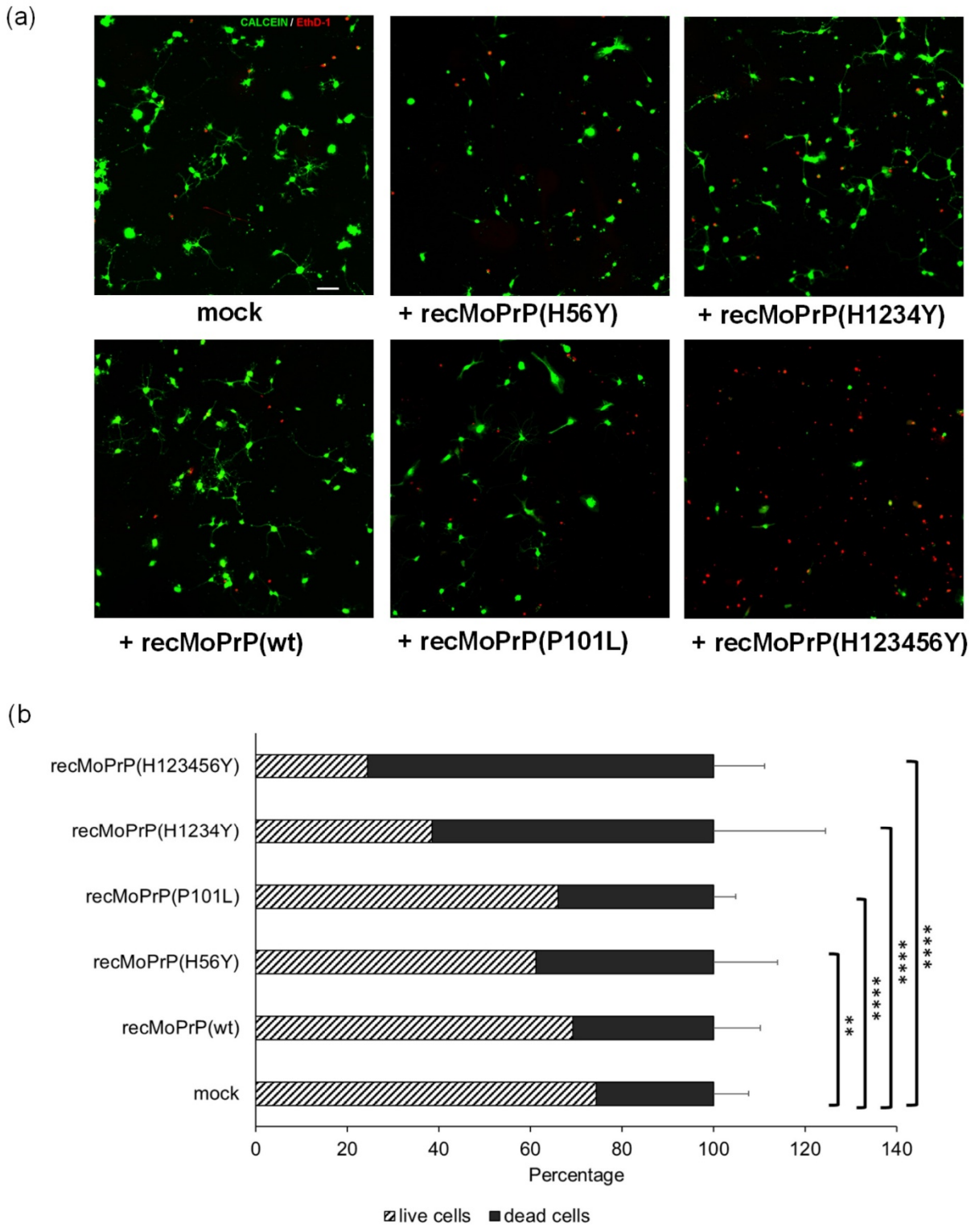

Figure S4– Assessment on cell viability after treatments with recMoPrP proteins. (a) Representative fluorescent images of calcein dye (green) as indicator for live cells and EthD-1 dye (red) as indicator for dead cells in P2 hippocampal mouse neuronal cultures after about 22

hours of incubation with mock control, 2μM recMoPrP(wt) or other mutant recMoPrP(s). Images were taken at 20X objective by the Nikon confocal microscope; scale bar 50μm. **(b)** Percentage of live and dead cells from above cultures calculated from many images ($n \geq 20$) taken from at least three independent experiments. Neuronal cultures treated with mutant recMoPrP had less live cells than those treated with mock control and recMoPrP(wt). recMoPrP(H123456Y) had highest toxicity to neurons. Data represent mean (SD). Statistical comparison by one-way ANOVA with Games-Howell post hoc test (**$p < 0.01$; ****$p < 0.0001$)

Supplementary video 1

GC stimulated with recMoPrP(P101L)

The GC responded to recMoPrP(P101L) by turning toward the protein source few times but then kept spontaneous movement without significant outgrowth. (To see the video, Ctrl-click on the protein name)

Supplementary video 2

GC stimulated with recMoPrP(H56Y)

The GC neither turned nor growth toward the protein source and retracted after some minutes in response to recMoPrP(H56Y). (To see the video, Ctrl-click on the protein name)

REFERENCES

1. Prusiner SB. *Neurodegenerative Diseases and Prions.* New England Journal of Medicine, 2001. **344**(20): p. 1516-1526.
2. Aguzzi A, Sigurdson C, and Heikenwaelder M. *Molecular Mechanisms of Prion Pathogenesis.* Annual Review of Pathology: Mechanisms of Disease, 2008. **3**(1): p. 11-40.
3. Clinton J, Forsyth C, Royston MC, and Roberts GW. *Synaptic degeneration is the primary neuropathological feature in prion disease: a preliminary study.* Neuroreport, 1993. **4**(1): p. 65-8.
4. Aguzzi A and Heikenwalder M. *Pathogenesis of prion diseases: current status and future outlook.* Nature Reviews Microbiology, 2006. **4**: p. 765.
5. Aguzzi A and Calella AM. *Prions: Protein Aggregation and Infectious Diseases.* Physiological Reviews, 2009. **89**(4): p. 1105-1152.
6. Williams ES and Miller MW. *Chronic wasting disease in deer and elk in North America.* Rev Sci Tech, 2002. **21**(2): p. 305-16.
7. Laurén J, Gimbel DA, Nygaard HB, Gilbert JW, and Strittmatter SM. *Cellular prion protein mediates impairment of synaptic plasticity by amyloid-β oligomers.* Nature, 2009. **457**: p. 1128.
8. Um JW, Nygaard HB, Heiss JK, Kostylev MA, Stagi M, Vortmeyer A, Wisniewski T, Gunther EC, and Strittmatter SM. *Alzheimer amyloid-β oligomer bound to postsynaptic prion protein activates Fyn to impair neurons.* Nature Neuroscience, 2012. **15**: p. 1227.
9. Cushman M, Johnson BS, King OD, Gitler AD, and Shorter J. *Prion-like disorders: blurring the divide between transmissibility and infectivity.* Journal of Cell Science, 2010. **123**(8): p. 1191-1201.
10. Mukherjee A, Morales-Scheihing D, Salvadores N, Moreno-Gonzalez I, Gonzalez C, Taylor-Presse K, Mendez N, Shahnawaz M, Gaber AO, Sabek OM, Fraga DW, and Soto C. *Induction of IAPP amyloid deposition and associated diabetic abnormalities by a prion-like mechanism.* The Journal of Experimental Medicine, 2017.
11. Martins VR, Beraldo FH, Hajj GN, Lopes MH, Lee KS, Prado MA, and Linden R. *Prion protein: orchestrating neurotrophic activities.* Curr Issues Mol Biol, 2010. **12**(2): p. 63-86.
12. Westergard L, Christensen HM, and Harris DA. *The Cellular Prion Protein (PrP(C)): Its Physiological Function and Role in Disease.* Biochimica et biophysica acta, 2007. **1772**(6): p. 629-644.
13. Málaga-Trillo E, Solis GP, Schrock Y, Geiss C, Luncz L, Thomanetz V, and Stuermer CAO. *Regulation of Embryonic Cell Adhesion by the Prion Protein.* PLoS Biology, 2009. **7**(3): p. e1000055.
14. Linden R, Martins VR, Prado MA, Cammarota M, Izquierdo I, and Brentani RR. *Physiology of the prion protein.* Physiol Rev, 2008. **88**(2): p. 673-728.
15. Roucou X, Gains M, and LeBlanc AC. *Neuroprotective functions of prion protein.* J Neurosci Res, 2004. **75**(2): p. 153-61.
16. Gasperini L, Meneghetti E, Pastore B, Benetti F, and Legname G. *Prion Protein and Copper Cooperatively Protect Neurons by Modulating NMDA Receptor Through S-nitrosylation.* Antioxidants & Redox Signaling, 2015. **22**(9): p. 772-784.

17. Pushie MJ, Pickering IJ, Martin GR, Tsutsui S, Jirik FR, and George GN. *Prion protein expression level alters regional copper, iron and zinc content in the mouse brain.* Metallomics, 2011. **3**(2): p. 206-214.
18. Büeler H, Aguzzi A, Sailer A, Greiner RA, Autenried P, Aguet M, and Weissmann C. *Mice devoid of PrP are resistant to scrapie.* Cell, 1993. **73**(7): p. 1339-1347.
19. Li A, Piccardo P, Barmada SJ, Ghetti B, and Harris DA. *Prion protein with an octapeptide insertion has impaired neuroprotective activity in transgenic mice.* The EMBO journal, 2007. **26**(11): p. 2777-2785.
20. Fevrier B, Vilette D, Archer F, Loew D, Faigle W, Vidal M, Laude H, and Raposo G. *Cells release prions in association with exosomes.* Proceedings of the National Academy of Sciences of the United States of America, 2004. **101**(26): p. 9683-9688.
21. Pinato G, Cojoc D, Lien LT, Ansuini A, Ban J, D'Este E, and Torre V. *Less than 5 Netrin-1 molecules initiate attraction but 200 Sema3A molecules are necessary for repulsion.* Scientific Reports, 2012. **2**: p. 675.
22. Sun B and Chiu DT. *Spatially and Temporally Resolved Delivery of Stimuli to Single Cells.* Journal of the American Chemical Society, 2003. **125**(13): p. 3702-3703.
23. Sun B and Chiu DT. *Determination of the Encapsulation Efficiency of Individual Vesicles Using Single-Vesicle Photolysis and Confocal Single-Molecule Detection.* Analytical Chemistry, 2005. **77**(9): p. 2770-2776.
24. Chen S, Mange A, Dong L, Lehmann S, and Schachner M. *Prion protein as trans-interacting partner for neurons is involved in neurite outgrowth and neuronal survival.* Mol Cell Neurosci, 2003. **22**(2): p. 227-33.
25. Kanaani J, Prusiner SB, Diacovo J, Baekkeskov S, and Legname G. *Recombinant prion protein induces rapid polarization and development of synapses in embryonic rat hippocampal neurons in vitro.* Journal of Neurochemistry, 2005. **95**(5): p. 1373-1386.
26. Santuccione A, Sytnyk V, Leshchyns'ka I, and Schachner M. *Prion protein recruits its neuronal receptor NCAM to lipid rafts to activate p59^{fyn} and to enhance neurite outgrowth.* The Journal of Cell Biology, 2005. **169**(2): p. 341-354.
27. Prusiner S. *Novel proteinaceous infectious particles cause scrapie.* Science, 1982. **216**(4542): p. 136-144.
28. Prusiner SB. *Prions.* Proceedings of the National Academy of Sciences of the United States of America, 1998. **95**(23): p. 13363-13383.
29. Pan KM, Baldwin M, Nguyen J, Gasset M, Serban A, Groth D, Mehlhorn I, Huang Z, Fletterick RJ, and Cohen FE. *Conversion of alpha-helices into beta-sheets features in the formation of the scrapie prion proteins.* Proceedings of the National Academy of Sciences, 1993. **90**(23): p. 10962-10966.
30. Colby DW and Prusiner SB. *Prions.* Cold Spring Harbor Perspectives in Biology, 2011. **3**(1): p. a006833.
31. Geschwind MD. *Prion Diseases.* Continuum (Minneapolis, Minn.), 2015. **21**(6 NEUROINFECTIOUS DISEASE): p. 1612-1638.
32. Bechtel K and Geschwind MD. *Ethics in Prion Disease.* Progress in neurobiology, 2013. **110**: p. 10.1016/j.pneurobio.2013.07.001.
33. Casalone C, Zanusso G, Acutis P, Ferrari S, Capucci L, Tagliavini F, Monaco S, and Caramelli M. *Identification of a second bovine amyloidotic spongiform encephalopathy: Molecular similarities with sporadic Creutzfeldt-Jakob disease.* Proceedings of the

National Academy of Sciences of the United States of America, 2004. **101**(9): p. 3065-3070.
34. Will RG. *Acquired prion disease: iatrogenic CJD, variant CJD, kuru.* Br Med Bull, 2003. **66**: p. 255-65.
35. Spencer MD, Knight RSG, and Will RG. *First hundred cases of variant Creutzfeldt-Jakob disease: retrospective case note review of early psychiatric and neurological features.* BMJ, 2002. **324**(7352): p. 1479-1482.
36. Stahl N and Prusiner SB. *Prions and prion proteins.* The FASEB Journal, 1991. **5**(13): p. 2799-2807.
37. Goldfarb L, Petersen R, Tabaton M, Brown P, LeBlanc A, Montagna P, Cortelli P, Julien J, Vital C, Pendelbury W, and et a. *Fatal familial insomnia and familial Creutzfeldt-Jakob disease: disease phenotype determined by a DNA polymorphism.* Science, 1992. **258**(5083): p. 806-808.
38. Hsiao K, Baker HF, Crow TJ, Poulter M, Owen F, Terwilliger JD, Westaway D, Ott J, and Prusiner SB. *Linkage of a prion protein missense variant to Gerstmann–Sträussler syndrome.* Nature, 1989. **338**: p. 342.
39. Goldgaber D, Goldfarb LG, Brown P, Asher DM, Brown WT, Lin S, Teener JW, Feinstone SM, Rubenstein R, Kascsak RJ, and et al. *Mutations in familial Creutzfeldt-Jakob disease and Gerstmann-Straussler-Scheinker's syndrome.* Exp Neurol, 1989. **106**(2): p. 204-6.
40. Mastrianni JA. *The genetics of prion diseases.* Genetics In Medicine, 2010. **12**: p. 187.
41. Hill AF, Desbruslais M, Joiner S, Sidle KCL, Gowland I, Collinge J, Doey LJ, and Lantos P. *The same prion strain causes vCJD and BSE.* Nature, 1997. **389**: p. 448.
42. Moore SJ, West Greenlee MH, Smith JD, Vrentas CE, Nicholson EM, and Greenlee JJ. *A Comparison of Classical and H-Type Bovine Spongiform Encephalopathy Associated with E211K Prion Protein Polymorphism in Wild-Type and EK211 Cattle Following Intracranial Inoculation.* Frontiers in Veterinary Science, 2016. **3**: p. 78.
43. Dudas S and Czub S. *Atypical BSE: Current Knowledge and Knowledge Gaps.* Food Safety, 2017. **advpub**.
44. Miller MW and Williams ES. *Chronic wasting disease of cervids.* Curr Top Microbiol Immunol, 2004. **284**: p. 193-214.
45. Stahl N, Borchelt DR, Hsiao K, and Prusiner SB. *Scrapie prion protein contains a phosphatidylinositol glycolipid.* Cell, 1987. **51**(2): p. 229-240.
46. Donne DG, Viles JH, Groth D, Mehlhorn I, James TL, Cohen FE, Prusiner SB, Wright PE, and Dyson HJ. *Structure of the recombinant full-length hamster prion protein PrP(29–231): The N terminus is highly flexible.* Proceedings of the National Academy of Sciences of the United States of America, 1997. **94**(25): p. 13452-13457.
47. Chakrabarti O, Ashok A, and Hegde RS. *Prion protein biosynthesis and its emerging role in neurodegeneration.* Trends in biochemical sciences, 2009. **34**(6): p. 287-295.
48. Hornemann S, Korth C, Oesch B, Riek R, Wider G, Wüthrich K, and Glockshuber R. *Recombinant full-length murine prion protein, mPrP(23–231): purification and spectroscopic characterization.* FEBS Letters, 1997. **413**(2): p. 277-281.
49. Riek R, Hornemann S, Wider G, Billeter M, Glockshuber R, and Wüthrich K. *NMR structure of the mouse prion protein domain PrP(121–231).* Nature, 1996. **382**: p. 180.
50. Lau A, McDonald A, Daude N, Mays CE, Walter ED, Aglietti R, Mercer RCC, Wohlgemuth S, van der Merwe J, Yang J, Gapeshina H, Kim C, Grams J, Shi B, Wille H,

Balachandran A, Schmitt-Ulms G, Safar JG, Millhauser GL, and Westaway D. *Octarepeat region flexibility impacts prion function, endoproteolysis and disease manifestation.* EMBO Molecular Medicine, 2015. **7**(3): p. 339-356.
51. Walter ED, Stevens DJ, Spevacek AR, Visconte MP, Dei Rossi A, and Millhauser GL. *Copper binding extrinsic to the octarepeat region in the prion protein.* Curr Protein Pept Sci, 2009. **10**(5): p. 529-35.
52. Jackson GS, Murray I, Hosszu LLP, Gibbs N, Waltho JP, Clarke AR, and Collinge J. *Location and properties of metal-binding sites on the human prion protein.* Proceedings of the National Academy of Sciences, 2001. **98**(15): p. 8531-8535.
53. Chattopadhyay M, Walter ED, Newell DJ, Jackson PJ, Aronoff-Spencer E, Peisach J, Gerfen GJ, Bennett B, Antholine WE, and Millhauser GL. *The Octarepeat Domain of the Prion Protein Binds Cu(II) with Three Distinct Coordination Modes at pH 7.4.* Journal of the American Chemical Society, 2005. **127**(36): p. 12647-12656.
54. H.C. A, Johannes P, Berta P, Frank D, Clemens F, Susanne K, and Markus G. *Roles of endoproteolytic α-cleavage and shedding of the prion protein in neurodegeneration.* The FEBS Journal, 2013. **280**(18): p. 4338-4347.
55. McDonald AJ and Millhauser GL. *PrP overdrive: Does inhibition of α-cleavage contribute to PrP(C) toxicity and prion disease?* Prion, 2014. **8**(2): p. 183-191.
56. Chen SG, Teplow DB, Parchi P, Teller JK, Gambetti P, and Autilio-Gambetti L. *Truncated Forms of the Human Prion Protein in Normal Brain and in Prion Diseases.* Journal of Biological Chemistry, 1995. **270**(32): p. 19173-19180.
57. Altmeppen HC, Puig B, Dohler F, Thurm DK, Falker C, Krasemann S, and Glatzel M. *Proteolytic processing of the prion protein in health and disease.* American Journal of Neurodegenerative Disease, 2012. **1**(1): p. 15-31.
58. Liang J, Wang W, Sorensen D, Medina S, Ilchenko S, Kiselar J, Surewicz WK, Booth SA, and Kong Q. *Cellular Prion Protein Regulates Its Own α-Cleavage through ADAM8 in Skeletal Muscle.* The Journal of Biological Chemistry, 2012. **287**(20): p. 16510-16520.
59. Westergard L, Turnbaugh JA, and Harris DA. *A Naturally Occurring C-terminal Fragment of the Prion Protein (PrP) Delays Disease and Acts as a Dominant-negative Inhibitor of PrP(Sc) Formation.* The Journal of Biological Chemistry, 2011. **286**(51): p. 44234-44242.
60. Sunyach C, Cisse MA, da Costa CA, Vincent B, and Checler F. *The C-terminal Products of Cellular Prion Protein Processing, C1 and C2, Exert Distinct Influence on p53-dependent Staurosporine-induced Caspase-3 Activation.* Journal of Biological Chemistry, 2007. **282**(3): p. 1956-1963.
61. Guillot-Sestier M-V, Sunyach C, Druon C, Scarzello S, and Checler F. *The α-Secretase-derived N-terminal Product of Cellular Prion, N1, Displays Neuroprotective Function in Vitro and in Vivo.* Journal of Biological Chemistry, 2009. **284**(51): p. 35973-35986.
62. McMahon HEM, Mangé A, Nishida N, Créminon C, Casanova D, and Lehmann S. *Cleavage of the Amino Terminus of the Prion Protein by Reactive Oxygen Species.* Journal of Biological Chemistry, 2001. **276**(3): p. 2286-2291.
63. Watt NT, Taylor DR, Gillott A, Thomas DA, Perera WSS, and Hooper NM. *Reactive Oxygen Species-mediated β-Cleavage of the Prion Protein in the Cellular Response to Oxidative Stress.* Journal of Biological Chemistry, 2005. **280**(43): p. 35914-35921.

64. Stahl N, Baldwin MA, Teplow DB, Hood L, Gibson BW, Burlingame AL, and Prusiner SB. *Structural studies of the scrapie prion protein using mass spectrometry and amino acid sequencing.* Biochemistry, 1993. **32**(8): p. 1991-2002.
65. Haigh CL, Drew SC, Boland MP, Masters CL, Barnham KJ, Lawson VA, and Collins SJ. *Dominant roles of the polybasic proline motif and copper in the PrP23-89-mediated stress protection response.* Journal of Cell Science, 2009. **122**(10): p. 1518-1528.
66. Lewis V, Johanssen VA, Crouch PJ, Klug GM, Hooper NM, and Collins SJ. *Prion protein "gamma-cleavage": characterizing a novel endoproteolytic processing event.* Cellular and Molecular Life Sciences, 2016. **73**(3): p. 667-683.
67. Hay B, Prusiner SB, and Lingappa VR. *Evidence for a secretory form of the cellular prion protein.* Biochemistry, 1987. **26**(25): p. 8110-5.
68. Tagliavini F, Prelli F, Porro M, Salmona M, Bugiani O, and Frangione B. *A soluble form of prion protein in human cerebrospinal fluid: Implications for prion-related encephalopathies.* Biochemical and Biophysical Research Communications, 1992. **184**(3): p. 1398-1404.
69. Parizek P, Roeckl C, Weber J, Flechsig E, Aguzzi A, and Raeber AJ. *Similar Turnover and Shedding of the Cellular Prion Protein in Primary Lymphoid and Neuronal Cells.* Journal of Biological Chemistry, 2001. **276**(48): p. 44627-44632.
70. Parkin ET, Watt NT, Turner AJ, and Hooper NM. *Dual Mechanisms for Shedding of the Cellular Prion Protein.* Journal of Biological Chemistry, 2004. **279**(12): p. 11170-11178.
71. Borchelt DR, Rogers M, Stahl N, Telling G, and Prusiner SB. *Release of the cellular prion protein from cultured cells after loss of its glycoinositol phospholipid anchor.* Glycobiology, 1993. **3**(4): p. 319-29.
72. S. LFR, P. AC, G. MA, Regina N, R. BR, and R. MV. *Cellular prion protein expression in astrocytes modulates neuronal survival and differentiation.* Journal of Neurochemistry, 2007. **103**(6): p. 2164-2176.
73. Meier P, Genoud N, Prinz M, Maissen M, Rülicke T, Zurbriggen A, Raeber AJ, and Aguzzi A. *Soluble Dimeric Prion Protein Binds PrP^{Sc} In Vivo and Antagonizes Prion Disease.* Cell, 2003. **113**(1): p. 49-60.
74. Chesebro B, Trifilo M, Race R, Meade-White K, Teng C, LaCasse R, Raymond L, Favara C, Baron G, Priola S, Caughey B, Masliah E, and Oldstone M. *Anchorless Prion Protein Results in Infectious Amyloid Disease Without Clinical Scrapie.* Science, 2005. **308**(5727): p. 1435-1439.
75. Mattei V, Barenco MG, Tasciotti V, Garofalo T, Longo A, Boller K, Löwer J, Misasi R, Montrasio F, and Sorice M. *Paracrine Diffusion of PrPC and Propagation of Prion Infectivity by Plasma Membrane-Derived Microvesicles.* PLOS ONE, 2009. **4**(4): p. e5057.
76. Clemens F, Alexander H, Inga G, Frank D, Hermann A, Christian B, Robin S, Dana T, Florian W, Pooja J, Claudia V, Susanne K, and Markus G. *Exosomal cellular prion protein drives fibrillization of amyloid beta and counteracts amyloid beta-mediated neurotoxicity.* Journal of Neurochemistry, 2016. **137**(1): p. 88-100.
77. Nishida N, Katamine S, Shigematsu K, Nakatani A, Sakamoto N, Hasegawa S, Nakaoke R, Atarashi R, Kataoka Y, and Miyamoto T. *Prion protein is necessary for latent learning and long-term memory retention.* Cell Mol Neurobiol, 1997. **17**(5): p. 537-45.

78. Coitinho AS, Roesler R, Martins VR, Brentani RR, and Izquierdo I. *Cellular prion protein ablation impairs behavior as a function of age.* NeuroReport, 2003. **14**(10): p. 1375-1379.
79. Criado JR, Sánchez-Alavez M, Conti B, Giacchino JL, Wills DN, Henriksen SJ, Race R, Manson JC, Chesebro B, and Oldstone MBA. *Mice devoid of prion protein have cognitive deficits that are rescued by reconstitution of PrP in neurons.* Neurobiology of Disease, 2005. **19**(1): p. 255-265.
80. S. CA, O. FAR, H. LM, M. HGN, Rafael R, Roger W, I. RJ, Martin C, Ivan I, R. MV, and R. BR. *The interaction between prion protein and laminin modulates memory consolidation.* European Journal of Neuroscience, 2006. **24**(11): p. 3255-3264.
81. Zanata SM, Lopes MH, Mercadante AF, Hajj GNM, Chiarini LB, Nomizo R, Freitas ARO, Cabral ALB, Lee KS, Juliano MA, de Oliveira E, Jachieri SG, Burlingame A, Huang L, Linden R, Brentani RR, and Martins VR. *Stress-inducible protein 1 is a cell surface ligand for cellular prion that triggers neuroprotection.* The EMBO Journal, 2002. **21**(13): p. 3307-3316.
82. Coitinho AS, Lopes MH, Hajj GNM, Rossato JI, Freitas AR, Castro CC, Cammarota M, Brentani RR, Izquierdo I, and Martins VR. *Short-term memory formation and long-term memory consolidation are enhanced by cellular prion association to stress-inducible protein 1.* Neurobiology of Disease, 2007. **26**(1): p. 282-290.
83. Berr C, Richard F, Dufouil C, Amant C, Alperovitch A, and Amouyel P. *Polymorphism of the prion protein is associated with cognitive impairment in the elderly.* The EVA study, 1998. **51**(3): p. 734-737.
84. Papassotiropoulos A, Wollmer MA, Aguzzi A, Hock C, Nitsch RM, and de Quervain DJF. *The prion gene is associated with human long-term memory.* Human Molecular Genetics, 2005. **14**(15): p. 2241-2246.
85. Leighton PLA, Nadolski NJ, Morrill A, Hamilton TJ, and Allison WT. *An ancient conserved role for prion protein in learning and memory.* Biology Open, 2018. **7**(1): p. bio025734.
86. Fournier JG, Escaig-Haye F, Billette de Villemeur T, and Robain O. *Ultrastructural localization of cellular prion protein (PrPc) in synaptic boutons of normal hamster hippocampus.* C R Acad Sci III, 1995. **318**(3): p. 339-44.
87. Herms J, Tings T, Gall S, Madlung A, Giese A, Siebert H, Schürmann P, Windl O, Brose N, and Kretzschmar H. *Evidence of Presynaptic Location and Function of the Prion Protein.* The Journal of Neuroscience, 1999. **19**(20): p. 8866-8875.
88. Haeberlé AM, Ribaut-Barassin C, Bombarde G, Mariani J, Hunsmann G, Grassi J, and Bailly Y. *Synaptic prion protein immuno-reactivity in the rodent cerebellum.* Microscopy Research and Technique, 2000. **50**(1): p. 66-75.
89. Nicole S, Raymonde H, Katia R, Luigi DG, Elisabeth T, Martial R, Philippe F, and L. MK. *Developmental expression of the cellular prion protein in elongating axons.* European Journal of Neuroscience, 2002. **15**(7): p. 1163-1177.
90. L. MK, Raymonde H, Christophe C, Isabelle L, and Luigi DG. *Enhanced detection and retrograde axonal transport of PrPc in peripheral nerve.* Journal of Neurochemistry, 2004. **88**(1): p. 155-160.
91. K.L. M, Raymonde H, C. BK, Hervé V, and Luigi DG. *Axonal transport of the cellular prion protein is increased during axon regeneration.* Journal of Neurochemistry, 2005. **92**(5): p. 1044-1053.

92. Caiati MD, Safiulina VF, Fattorini G, Sivakumaran S, Legname G, and Cherubini E. *PrPC Controls via Protein Kinase A the Direction of Synaptic Plasticity in the Immature Hippocampus.* The Journal of Neuroscience, 2013. **33**(7): p. 2973-2983.
93. R. BD, St.J. NR, and Laura C. *Lack of prion protein expression results in a neuronal phenotype sensitive to stress.* Journal of Neuroscience Research, 2002. **67**(2): p. 211-224.
94. Weise J, Sandau R, Schwarting S, Crome O, Wrede A, Schulz-Schaeffer W, Zerr I, and Bahr M. *Deletion of cellular prion protein results in reduced Akt activation, enhanced postischemic caspase-3 activation, and exacerbation of ischemic brain injury.* Stroke, 2006. **37**(5): p. 1296-300.
95. Takashi O, Akikazu S, Hirokazu T, and Shigeyoshi I. *Review of studies that have used knockout mice to assess normal function of prion protein under immunological or pathophysiological stress.* Microbiology and Immunology, 2014. **58**(7): p. 361-374.
96. Boon-Seng W, Tong L, Ruliang L, Tao P, B. PR, A. SM, Pierluigi G, George P, C. MJ, R. BD, and Man-Sun S. *Increased levels of oxidative stress markers detected in the brains of mice devoid of prion protein.* Journal of Neurochemistry, 2001. **76**(2): p. 565-572.
97. Khosravani H, Zhang Y, Tsutsui S, Hameed S, Altier C, Hamid J, Chen L, Villemaire M, Ali Z, Jirik FR, and Zamponi GW. *Prion protein attenuates excitotoxicity by inhibiting NMDA receptors.* The Journal of Cell Biology, 2008. **181**(3): p. 551-565.
98. You H, Tsutsui S, Hameed S, Kannanayakal TJ, Chen L, Xia P, Engbers JDT, Lipton SA, Stys PK, and Zamponi GW. *Aβ neurotoxicity depends on interactions between copper ions, prion protein, and N-methyl-d-aspartate receptors.* Proceedings of the National Academy of Sciences of the United States of America, 2012. **109**(5): p. 1737-1742.
99. K. SP, Haitao Y, and W. ZG. *Copper-dependent regulation of NMDA receptors by cellular prion protein: implications for neurodegenerative disorders.* The Journal of Physiology, 2012. **590**(6): p. 1357-1368.
100. Fluharty BR, Biasini E, Stravalaci M, Sclip A, Diomede L, Balducci C, La Vitola P, Messa M, Colombo L, Forloni G, Borsello T, Gobbi M, and Harris DA. *An N-terminal Fragment of the Prion Protein Binds to Amyloid-β Oligomers and Inhibits Their Neurotoxicity in Vivo.* Journal of Biological Chemistry, 2013. **288**(11): p. 7857-7866.
101. Steele AD, Emsley JG, Özdinler PH, Lindquist S, and Macklis JD. *Prion protein (PrP(c)) positively regulates neural precursor proliferation during developmental and adult mammalian neurogenesis.* Proceedings of the National Academy of Sciences of the United States of America, 2006. **103**(9): p. 3416-3421.
102. G. ST, R. SI, Bruno C-S, Paula LA, R. MV, and H. LM. *Enhanced Neural Progenitor/Stem Cells Self-Renewal via the Interaction of Stress-Inducible Protein 1 with the Prion Protein.* STEM CELLS, 2011. **29**(7): p. 1126-1136.
103. Deng W, Aimone JB, and Gage FH. *New neurons and new memories: how does adult hippocampal neurogenesis affect learning and memory?* Nature Reviews Neuroscience, 2010. **11**: p. 339.
104. Doeppner TR, Kaltwasser B, Schlechter J, Jaschke J, Kilic E, Bähr M, Hermann DM, and Weise J. *Cellular prion protein promotes post-ischemic neuronal survival, angioneurogenesis and enhances neural progenitor cell homing via proteasome inhibition.* Cell Death & Disease, 2015. **6**(12): p. e2024.
105. Relaño-Ginès A, Gabelle A, Hamela C, Belondrade M, Casanova D, Mourton-Gilles C, Lehmann S, and Crozet C. *Prion Replication Occurs in Endogenous Adult Neural Stem*

Cells and Alters Their Neuronal Fate: Involvement of Endogenous Neural Stem Cells in Prion Diseases. PLOS Pathogens, 2013. **9**(8): p. e1003485.
106. Rieger R, Edenhofer F, Lasmézas CI, and Weiss S. *The human 37-kDa laminin receptor precursor interacts with the prion protein in eukaryotic cells.* Nature Medicine, 1997. **3**: p. 1383.
107. Hundt C, Peyrin J-M, Haïk S, Gauczynski S, Leucht C, Rieger R, Riley ML, Deslys J-P, Dormont D, Lasmézas CI, and Weiss S. *Identification of interaction domains of the prion protein with its 37-kDa/67-kDa laminin receptor.* The EMBO Journal, 2001. **20**(21): p. 5876-5886.
108. Gauczynski S, Peyrin J-M, Haïk S, Leucht C, Hundt C, Rieger R, Krasemann S, Deslys J-P, Dormont D, Lasmézas CI, and Weiss S. *The 37-kDa/67-kDa laminin receptor acts as the cell-surface receptor for the cellular prion protein.* The EMBO Journal, 2001. **20**(21): p. 5863-5875.
109. Graner E, Mercadante AF, Zanata SM, Forlenza OV, Cabral ALB, Veiga SS, Juliano MA, Roesler R, Walz R, Minetti A, Izquierdo I, Martins VR, and Brentani RR. *Cellular prion protein binds laminin and mediates neuritogenesis.* Molecular Brain Research, 2000. **76**(1): p. 85-92.
110. Hajj GNM, Lopes MH, Mercadante AF, Veiga SS, da Silveira RB, Santos TG, Ribeiro KCB, Juliano MA, Jacchieri SG, Zanata SM, and Martins VR. *Cellular prion protein interaction with vitronectin supports axonal growth and is compensated by integrins.* Journal of Cell Science, 2007. **120**(11): p. 1915-1926.
111. Lopes MH, Hajj GNM, Muras AG, Mancini GL, Castro RMPS, Ribeiro KCB, Brentani RR, Linden R, and Martins VR. *Interaction of Cellular Prion and Stress-Inducible Protein 1 Promotes Neuritogenesis and Neuroprotection by Distinct Signaling Pathways.* The Journal of Neuroscience, 2005. **25**(49): p. 11330-11339.
112. Caetano FA, Lopes MH, Hajj GNM, Machado CF, Arantes CP, Magalhães AC, Vieira MDPB, Américo TA, Massensini AR, Priola SA, Vorberg I, Gomez MV, Linden R, Prado VF, Martins VR, and Prado MAM. *Endocytosis of prion protein is required for ERK1/2 signaling induced by stress-inducible protein 1.* The Journal of neuroscience : the official journal of the Society for Neuroscience, 2008. **28**(26): p. 6691-6702.
113. Schmitt-Ulms G, Legname G, Baldwin MA, Ball HL, Bradon N, Bosque PJ, Crossin KL, Edelman GM, DeArmond SJ, Cohen FE, and Prusiner SB. *Binding of neural cell adhesion molecules (N-CAMs) to the cellular prion protein11Edited by P. E. Wright.* Journal of Molecular Biology, 2001. **314**(5): p. 1209-1225.
114. Slapšak U, Salzano G, Amin L, Abskharon RNN, Ilc G, Zupančič B, Biljan I, Plavec J, Giachin G, and Legname G. *The N Terminus of the Prion Protein Mediates Functional Interactions with the Neuronal Cell Adhesion Molecule (NCAM) Fibronectin Domain.* The Journal of Biological Chemistry, 2016. **291**(42): p. 21857-21868.
115. Zatta P and Frank A. *Copper deficiency and neurological disorders in man and animals.* Brain Research Reviews, 2007. **54**(1): p. 19-33.
116. Dobrowolska J, Dehnhardt M, Matusch A, Zoriy M, Palomero-Gallagher N, Koscielniak P, Zilles K, and Becker JS. *Quantitative imaging of zinc, copper and lead in three distinct regions of the human brain by laser ablation inductively coupled plasma mass spectrometry.* Talanta, 2008. **74**(4): p. 717-723.

117. Que EL, Domaille DW, and Chang CJ. *Metals in Neurobiology: Probing Their Chemistry and Biology with Molecular Imaging.* Chemical Reviews, 2008. **108**(5): p. 1517-1549.
118. E.D. G, B.A. E, and R.E. M. *Copper signaling in the mammalian nervous system: Synaptic effects.* Journal of Neuroscience Research, 2013. **91**(1): p. 2-19.
119. Telianidis J, Hung YH, Materia S, and Fontaine SL. *Role of the P-Type ATPases, ATP7A and ATP7B in brain copper homeostasis.* Frontiers in Aging Neuroscience, 2013. **5**: p. 44.
120. Turski ML and Thiele DJ. *New Roles for Copper Metabolism in Cell Proliferation, Signaling, and Disease.* The Journal of Biological Chemistry, 2009. **284**(2): p. 717-721.
121. Schlief ML and Gitlin JD. *Copper homeostasis in the CNS.* Molecular Neurobiology, 2006. **33**(2): p. 81-90.
122. Rajan KS, Colburn RW, and Davis JM. *Distribution of metal ions in the subcellular fractions of several rat brain areas.* Life Sciences, 1976. **18**(4): p. 423-431.
123. Weiser T and Wienrich M. *The effects of copper ions on glutamate receptors in cultured rat cortical neurons.* Brain Research, 1996. **742**(1): p. 211-218.
124. Kim H and Macdonald RL. *An N-Terminal Histidine Is the Primary Determinant of α Subunit-Dependent Cu²⁺ Sensitivity of αβ3γ2L GABA_A Receptors.* Molecular Pharmacology, 2003. **64**(5): p. 1145-1152.
125. S. AC, C. SR, Xudong H, D. MR, D. JW, P. FD, E. TR, and I. BA. *Characterization of Copper Interactions with Alzheimer Amyloid β Peptides.* Journal of Neurochemistry, 2000. **75**(3): p. 1219-1233.
126. Huang X, Cuajungco MP, Atwood CS, Hartshorn MA, Tyndall JDA, Hanson GR, Stokes KC, Leopold M, Multhaup G, Goldstein LE, Scarpa RC, Saunders AJ, Lim J, Moir RD, Glabe C, Bowden EF, Masters CL, Fairlie DP, Tanzi RE, and Bush AI. *Cu(II) Potentiation of Alzheimer Aβ Neurotoxicity: CORRELATION WITH CELL-FREE HYDROGEN PEROXIDE PRODUCTION AND METAL REDUCTION.* Journal of Biological Chemistry, 1999. **274**(52): p. 37111-37116.
127. You H, Tsutsui S, Hameed S, Kannanayakal TJ, Chen L, Xia P, Engbers JDT, Lipton SA, Stys PK, and Zamponi GW. *Aβ neurotoxicity depends on interactions between copper ions, prion protein, and N-methyl-d-aspartate receptors.* Proceedings of the National Academy of Sciences, 2012. **109**(5): p. 1737-1742.
128. Harris ZL and Gitlin JD. *Genetic and molecular basis for copper toxicity.* The American Journal of Clinical Nutrition, 1996. **63**(5): p. 836S-841S.
129. Waggoner DJ, Bartnikas TB, and Gitlin JD. *The Role of Copper in Neurodegenerative Disease.* Neurobiology of Disease, 1999. **6**(4): p. 221-230.
130. Walter ED, Stevens DJ, Visconte MP, and Millhauser GL. *The Prion Protein is a Combined Zinc and Copper Binding Protein: Zn(2+) Alters the Distribution of Cu(2+) Coordination Modes.* Journal of the American Chemical Society, 2007. **129**(50): p. 15440-15441.
131. Aronoff-Spencer E, Burns CS, Avdievich NI, Gerfen GJ, Peisach J, Antholine WE, Ball HL, Cohen FE, Prusiner SB, and Millhauser GL. *Identification of the Cu(2+) Binding Sites in the N-Terminal Domain of the Prion Protein by EPR and CD Spectroscopy.* Biochemistry, 2000. **39**(45): p. 13760-13771.

132. Miura T, Hori-i A, Mototani H, and Takeuchi H. *Raman Spectroscopic Study on the Copper(II) Binding Mode of Prion Octapeptide and Its pH Dependence.* Biochemistry, 1999. **38**(35): p. 11560-11569.
133. Wells Mark A, Jackson Graham S, Jones S, Hosszu Laszlo L P, Craven C J, Clarke Anthony R, Collinge J, and Waltho Jonathan P. *A reassessment of copper(II) binding in the full-length prion protein.* Biochemical Journal, 2006. **399**(Pt 3): p. 435-444.
134. Giachin G, Mai PT, Tran TH, Salzano G, Benetti F, Migliorati V, Arcovito A, Longa SD, Mancini G, D'Angelo P, and Legname G. *The non-octarepeat copper binding site of the prion protein is a key regulator of prion conversion.* Scientific Reports, 2015. **5**: p. 15253.
135. Burns CS, Aronoff-Spencer E, Legname G, Prusiner SB, Antholine WE, Gerfen GJ, Peisach J, and Millhauser GL. *Copper Coordination in the Full-Length, Recombinant Prion Protein†.* Biochemistry, 2003. **42**(22): p. 6794-6803.
136. Kramer ML, Kratzin HD, Schmidt B, Römer A, Windl O, Liemann S, Hornemann S, and Kretzschmar H. *Prion Protein Binds Copper within the Physiological Concentration Range.* Journal of Biological Chemistry, 2001. **276**(20): p. 16711-16719.
137. Burns CS, Aronoff-Spencer E, Legname G, Prusiner SB, Antholine WE, Gerfen GJ, Peisach J, and Millhauser GL. *Copper Coordination in the Full-Length, Recombinant Prion Protein.* Biochemistry, 2003. **42**(22): p. 6794-6803.
138. Vassallo N and Herms J. *Cellular prion protein function in copper homeostasis and redox signalling at the synapse.* Journal of Neurochemistry, 2003. **86**(3): p. 538-544.
139. Millhauser GL. *Copper and the Prion Protein: Methods, Structures, Function, and Disease.* Annual review of physical chemistry, 2007. **58**: p. 299-320.
140. Berlett BS and Stadtman ER. *Protein Oxidation in Aging, Disease, and Oxidative Stress.* Journal of Biological Chemistry, 1997. **272**(33): p. 20313-20316.
141. Bounhar Y, Zhang Y, Goodyer CG, and LeBlanc A. *Prion Protein Protects Human Neurons against Bax-mediated Apoptosis.* Journal of Biological Chemistry, 2001. **276**(42): p. 39145-39149.
142. Brown LR and Harris DA. *Copper and zinc cause delivery of the prion protein from the plasma membrane to a subset of early endosomes and the Golgi.* Journal of Neurochemistry, 2003. **87**(2): p. 353-363.
143. Pauly PC and Harris DA. *Copper Stimulates Endocytosis of the Prion Protein.* Journal of Biological Chemistry, 1998. **273**(50): p. 33107-33110.
144. Whittal RM, Ball HL, Cohen FE, Burlingame AL, Prusiner SB, and Baldwin MA. *Copper binding to octarepeat peptides of the prion protein monitored by mass spectrometry.* Protein Science : A Publication of the Protein Society, 2000. **9**(2): p. 332-343.
145. Miura T, Sasaki S, Toyama A, and Takeuchi H. *Copper Reduction by the Octapeptide Repeat Region of Prion Protein: pH Dependence and Implications in Cellular Copper Uptake.* Biochemistry, 2005. **44**(24): p. 8712-8720.
146. McDonald AJ, Dibble JP, Evans EGB, and Millhauser GL. *A New Paradigm for Enzymatic Control of α-Cleavage and β-Cleavage of the Prion Protein.* Journal of Biological Chemistry, 2014. **289**(2): p. 803-813.
147. McKenzie D, Bartz J, Mirwald J, Olander D, Marsh R, and Aiken J. *Reversibility of Scrapie Inactivation Is Enhanced by Copper.* Journal of Biological Chemistry, 1998. **273**(40): p. 25545-25547.

148. Wadsworth JDF, Hill AF, Joiner S, Jackson GS, Clarke AR, and Collinge J. *Strain-specific prion-protein conformation determined by metal ions.* Nature Cell Biology, 1999. **1**: p. 55.
149. Quaglio E, Chiesa R, and Harris DA. *Copper Converts the Cellular Prion Protein into a Protease-resistant Species That Is Distinct from the Scrapie Isoform.* Journal of Biological Chemistry, 2001. **276**(14): p. 11432-11438.
150. Sigurdsson EM, Brown DR, Alim MA, Scholtzova H, Carp R, Meeker HC, Prelli F, Frangione B, and Wisniewski T. *Copper Chelation Delays the Onset of Prion Disease.* Journal of Biological Chemistry, 2003. **278**(47): p. 46199-46202.
151. Bocharova OV, Breydo L, Salnikov VV, and Baskakov IV. *Copper(II) Inhibits in Vitro Conversion of Prion Protein into Amyloid Fibrils.* Biochemistry, 2005. **44**(18): p. 6776-6787.
152. Fischer M, Rülicke T, Raeber A, Sailer A, Moser M, Oesch B, Brandner S, Aguzzi A, and Weissmann C. *Prion protein (PrP) with amino-proximal deletions restoring susceptibility of PrP knockout mice to scrapie.* The EMBO Journal, 1996. **15**(6): p. 1255-1264.
153. Flechsig E, Shmerling D, Hegyi I, Raeber AJ, Fischer M, Cozzio A, von Mering C, Aguzzi A, and Weissmann C. *Prion Protein Devoid of the Octapeptide Repeat Region Restores Susceptibility to Scrapie in PrP Knockout Mice.* Neuron, 2000. **27**(2): p. 399-408.
154. Moore RA, Herzog C, Errett J, Kocisko DA, Arnold KM, Hayes SF, and Priola SA. *Octapeptide repeat insertions increase the rate of protease-resistant prion protein formation.* Protein Science : A Publication of the Protein Society, 2006. **15**(3): p. 609-619.
155. Stevens DJ, Walter ED, Rodríguez A, Draper D, Davies P, Brown DR, and Millhauser GL. *Early Onset Prion Disease from Octarepeat Expansion Correlates with Copper Binding Properties.* PLoS Pathogens, 2009. **5**(4): p. e1000390.
156. Cox DL, Pan J, and Singh RRP. *A Mechanism for Copper Inhibition of Infectious Prion Conversion.* Biophysical Journal, 2006. **91**(2): p. L11-L13.
157. Novitskaya V, Bocharova OV, Bronstein I, and Baskakov IV. *Amyloid Fibrils of Mammalian Prion Protein Are Highly Toxic to Cultured Cells and Primary Neurons.* Journal of Biological Chemistry, 2006. **281**(19): p. 13828-13836.
158. Hu PP and Huang CZ. *Prion protein: structural features and related toxicity.* Acta Biochimica et Biophysica Sinica, 2013. **45**(6): p. 435-441.
159. Brown DR, Nicholas RSJ, and Canevari L. *Lack of prion protein expression results in a neuronal phenotype sensitive to stress.* Journal of Neuroscience Research, 2002. **67**(2): p. 211-224.
160. bio Klamt F, Dal-Pizzol F, Conte da Frota ML, Walz R, Andrades ME, da Silva EG, Brentani RR, n Izquierdo I, and Fonseca Moreira JC. *Imbalance of antioxidant defense in mice lacking cellular prion protein.* Free Radical Biology and Medicine, 2001. **30**(10): p. 1137-1144.
161. Weissmann C and Flechsig E. *PrP knock-out and PrP transgenic mice in prion research.* British Medical Bulletin, 2003. **66**(1): p. 43-60.
162. Swietnicki W, Petersen RB, Gambetti P, and Surewicz WK. *Familial Mutations and the Thermodynamic Stability of the Recombinant Human Prion Protein.* Journal of Biological Chemistry, 1998. **273**(47): p. 31048-31052.

163. Kim H-J, Choi H-S, Park J-H, Kim M-J, Lee H-g, Petersen RB, Kim Y-S, Park J-B, and Choi E-K. *Regulation of RhoA activity by the cellular prion protein.* Cell Death & Disease, 2017. **8**(3): p. e2668.
164. Westergard L, Christensen HM, and Harris DA. *The cellular prion protein (PrPC): Its physiological function and role in disease.* Biochimica et Biophysica Acta (BBA) - Molecular Basis of Disease, 2007. **1772**(6): p. 629-644.
165. van den Ent F and Löwe J. *RF cloning: A restriction-free method for inserting target genes into plasmids.* Journal of Biochemical and Biophysical Methods, 2006. **67**(1): p. 67-74.
166. Giachin G, Narkiewicz J, Scaini D, Ngoc AT, Margon A, Sequi P, Leita L, and Legname G. *Prion Protein Interaction with Soil Humic Substances: Environmental Implications.* PLOS ONE, 2014. **9**(6): p. e100016.
167. Hub HH, Zimmermann U, and Ringsdorf H. *Preparation of large unilamellar vesicles.* FEBS Letters, 1982. **140**(2): p. 254-256.
168. Pinato G, Raffaelli T, D'Este E, Tavano F, and Cojoc D-A. *Optical delivery of liposome encapsulated chemical stimuli to neuronal cells*. 2011. SPIE.
169. Göttfert F, Wurm Christian A, Mueller V, Berning S, Cordes Volker C, Honigmann A, and Hell Stefan W. *Coaligned Dual-Channel STED Nanoscopy and Molecular Diffusion Analysis at 20 nm Resolution.* Biophysical Journal, 2013. **105**(1): p. L01-L03.
170. Berens P. *CircStat: A MATLAB Toolbox for Circular Statistics.* 2009, 2009. **31**(10): p. 21.
171. Amin L, Nguyen XTA, Rolle IG, Este E, Giachin G, Tran TH, Šerbec VČ, Cojoc D, and Legname G. *Characterization of prion protein function by focal neurite stimulation.* Journal of Cell Science, 2016.
172. Loubet D, Dakowski C, Pietri M, Pradines E, Bernard S, Callebert J, Ardila-Osorio H, Mouillet-Richard S, Launay JM, Kellermann O, and Schneider B. *Neuritogenesis: the prion protein controls beta1 integrin signaling activity.* Faseb j, 2012. **26**(2): p. 678-90.
173. Hornemann S, Schorn C, and Wüthrich K. *NMR structure of the bovine prion protein isolated from healthy calf brains.* EMBO Reports, 2004. **5**(12): p. 1159-1164.
174. Redecke L, Binder S, Elmallah MIY, Broadbent R, Tilkorn C, Schulz B, May P, Goos A, Eich A, Rübhausen M, and Betzel C. *UV-light-induced conversion and aggregation of prion proteins.* Free Radical Biology and Medicine, 2009. **46**(10): p. 1353-1361.
175. Premzl M, Sangiorgio L, Strumbo B, Marshall Graves JA, Simonic T, and Gready JE. *Shadoo, a new protein highly conserved from fish to mammals and with similarity to prion protein.* Gene, 2003. **314**: p. 89-102.
176. Moore SW, Tessier-Lavigne M, and Kennedy TE, *Netrins and Their receptors*, in *Axon Growth and Guidance*, D. Bagnard, Editor. 2007, Springer New York: New York, NY. p. 17-31.
177. Barmada S, Piccardo P, Yamaguchi K, Ghetti B, and Harris DA. *GFP-tagged prion protein is correctly localized and functionally active in the brains of transgenic mice.* Neurobiology of Disease, 2004. **16**(3): p. 527-537.
178. Bian J, Nazor KE, Angers R, Jernigan M, Seward T, Centers A, Green M, and Telling GC. *GFP-tagged PrP supports compromised prion replication in transgenic mice.* Biochemical and Biophysical Research Communications, 2006. **340**(3): p. 894-900.
179. Petsch B, Müller-Schiffmann A, Lehle A, Zirdum E, Prikulis I, Kuhn F, Raeber AJ, Ironside JW, Korth C, and Stitz L. *Biological Effects and Use of PrPSc- and PrP-Specific*

Antibodies Generated by Immunization with Purified Full-Length Native Mouse Prions. Journal of Virology, 2011. **85**(9): p. 4538-4546.
180. Perrier V, Solassol J, Crozet C, Frobert Y, Mourton-Gilles C, Grassi J, and Lehmann S. *Anti-PrP antibodies block PrPSc replication in prion-infected cell cultures by accelerating PrPC degradation.* Journal of Neurochemistry, 2004. **89**(2): p. 454-463.
181. Didonna A, Venturini AC, Hartman K, Vranac T, Čurin Šerbec V, and Legname G. *Characterization of four new monoclonal antibodies against the distal N-terminal region of PrP(c).* PeerJ, 2015. **3**: p. e811.
182. Ochs K and Málaga-Trillo E. *Common themes in PrP signaling: the Src remains the same.* Frontiers in Cell and Developmental Biology, 2014. **2**(63).
183. Klar TA, Jakobs S, Dyba M, Egner A, and Hell SW. *Fluorescence microscopy with diffraction resolution barrier broken by stimulated emission.* Proceedings of the National Academy of Sciences of the United States of America, 2000. **97**(15): p. 8206-8210.
184. Walter ED, Stevens DJ, Spevacek AR, Visconte MP, Rossi AD, and Millhauser GL. *Copper Binding Extrinsic to the Octarepeat Region in the Prion Protein.* Current protein & peptide science, 2009. **10**(5): p. 529-535.
185. Pearson G, Robinson F, Beers Gibson T, Xu B-e, Karandikar M, Berman K, and Cobb MH. *Mitogen-Activated Protein (MAP) Kinase Pathways: Regulation and Physiological Functions*.* Endocrine Reviews, 2001. **22**(2): p. 153-183.
186. Ulla J, Vera N, Nina P, Palle S, Vladimir B, and Elisabeth B. *The transcription factors CREB and c-Fos play key roles in NCAM-mediated neuritogenesis in PC12-E2 cells.* Journal of Neurochemistry, 2001. **79**(6): p. 1149-1160.
187. Harris DA, Huber MT, Van Dijken P, Shyng SL, Chait BT, and Wang R. *Processing of a cellular prion protein: identification of N- and C-terminal cleavage sites.* Biochemistry, 1993. **32**(4): p. 1009-1016.
188. Lilien J and Balsamo J. *The regulation of cadherin-mediated adhesion by tyrosine phosphorylation/dephosphorylation of β-catenin.* Current Opinion in Cell Biology, 2005. **17**(5): p. 459-465.
189. Cantley LC. *The Phosphoinositide 3-Kinase Pathway.* Science, 2002. **296**(5573): p. 1655-1657.
190. Chang C, Adler CE, Krause M, Clark SG, Gertler FB, Tessier-Lavigne M, and Bargmann CI. *MIG-10/Lamellipodin and AGE-1/PI3K Promote Axon Guidance and Outgrowth in Response to Slit and Netrin.* Current Biology, 2006. **16**(9): p. 854-862.
191. Li Y, Jia Y-C, Cui K, Li N, Zheng Z-Y, Wang Y-z, and Yuan X-b. *Essential role of TRPC channels in the guidance of nerve growth cones by brain-derived neurotrophic factor.* Nature, 2005. **434**: p. 894.
192. Zahn R, Liu A, Lührs T, Riek R, von Schroetter C, López García F, Billeter M, Calzolai L, Wider G, and Wüthrich K. *NMR solution structure of the human prion protein.* Proceedings of the National Academy of Sciences, 2000. **97**(1): p. 145-150.
193. Spevacek Ann R, Evans Eric GB, Miller Jillian L, Meyer Heidi C, Pelton Jeffrey G, and Millhauser Glenn L. *Zinc Drives a Tertiary Fold in the Prion Protein with Familial Disease Mutation Sites at the Interface.* Structure, 2013. **21**(2): p. 236-246.
194. Thakur AK, Srivastava AK, Srinivas V, Chary KVR, and Rao CM. *Copper Alters Aggregation Behavior of Prion Protein and Induces Novel Interactions between Its N- and C-terminal Regions.* Journal of Biological Chemistry, 2011. **286**(44): p. 38533-38545.

195. Schrock Y, Solis GP, and Stuermer CAO. *Regulation of focal adhesion formation and filopodia extension by the cellular prion protein (PrPC).* FEBS Letters, 2009. **583**(2): p. 389-393.
196. Wulf M-A, Senatore A, and Aguzzi A. *The biological function of the cellular prion protein: an update.* BMC Biology, 2017. **15**: p. 34.
197. Steele AD, Emsley JG, Özdinler PH, Lindquist S, and Macklis JD. *Prion protein (PrP^c) positively regulates neural precursor proliferation during developmental and adult mammalian neurogenesis.* Proceedings of the National Academy of Sciences of the United States of America, 2006. **103**(9): p. 3416-3421.
198. Kardos J, Kovács I, Hajós F, Kálmán M, and Simonyi M. *Nerve endings from rat brain tissue release copper upon depolarization. A possible role in regulating neuronal excitability.* Neuroscience Letters, 1989. **103**(2): p. 139-144.
199. Pushkar Y, Robison G, Sullivan B, Zheng W, Fu SX, Kohne M, Jiang W, Rohr S, Lai B, Marcus MA, and Zakharova T. *Aging results in copper accumulations in GFAP-positive cells in the subventricular zone.* Aging cell, 2013. **12**(5): p. 823-832.
200. Hunt CD and Idso JP. *Moderate Copper Deprivation during Gestation and Lactation Affects Dentate Gyrus and Hippocampal Maturation in Immature Male Rats.* The Journal of Nutrition, 1995. **125**(10): p. 2700-2710.
201. Toni M, Massimino ML, Griffoni C, Salvato B, Tomasi V, and Spisni E. *Extracellular copper ions regulate cellular prion protein (PrPC) expression and metabolism in neuronal cells.* FEBS Letters, 2005. **579**(3): p. 741-744.
202. Perron JC and Bixby JL. *Distinct Neurite Outgrowth Signaling Pathways Converge on ERK Activation.* Molecular and Cellular Neuroscience, 1999. **13**(5): p. 362-378.
203. Cohen MR, Johnson WM, Pilat JM, Kiselar J, DeFrancesco-Lisowitz A, Zigmond RE, and Moiseenkova-Bell VY. *NGF regulates TRPV2 via ERK signaling to enhance neurite outgrowth in developing neurons.* Molecular and Cellular Biology, 2015.